The molecular interaction of feline immunodeficiency virus Vif with feline APOBEC3 and Cullin 5

INAUGURAL-DISSERTATION

zur Erlangung des Grades eines

Dr.biol.anim.

beim Fachbereich Veterinärmedizin

der Justus-Liebig-Universität Gießen

Qinyong Gu

Aus dem Institut für Virologie

der Justus-Liebig-Universität Gießen

Betreuer: Prof. Dr. Gergely Tekes

und

Aus der Klinik für Gastroenterologie, Hepatologie und Infektiologie

der Heinrich-Heine-Universität Düsseldorf

Betreuer: Prof. Dr. Carsten Münk

The molecular interaction of feline immunodeficiency virus Vif with feline APOBEC3 and Cullin 5

INAUGURAL-DISSERTATION

zur Erlangung des Grades eines

Dr.biol.anim.

beim Fachbereich Veterinärmedizin

der Justus-Liebig-Universität Gießen

Eingereicht von

Qinyong Gu

Aus China

Giessen 2018

Mit Genehmigung des Fachbereichs Veterinärmedizin

der Justus-Liebig-Universität Gießen

Dekan: Prof. Dr. Martin Kramer

Gutachter: Prof. Dr. Gergely Tekes

Prof. Dr. Carsten Münk

Tag der Disputation: 29-06-2018

Declaration

I declare under oath that I have compiled my dissertation independently and without any undue assistance by third parties under consideration of the 'Principles for the Safeguarding of Good Scientific Practice at Justus -Liebig-Universität Gießen'

Gießen/ Düsseldorf

Date: 29-06-2018

Qinyong Gu

Publications

This thesis is based on the following publications:

1. Gu Q, Zhang Z, Cano Ortiz L, Franco AC, Häussinger D, Münk C. 2016. Feline Immunodeficiency Virus Vif N-Terminal Residues Selectively Counteract Feline APOBEC3s. **Journal of virology** 90:10545-10557.

2. Gu Q, Zhang Z, Gertzen CGW, Häussinger D, Gohlke H, Münk C. 2017. Identification of a conserved interface of HIV-1 and FIV Vifs with Cullin 5. **Journal of virology**. 2017 Dec 20. pii: JVI.01697-17. doi: 10.1128/JVI.01697-17.

This thesis is also partially based on the following publication:

1. Zhang Z**,** Gu Q, Jaguva Vasudevan AA, Hain A, Kloke BP, Hasheminasab S, Mulnaes D, Sato K, Cichutek K, Häussinger D, Bravo IG, Smits SH, Gohlke H, Münk C. 2016. Determinants of FIV and HIV Vif sensitivity of feline APOBEC3 restriction factors. **Retrovirology** 13:46.

Statement

Most of data in current thesis are produced by me. To retain the integrity of the written thesis, several figures produced by my project cooperators are included with their permission. The contribution of these data is clearly indicated.

Table of contents

List of figures

List of tables

List of abbreviations

A3	apolipoprotein B mRNA-editing enzyme, catalytic polypeptide-like 3
Vif	viral infectivity factor
FIV	feline immunodeficiency virus
CUL	cullin
ELOB	elongin B
ELOC	elongin C
HIV	human immunodeficiency virus
ALV	avian leukosis virus
MMTV	mouse mammary tumor virus
MLV	mice leukemia virus
AIDS	acquired immunodeficiency syndrome
SIV	simian immunodeficiency virus
HTLV	human T-lymphotropic virus
FLV	feline leukemia virus
BLV	bovine leukemia virus
WDSV	walleye dermal sarcoma virus
SFV	simian foamy virus
FFV	feline foamy virus
ERV	endogenous retroviruses
MA	matrix
CA	capsid
NC	nucleocapsid
PR	protease
RT	reverse transcriptase
IN	integrase

SU	surface
TM	transmembrane
Nef	negative factor
Rev	reticuloendotheliosis virus
Vpr	viral protein R
Vpu	viral protein U
Vpx	viral protein X
Vif	viral infectivity factor
Tat	transactivator (of HIV)
Env	envelope
LTR	long terminal repeats
CD4	cluster of differentiation 4
CCR5	C-C chemokine receptor type 5
CXCR4	C-X-C chemokine receptor type 4
CD134	tumor necrosis factor receptor superfamily, member 4
cDNA	complementary DNA
EIAV	equine Infectious Anemia Virus
VLPs	viral like particles
ART	antiretroviral treatment
SIVcpz	SIV of chimpanzees
SIVsm	SIV of sooty mangabeys
SIVgor	SIV of gorilla
ELISA	enzyme-linked immunosorbent assay
IFA	immunofluorescence assays
FIVple	FIV infects lion
FIVpco	FIV infects puma

PLV	puma lentivirus
OrfA	open reading frame A
Fca	felis catus
FeLV	feline leukemia virus
FFV	feline foamy virus
SIN	self-inactivating
GFP	green fluorescent protein
VSV-G	envelope glycoprotein of vesicular stomatitis virus
CMV	cytomegalovirus
neoR	neomycin phosphotransferase
TRIM	tripartite motif-containing protein
SAMHD	SAM and HD domain-containing protein
Mx	myxovirus resistan
SERINC	serine incorporator protein
IFN	interferon
GPI	glycophosphatidylinositol
RING	really interesting new gene
E1	ubiquitin activating enzymes
E2	ubiquitin conjugating enzymes
E3	ubiquitin ligases
dNTP	deoxynucleotide triphosphates
DNA	deoxyribonucleic acid
RNA	ribonucleic acid
mRNA	messenger RNA
HBV	hepatitis B virus
PFV	prototype foamy virus

glycoGag	glycosylated Gag
Ub	ubiquitin
ATP	adenosine triphosphate
CRLs	cullin-RING ubiquitin ligases
Δ	deficient
CBF-β	core binding factor β
MVV	maedi-visna virus
CAEV	caprine arthritis encephalitis virus
BIV	bovine immunodeficiency virus
CYPA	cellular cyclophilin A
CTD	C-terminal domain
CoIP	co-immunoprecipitation assays
DMEM	dulbecco's high-glucose modified eagle's medium
FBS	fetal bovine serum
HA	hemagglutinin
DMSO	dimethyl sulfoxide
FIV-luc	FIV single-cycle luciferase viruses
RIPA	radioimmunoprecipitation assay
SDS	sodium dodecyl sulfate
PBS	phosphate buffered saline
DN	dominant negative

1. Introduction

1.1 Retroviruses

1.1.1 Discovery of retroviruses

In 1908, Vilhelm Ellermann and Oluf Bang who were part of a Danish physician–veterinarian team found chicken leukosis, a form of leukemia and lymphoma, which was caused by a virus (Retroviruses 1997, Cold Spring Harbor Laboratory Press). Today, this virus is known as avian leukosis virus (ALV) (1). In 1936, John Bittner found that mice mammary carcinomas were caused by a kind of milk-transmitted, filterable agent, which was identified as mouse mammary tumor virus (MMTV) (2). In 1957, Ludwik Gross reported murine leukemia virus (MLV) (3).

Human immunodeficiency virus (HIV) is a lentivirus, which is a subgroup of retroviruses. HIV can attack the immune system and cause acquired immunodeficiency syndrome (AIDS) in humans (4). Similarly, the simian immunodeficiency virus (SIV) attacks the immune systems of monkeys and apes (5). By analyzing the "family tree" of HIV and SIV, scientists found that HIV-1 was transmitted from chimpanzees to humans in Kinshasa (Democratic Republic of Congo) around 1920 (4). HIV-1 had already rapidly spread to five continents (Africa, Europe, Australia, North America, and South America) by 1980 (4). A second HIV virus, HIV-2, originates from the cross-species transmission of SIV from sooty mangabey (6). In 1986, the feline immunodeficiency virus (FIV) was discovered in the domestic cat (7). FIV can cause AIDS in domestic cats and the pathogenesis and genomic organization of FIV are similar to HIV (8). Thus, FIV has been used as an experimental model for HIV-1 in the investigation of immune-pathogenesis and antiviral drugs (9).

1.1.2 Classification of retroviruses

Retroviruses include exogenous retroviruses and endogenous retroviruses. Exogenous retroviruses include seven genera that are Alpharetroviruses, Betaretroviruses, Gammaretroviruses, Deltaretroviruses, Epsilonretroviruses, Lentiviruses and Spumaviruses (10). The classification of exogenous retroviruses is shown in table 1.1. Among the

exogenous retroviruses, only HIV and human T-lymphotropic virus (HTLV) cause diseases in humans.

Genus	Type species
Alpharetrovirus	ALV
Betaretrovirus	MMTV
Gammaretrovirus	MLV, FLV
Deltaretrovirus	BLV, HTLV
Epsilonretrovirus	WDSV
Lentivirus	FIV, SIV, HIV
spumavirus	SFV, FFV,

Table 1.1 The genera of exogenous retrovirus. ALV: Avian leucosis virus, MMTV: Mouse mammary tumor virus, MLV: Murine leukemia virus, FLV: Feline leukemia virus, BLV: Bovine leukemia virus, HTLV: Human T-lymphotropic virus, WDSV: Walleye dermal sarcoma virus, FIV: Feline immunodeficiency virus, SIV: Simian immunodeficiency virus, HIV: Human immunodeficiency virus, SFV: Simian foamy virus, FFV: Feline foamy virus.

There are endogenous viral elements in mammal and other genomes, which are called endogenous retroviruses (ERVs). Depending on the relatedness to exogenous retrovirus, endogenous retroviruses are classified into three classes: Class I is similar to the gammaretroviruses, Class II is closely related to the betaretroviruses and alpharetroviruses, Class III resembles the spumaviruses (10). Around 8% of the human genome consists of endogenous retroviral sequences that play important biological roles in humans (11).

1.1.3 Retrovirus genome structure

Retroviruses are enveloped single-stranded positive-sense RNA viruses, which have a reverse transcriptase that converts viral RNA to DNA and an integrase that incorporates the viral DNA into the host cellular genome. The integrated viral genome is referred to as a provirus, which replicates together with the host genome. The diameter of a retrovirus virion is around 80–120 nm and the length of single-stranded RNA molecule is around 7–12 kb. The

retroviral genome includes four main genes: *gag*, *pro*, *pol,* and *env*. The *gag* gene encodes viral structural proteins: matrix (MA), capsid (CA), and nucleocapsid (NC). The *pro* gene encodes a protease (PR) that cleaves or induces proteolysis of proteins produced by *gag*, *pro*, *pol,* and *env*. The *pol* gene encodes the viral enzymes reverse transcriptase (RT), integrase (IN), and RNase H. The *pro* gene is found in *pol* in some viruses. The *env* gene encodes the viral envelope proteins surface (SU) glycoprotein and transmembrane (TM) protein. In addition, some retroviral genomes also include several regulatory genes, including *tat*, *rex*, *nef*, *rev*, *vpr*, *vif,* and *vpu*. These regulator proteins play an important role in virus infection, production, and pathogenesis. At the termini of the viral genomes, there are two long terminal repeats (5'-LTR and 3'-LTR, respectively). The two LTRs are essential for viral transcription and integration (Fig. 1.1) (Retroviruses 1997, Cold Spring Harbor Laboratory Press).

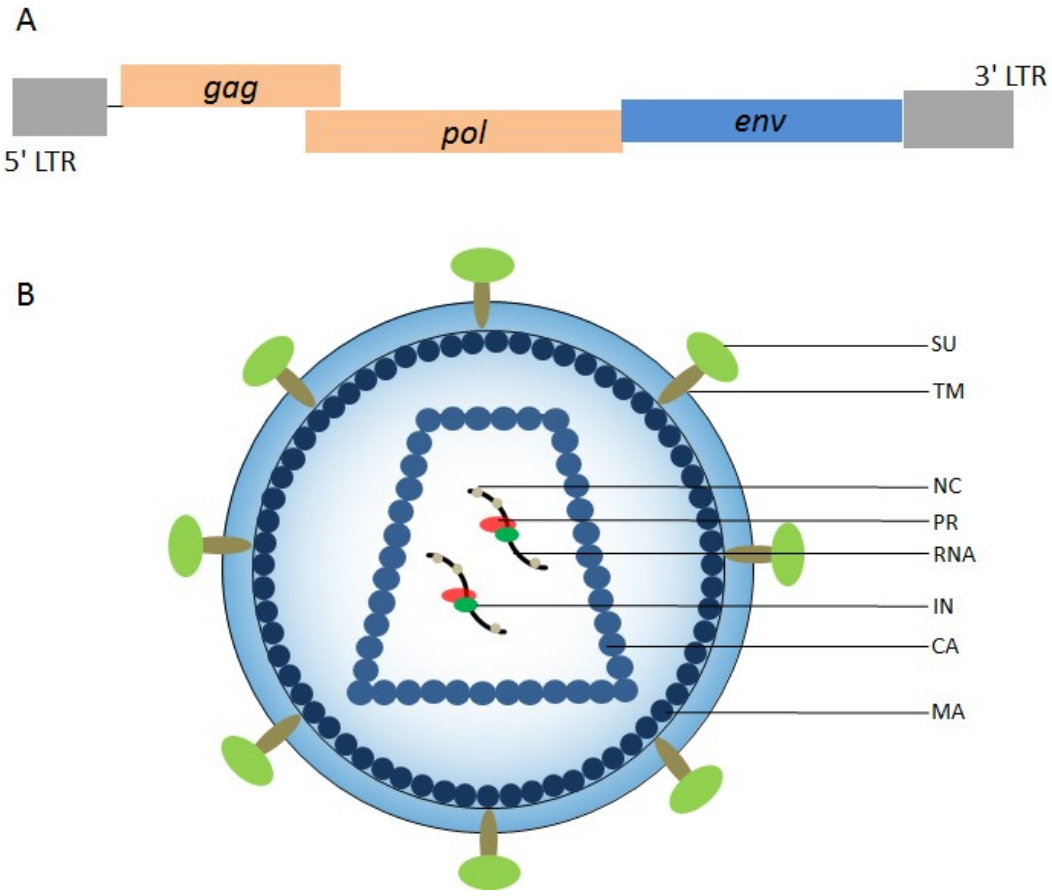

Fig. 1.1 Schematic representation of retroviral genome and particles. (A) The *gag*, *pol* and *env* are main genes of retrovirus. Both 5’ and 3’ termini of viral genomes contain long terminal repeats (LTRs). (B) The retroviral particle contains RNA genomes and viral proteins.

The *env* encodes virus envelope proteins: surface (SU) glycoprotein and transmembrane (TM) protein. The *gag* encodes virus structural proteins: matrix (MA), capsid (CA), nucleocapsid (NC). The *pol* encodes virus enzymes: protease (PR), integrase (IN).

1.1.4 Retroviral lifecycle

The retroviral lifecycle starts at the point of attachment of the retroviral envelope glycoproteins to specific host cell receptors. HIV-1 attaches to the host cell by binding to the CD4 receptor and co-receptors CCR5 or CXCR4 (12). The receptor for FIV is CD134 and CXCR4 (13-15). Once the retrovirus attaches to the host cell, the virion envelope fuses with the plasma membrane of the host cell. This fusion step leads to the release of the viral capsid into the cytoplasm. After entering the host cell, the reverse transcriptase of the virus transcribes the single-stranded RNA into complementary DNA (cDNA), and then the viral double-stranded DNA is synthesized using the cDNA as the template. Following this, the viral integrase incorporates the double-stranded DNA into the host genome. After integration, the 5⁻LTR acts as a promoter to induce viral transcription. The retrovirus hijacks the host cellular translation and transcription machinery for its own replication. Next, newly synthesized viral proteins and the full-length viral genome are assembled. Most retroviruses express envelope proteins from the spliced mRNA and Gag and GagPol proteins from unspliced mRNA. Pol is expressed in most cases as GagPol polyprotein by repressing a stop codon of Gag either by stop-codon suppression or ribosomal frameshifting. Different retroviruses choose distinct cellular assembly sites. For example, equine infectious anemia virus (EIAV) assembly starts at the trans-Golgi while HIV-1 selectively assembles on the cellular plasma membrane (16). The retroviral Gag protein alone is sufficient to form virus-like particles (VLPs). However, retroviruses need to obtain envelope proteins, and be released from the cell membrane to form infectious virions; this step is called viral budding. The viral maturation is induced by a viral protease by cleaving the Gag and GagPol proteins. The mature viruses are able to repeat this cycle in new target cells (Retroviruses 1997, Cold Spring Harbor Laboratory Press) (Fig. 1.2).

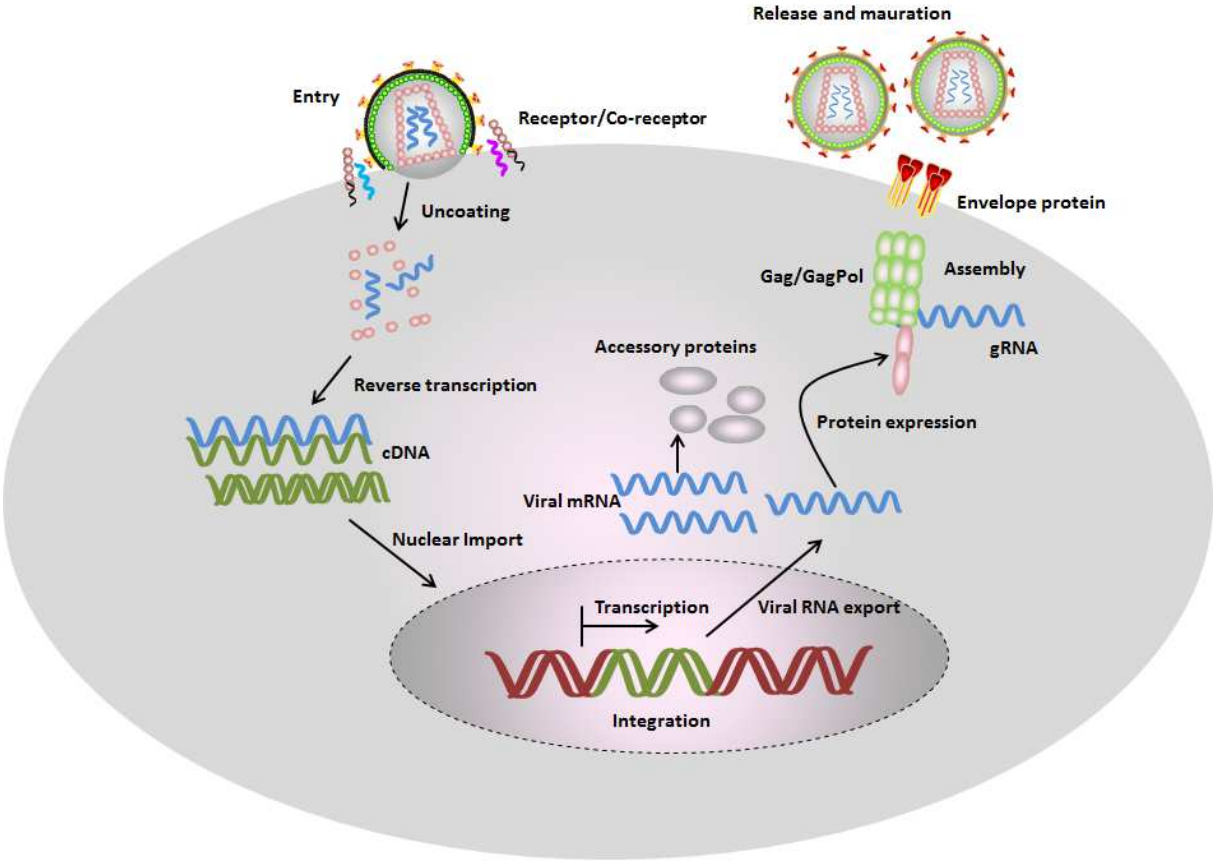

Fig. 1.2 The replication cycle of retroviruses. Four main steps are included: Viral entry and uncoating; reverse transcription and integration; transcription and splicing; assembly and release.

1.2 Human immunodeficiency virus

HIV is a lentivirus that attacks and destroys the human immune system. HIV infects $CD4^+$ T cells, macrophages, and dendritic cells (17). HIV may be present in several body fluids, including blood, semen, pre-ejaculate, vaginal fluids, rectal fluids, breast milk, and wound secretions. HIV has several transmission pathways: vaginal sexual intercourse; anal sexual intercourse; intravenous blood exposure by sharing needles; blood transfusions; mother-to-child transmission during childbirth; and breastfeeding (18). However, HIV cannot be transmitted through sweat, saliva, or urine. In the early stage of HIV infection, the patient may not have any symptoms. However, ultimately, HIV attacks the immune system and finally causes acquired immune deficiency syndrome (AIDS). Clinically, HIV replication is inhibited using antiretroviral treatment (ART) (19). Without treatment, the immune system

of the HIV patient will be lethally damaged after 10–15 years. Under effective and correct ART therapy, HIV replication in patients is controlled and patient immune system is protected. However, drug resistance is becoming increasingly common (20) and scientists are currently trying to identify new antiretroviral drugs. These drugs may interrupt the HIV lifecycle by interfering with viral reverse transcription, stopping the virus fusing with the host cell, inhibiting viral integration into the host genome, or by inhibiting release of new HIV particles from the producer cell.

HIV includes two main strains, HIV-1 and HIV-2, which are very similar, but they are two distinct viruses (4). The origin of HIV-1 is from SIV of chimpanzees (SIVcpz) and the origin of HIV-2 is from SIV of sooty mangabeys (SIVsm). HIV-1 is most common and causes around 95% of HIV infections worldwide. HIV-1 can be divided into four groups: M, N, O, and P (4). Among the four groups, M is the major group, whereas viruses of N and P are only found in a few infected individuals. The O group of HIV-1 is mainly distributed in west-central Africa and has a low prevalence rate (less than 1% of global HIV-1 infections) (4). Recent data indicate that the O and P groups of HIV-1 originate from the cross-species transmission of SIV of gorilla (SIVgor) (21). In addition, group M is mainly responsible for the AIDS pandemic and is subdivided into 11 subtypes (subtypes A–K) based on the genetic sequence data (22). HIV-2 is less infectious and progresses more slowly than HIV-1 and HIV-2 infection cases are limited to a few West African countries. Currently, HIV-2 is divided into eight groups (groups A–H). However, only group A and group B are pandemic; the other six groups (C–H) were rarely found (23, 24). The HIV subtype information is described in Table 1.2.

	Major types	Groups	Subtypes	Prevalence
HIV	**HIV-1**	**Group M**	Subtype A	Is common in West Africa
			Subtype B	is most common in the Middle East and North Africa, Europe, the Americas, Japan, and Australia
			Subtype C	is dominant form in Southern Africa, Eastern Africa, India, Nepal, and parts of China
			Subtype D	generally is only seen in Eastern and central Africa
			Subtype E	is dominant form in Southeast Asia
			Subtype F	was found in central Africa, South America and Eastern Europe
			Subtype G	have been found in Africa and central Europe
			Subtype H	is limited to central Africa
			Subtype I	a strain with the cpx for a "complex"

				recombination of several subtypes
			Subtype J	is primarily found in North, Central and West Africa, and the Caribbean
			Subtype K	is limited to the Democratic Republic of Congo and Cameroon
		Group N		was firstly isolated from a Cameroonian woman in 1998
		Group O		is most common in Cameroon and unusually seen outside of West-central Africa
		Group P		was isolated from a Cameroonian woman residing in France in 2009
	HIV-2	Subtype **A**		is found mainly in West Africa, but has also spread globally to Angola, Mozambique, Brazil, India, Europe, and the US
		Subtype **B**		is mainly limited to West Africa
		Subtype **C**		is found in just one person from Liberia
		Subtype **D**		is found in just one person from Liberia
		Subtype **E**		is found in just one person from Sierra Leone
		Subtype **F**		is found in just one person from Sierra Leone
		Subtype **G**		is found in just one person from Ivory Coast
		Subtype **H**		is found in just one person from Ivory Coast

Table 1.2 The classification of HIV.

The genome of HIV-1 contains *LTR*, *gag*, *pol*, *env*, and some accessary genes (*vif*, *vpr*,*nef*, *vpu*). The genome of HIV-2 contains *LTR*, *gag*, *pol*, *env*, and some accessary genes (*vif*, *vpr*,*nef*, *vpx*). Vpu is unique for HIV-1, such as Vpx is special for HIV-2. These different accessory genes are important for HIV replication and pathogenesis (25) (Fig. 1.3).

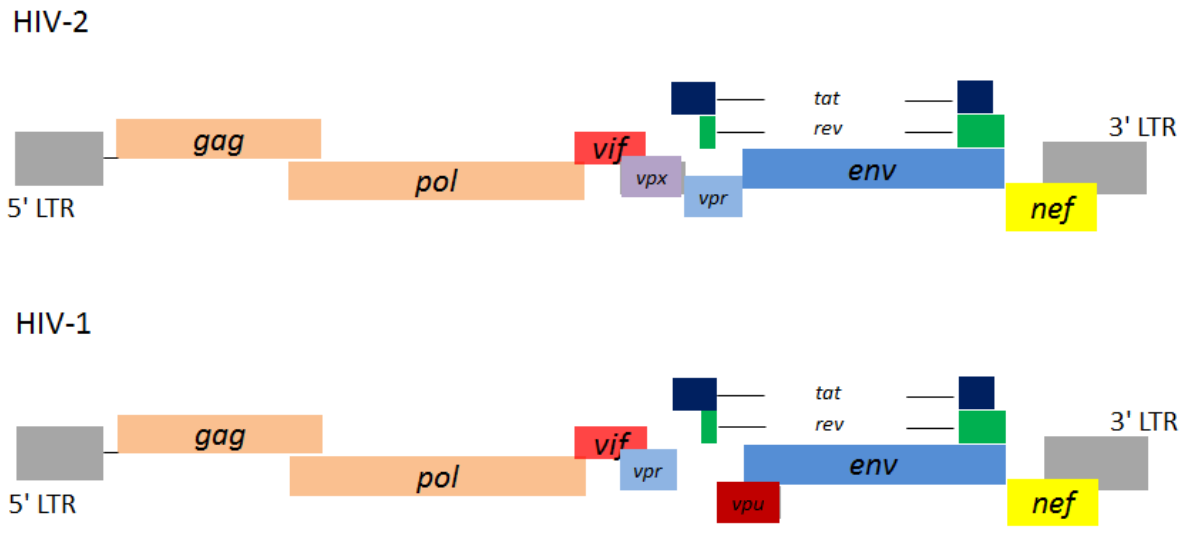

Fig. 1.3 HIV-1 and HIV-2 genome structure. Both HIV-1 and HIV-2 contain two long terminal repeats (LTRs) and the genes *gag*, *pol*, *env*, *vif*, *vpr*, *tat*, *rev*, and *nef*. HIV-2 uniquely contains *vpx* gene, while HIV-1 contains *vpu* gene.

1.3 Feline immunodeficiency virus

1.3.1 FIV-caused disease

FIV is a lentivirus that attacks the cat immune system and was isolated in 1986 by Dr. Smith at the University of California (7). Around 2.5–4.4% of cats are infected with FIV worldwide (8). FIV cannot infect humans and can only be transmitted from cat to cat. The spread of FIV among cats passes through deep bite wounds. It can also be transmitted from infected mother cats to offspring but this transmission mode is rare. In semen FIV can be detected, but sexual transmission is uncommon. Cats infected with FIV may not show symptoms for several years because FIV is a slow-acting virus, but once the cat immune system is impaired, various secondary infections will occur. FIV-infected cats may display several symptoms including enlarged lymph nodes, fever, anemia, weight loss, disheveled coat, poor appetite, diarrhea, conjunctivitis, gingivitis, stomatitis, dental disease, skin redness or hair loss, wounds that don’t heal, sneezing, discharge from eyes or nose, frequent urination, straining to urinate or urinating outside of litter box, and behavioral changes (8). When a cat is diagnosed with FIV, the survival time is around 5 years. Normally, FIV infection is diagnosed by blood testing using an enzyme-linked immunosorbent assay (ELISA), Western blotting, or immunofluorescence (IFA) assays. Some anti-HIV-1 inhibitors or drugs can be used for antiviral treatment of FIV (26). In addition, the development of an FIV vaccine is underway and several commercial dual-subtypes FIV vaccines are available (27).

In fact, only a small proportion of FIV-infected domestic cats progress into an immunodeficiency disease similar to HIV-1-induced AIDS (28). However, highly pathogenic FIV isolates can lead to mortality rate up to 60% under experimental conditions (29-31). Thus, FIV-infected domestic cat is a valuable animal model to study the pathogenesis of HIV-1 and the progression of AIDS (32-34). In addition to the domestic cat, species-specific FIVs isolated from many Felidae might cause disease in these natural hosts (35).

1.3.2 FIV subgroups and cross-species transmission

FIV has five subtypes (subtypes A–E; Table 1.3) (36), which are classified through envelope gene polymorphisms. Subtype A has been found in Northern Europe and California. Subtype B was reported in southern European countries and central and eastern USA. Subtype C is dominant in California and British Columbia, whereas subtype D was reported in Japan and also Argentina. The prevalence of FIV infection shows that older cats (6 years or older) are more frequently infected, male cats are four times more likely to be infected than female cats, and outdoor cats are more likely to be infected than indoor cats (37). Different strains of FIV can infect both domestic and wild feline species, including cheetah, lion, puma, bobcat, leopard, and Pallas' cat. The FIV that infects lions is called FIVple and has a subtype composition that may affect disease outcome in African lions (38, 39). One previous study showed that more than 40% of Serengeti lions in Tanzania are multiply infected with different FIVple subtypes, including subtypes A, B, and C, and it was also suggested that the circulation of FIVple within this large population may offer opportunities for recombination (40). The FIV that infects puma is named FIVpco, while some studies describe FIVpco as puma lentivirus (PLV) (38, 39, 41-44). PLV includes subtypes A and B (PLVA and PLVB). PLVB infects puma throughout North and South America. PLVA infects puma in southern California and Florida, and bobcats in these two regions are also infected with PLVA (41). PLVA and PLVB are highly divergent in infected pumas and bobcats (41).

	Subtype	Prevalence
FIV	A	northern Europe, California.
	B	southern European countries, the central and eastern USA
	C	California, British Columbia
	D	Japan
	E	Argentina

Table 1.3 The classification of FIV.

It is known that the pandemic of HIV originated from cross-species transmission events of SIVs to humans (4). As described for inter-species infections of primate lentiviruses, cross-

species transmission of FIV between several Felidae were observed (39). For example, pumas are described to be occasionally infected by FIV of domestic cats and bobcats, and the lion FIV can be transmitted to tigers and leopards (43, 45-48). However, phylogenetic evidence indicated that these FIV transmissions are exceedingly rare events between wildlife cat species, and restriction factors of the host may act as barriers to prevent the spread of FIV (39, 42, 49).

1.3.3 FIV genome structure

FIV infects T cells, monocytes/macrophages, dendritic cells, and also B lymphocytes. Unlike HIV, FIV uses CD134 as a receptor and CXCR4 as a co-receptor (13-15); however, FIV and HIV entry mechanisms are similar. The genome of FIV contains *gag*, *pol*, *env*, *vif*, and *orfA*, coding for Gag, Pol, and Envelope structural and enzymatic proteins, and accessory proteins of Vif and OrfA (Fig. 1.4). During viral replication, the expression of Vif and OrfA is very low, but both are important for viral replication and infection. Vif protein prevents the restriction of feline APOBEC3 by inducing degradation via E3 ubiquitination (50). The OrfA protein downregulates the CD134 receptor from the cell surface and increases virus release and replication (51, 52). Sundstrom *et al.* also indicated that FIV OrfA alters the expression of cellular splicing factors and proteasome-ubiquitination proteins (53).

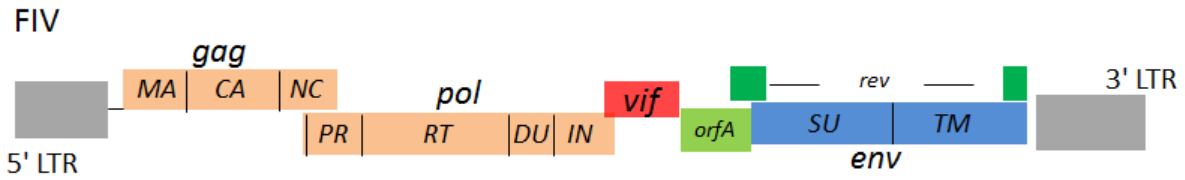

Fig. 1.4 FIV genome structure. Two long terminal repeats (LTRs) locate at 5' and 3' termini. The structural genes of FIV are *gag*, *pol*, and *env*. The regulatory genes of FIV are *vif*, *orfA*, and *rev*. The *gag* encodes virus structural proteins: matrix (MA), capsid (CA), nucleocapsid (NC). The *pol* encodes virus enzymes: protease (PR), reverse transcriptase (RT), integrase (IN) and dUTPase (DU). The *env* encodes virus envelope proteins: surface (SU) glycoprotein and transmembrane (TM) protein.

1.3.4 FIV based lentivirus vectors

Viral vectors are common tools to deliver viral genomes into cells *in vivo* and *in vitro*. In the 1970s, the viral vector system was first developed by Paul Berg who received the Nobel Prize for Chemistry in 1980. Berg delivered a modified simian virus 40 (SV40) containing DNA from the bacteriophage λ to monkey kidney cells (54).

For gene therapy, viral vectors should be safe, non-tocxic, stable, and have wide cell-type-specificity. Currently, there are several types of viral vectors available: retroviral vectors (55, 56), lentiviral vectors (57), adenoviral vectors (58), and adeno-associated viral vectors (59).

HIV-1-based vectors can be utilized for gene therapy and the first lentiviral vector was designed based on HIV-1 (60) while the first non-primate lentiviral vector was based on FIV (61). The FIV vector can effectively transduce cells in the brain, eye, airway, hematopoietic system, liver, muscle, and pancreas (61, 62). The FIV vector system includes three components: FIV transfer vector, e.g., pGINSIN, a packaging construct, e.g., pFP93, and non-lentiviral glycoprotein pseudotyping construct, e.g., pMD.G. The pGINSIN plasmid is a self-inactivating (SIN) vector with a U3 deletion that can deliver an exogene to the target cells. pGINSIN encodes a GFP exogene that can be used as a marker to evaluate the transduction efficiency; pFP93 is a minimal FIV packaging plasmid encoding Gag, Gag/Pol precursor, and Rev proteins; pMD.G is an envelope pseudotyping plasmid that expresses the envelope glycoprotein of vesicular stomatitis virus (VSV-G); VSV-G pseudotyped FIV particles have a wide cell tropism. However, other viral envelope glycoproteins can also be applied to the FIV vector system (63) (Fig. 1.5).

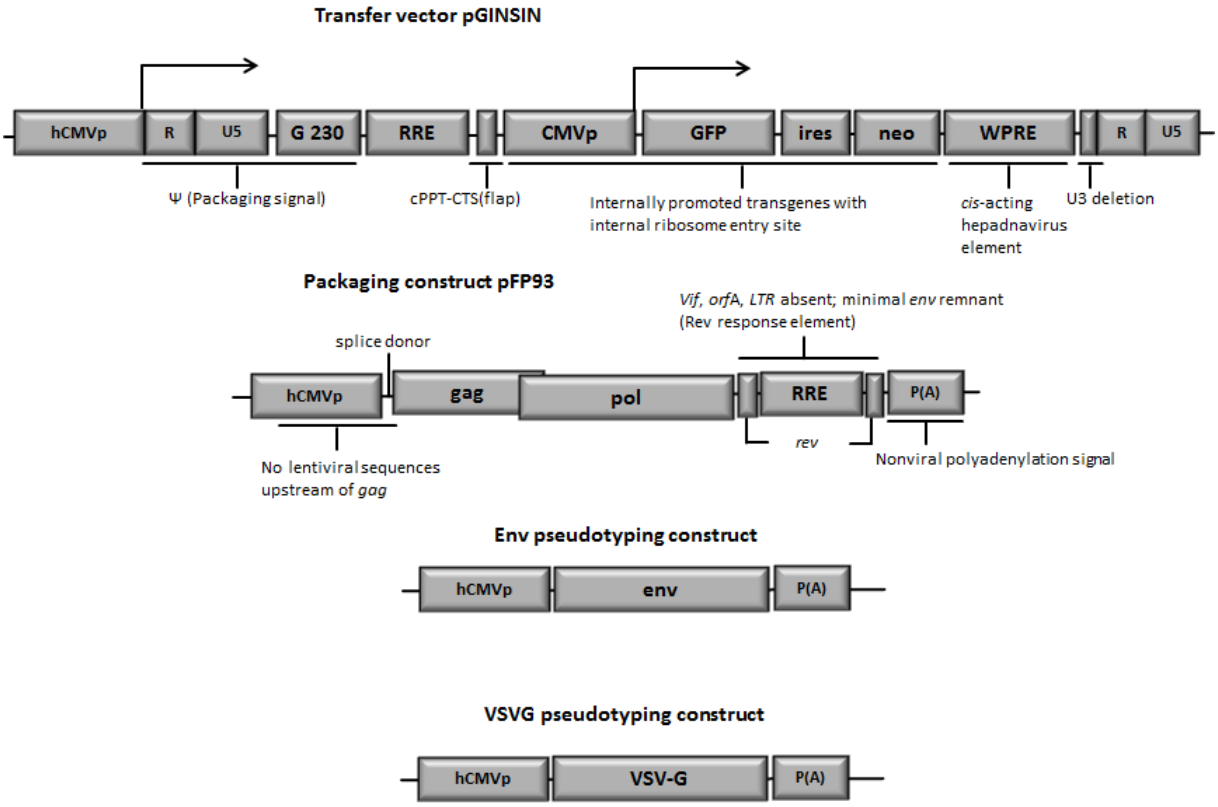

Fig. 1.5 Diagram of FIV-based lentiviral vector system. In FIV transfer vector pGINSIN, the U3 of 5' LTR is replaced by CMV promoter (hCMVp). Only the 5' 230bp of gag are present named G230. pGINSIN contains a (ϕ) packaging signal and also encodes enhanced green fluorescent protein (GFP), which is linked monocistronically via an internal ribosome entry site (IRES) to the gene of neomycin phosphotransferase (neoR). RRE is Rev responsive element. cPPT is central polypurine tract. CTS is central termination sequence. WPRE facilitates mRNA stability. U3 of 3' LTR has a central 167-nucleotide deletion. pFP93 is a FIV packaging construct encoding Gag, Gag/Pol precursor, and Rev proteins. A variety of viral envelope proteins (e.g. FIV env or VSV-G) can be used for pseudotyping.

1.4 Feline restriction factors

Restriction factors are innate cellular proteins that inhibit retrovirus replication by different mechanisms. Most of the restriction factors are IFN-inducible. However, retroviruses are able to escape the inhibition of restriction factor by specific counteraction mechanisms. Until now, many restriction factors were identified: Tetherin, tripartite motif-containing protein 5α (TRIM5α), SAM and HD domain-containing protein 1 (SAMHD1), myxovirus resistance B

(MxB), and serine incorporator protein 3/5 (SERINC3/5), apolipoprotein B mRNA-editing enzyme, catalytic polypeptide-like 3 (APOBEC3) (64).

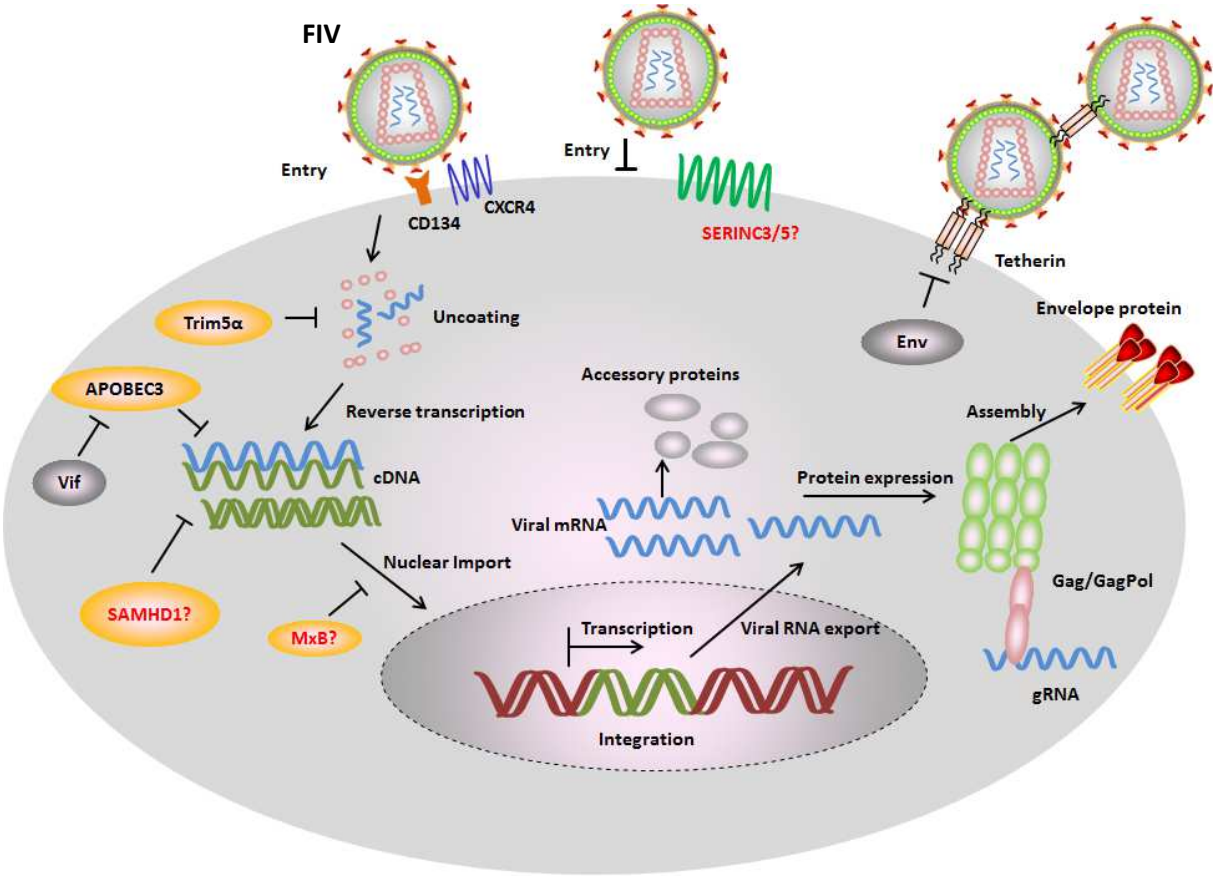

Fig. 1.6 Feline restriction factors and FIV counteraction mechanisms. In the absence of viral antagonists, several cellular proteins called restriction factors inhibit different stages of viral replication cycle. Monkey TRIM5α interacts with FIV capsid and inhibits an early infection step. Felines expresses a truncated TRIM5 gene that appears to have no antiretroviral activity, while the artificial fusion protein of feline TRIM5 with feline CypA displays potential inhibition against FIV. Feline APOBEC3s induce hypermutations of FIV genomes by its cytidine deamination activity. It is still unkown whether SERINC3/5 are expressed in feline cells and whether they confer antiviral activity. Cats have mutation in the MxB gene resulting in a very short transcript not encoding a functional protein. Feline tetherin prevents FIV release from cell surface. The restriction factors are counteracted by FIV encoded proteins. FIV Vif interacts with feline APOBEC3s and induces their degradation by the proteasome pathway. FIV Env counteracts the restriction of tetherin.

1.4.1 Tetherin:

Tetherin (also called BST2, CD317, or HM1.24) is a type I interferon (IFN-I)-inducible factor that can inhibit the release of many enveloped viruses from the cell surface. Tetherin is a type II transmembrane protein with an N-terminus transmembrane anchor, single-pass transmembrane domain, an extracellular domain, and a C-terminus glycophosphatidylinositol (GPI) lipid anchor. The N-terminus transmembrane domains are inserted into the cell membrane and the GPI anchors are incorporated into the lipid envelope of the virion particles. The extracellular domain promotes dimerization of adjacent tetherin molecules with disulfide links between the cell and the virus. Then, the tetherin protein spans both the virion and cell membranes after completion of budding. Some proteins encoded by viruses are able to counteract the inhibition of tetherin, including Vpu of HIV-1 and the Nef proteins of SIVmus/gsn/mon, both of which induce tetherin internalization and thus tetherin downregulation at the cell surface. The Env proteins of HIV-2, SIVtan, FIV, EIAV, and Ebola virus can sequester tetherin in intracellular compartments (65-68). Feline tetherin has the capability of preventing the release of FIV and HIV-1, which is antagonized by FIV Env (69-71).

1.4.2 Trim5α:

After retroviral fusion into the cytoplasm of the target cell, a conical core that contains capsid proteins (CA), two viral genomic RNAs, and several viral proteins are released into the cytoplasm. In the cytoplasm of the target cell, CAs are separated from the viral complex in a process named uncoating. During the uncoating process, the viral genome is reverse transcribed. Changing the stability of the lentivirus core can cause impaired reverse transcription or nuclear import (72-74).

The tripartite motif (TRIM) family member 5 with its splice variant alpha (TRIM5α) is expressed in cells of primates and most mammals and inhibits lentiviral infection by disturbing the uncoating process and thus provides an effective species-specific barrier to retroviral infection. Members of the TRIM family can be induced by interferons. TRIM proteins have a functional motif at the N-terminus, which includes RING (really interesting

new gene), B-box, and coiled-coil domains (75). The alpha isoform of TRIM5 (TRIM5α) additionally includes a C-terminal PRYSPRY (B30.2) domain (74-77), which directly interacts with the HIV-1 and FIV capsid core (78-81) and induces the anti-HIV-1 activity of TRIM5α. However, this kind of interaction is very weak (millimolar-level affinity). Thus, it requires both TRIM5α dimerization and assembly of the dimers into a multivalent hexagonal lattice to facilitate that interaction (82). The RING domains of TRIM5α have E3 ubiquitin ligase activity, and it can induce the proteasome-dependent degradation of the HIV-1 core (74, 83). Feline expresses a truncated TRIM5 gene that appears to have no antiretroviral activity (84). However, the fusion protein of feline TRIM5 with feline CypA displays potential inhibition against FIV and HIV-1 (85).

1.4.3 SAMHD1：

SAMHD1 (sterile α motif and histidine-aspartic acid domain-containing protein 1) is an enzyme that can inhibit retroviral reverse transcription by hydrolyzing intracellular deoxynucleotide triphosphates (dNTPs) (86, 87) during the early step of the viral lifecycle (88). This dNTP hydrolyzation function of SAMHD1 decreases the concentration of intracellular dNTP, which are essential for viral cDNA synthesis, and thus inhibits viral replication (86). The phosphorylation of SAMHD1 regulates its antiretroviral activity (89, 90). SAMHD1 can prevent the infection of HIV-1 in $CD4^+$ T cells but this antiviral activity can be inhibited by viral accessory protein Vpx from HIV-2/SIV, which causes proteasomal degradation of SAMHD1 (91, 92). The SAMHD1 protein also has single-stranded DNA- and RNA-binding activity, and it is possible that SAMHD1 directly digests genomic HIV-1 RNA to restrict HIV-1 infection (93). SAMHD1 is an IFN-α inducible protein (94), which can also block the replication of several DNA viruses such as Hepatitis B virus (HBV) in liver cells (94, 95). All retroviruses tested so far, except for prototype foamy virus (PFV) and human T cell leukemia virus type I (HTLV-1), can be restricted by SAMHD1 (96). Before virus entry, PFV has already completed reverse transcription and so escapes SAMHD1 restriction (96).

The infection of FIV is evidently inhibited by human SAMHD1 (97). One recent study indicates that feline SAMHD1 expresses in a wide range of cat tissues, such as skin, mucosal epithelium

spermatogenic tissues, and FIV susceptible cell lines (98). However, no study demonstrated whether feline SAMHD1 has the ability of restricting FIV or other retroviruses.

1.4.4 MxB:

Mx proteins are encoded by the *Mx* genes and are interferon-induced GTPases that act as restriction factors. Most mammals have two *Mx* genes: *MxA* (also called *Mx1*) and *MxB* (also called *Mx2*) (99). The amino acid sequence similarity of MxA and MxB is 63% and they have a similar domain structure and architecture (99). Human MxA protein can restrict many viral pathogens such as influenza viruses (100, 101) and it probably provides a barrier to the cross-species transmission of zoonotic influenza A viruses to humans (102). The human MxA protein is localized within the intracellular membranes, predominantly in the endoplasmic reticulum/Golgi intermediate compartment, which is an intracellular replication site of many viral pathogens (101). MxB protein is a capsid-interacting restriction factor that targets HIV after reverse transcription but before integration (103, 104). In the MxB knockout cell lines, the replication of HIV is increased compared to the wild-type cell lines. However, MxA cannot inhibit the replication of HIV (103, 104). MxB protein accumulates at the nuclear envelope (NE), throughout the cytoplasm, and in cytoplasmic granules (105) and some studies indicate that the oligomerization of MxB is essential for its antiviral activity (105-110). In addition, one study indicates that MxB is not a restriction factor of foamy viruses (111). In IFN-α-treated human cells, MxB directly interacts with the core of HIV-1 to inhibit the uncoating process of HIV-1 (112, 113). An HIV-1G208R mutant inhibits the interaction of MxB with the viral core (114). The 11RRR13 motif of MxB is important for binding to the capsid and to restrict HIV-1 infection (105).

Interestingly, human MxB does not inhibit several non-primate retroviruses, such as FIV, EIAV, and MLV (103). It is unknown whether MxB or MxA from the host of these non-primate retroviruses contains antiviral activity. Two studies identified that cats have a highly damaged and inactivated MxB gene (115, 116)

1.4.5 SERINC:

The serine incorporator (SERINC) family contains five members (SERINC1–5), all of which contain multiple transmembrane domains (117, 118). These five SERINC proteins are discussed to be eukaryotic cell membrane transporter proteins that incorporate serine into membrane lipid (117). In eukaryotes, SERINC proteins are highly conserved but there is no amino acid homology between SERINC and other proteins (117). SERINC3 and SERINC5 can be incorporated into HIV-1 particles and restrict the fusion of virions with target cells (119-121). It is likely that SERINC3 and SERINC5 restrict the expansion of the viral fusion pore and then prevent the release of the viral core into the cytoplasm (119-121). However, this antiviral activity is counteracted by the Nef protein from HIV-1 and SIVs (119, 120, 122). HIV-1 Nef and mouse leukemia virus glycosylated Gag (glycoGag) increases the infectivity of HIV-1 via inhibition of SERINC3 and SERINC5 (119, 120). Furthermore, in SERINC3 and SERINC5 double-knockout human $CD4^+$ T cells, the infectivity of *nef*-deficient virions increased more than 100-fold (119, 120). Nef protein of HIV-1 antagonizes SERINC5 by downregulating SERINC5 expression at the cell surface and blocking SERINC5 incorporation into virions. In addition, the Env protein of some HIV-1 strains (AD8-1 and YU-2) and glycoproteins of vesicular stomatitis virus (VSV) and Ebola virus can also prevent SERINC5 antiviral activity (118). However, why HIV-1 uses two proteins, Nef and Env, to counteract SERINC5 is not known (118). Both EIAV S2 and Env proteins partially counteract the antiviral activity of SERINC5 (123). EIAV Env also inhibits Tetherin (67).

1.4.6 APOBEC3:

Apolipoprotein B mRNA editing enzyme, catalytic polypeptide-like (APOBEC3, A3) family of DNA cytidine deaminases are found in placental mammals with different clade-specific gene copies and arrangements, which plays a vital role for innate immune defense against retroviruses (see recent reviews (124, 125). A3 proteins target retroviruses by interacting with viral Gag protein and viral RNA, and then A3 is packaged into viral particles (126). In the next round of infection, A3 inhibits viral replication by deamination of cytidines in viral single-strand DNA that forms during reverse transcription, introducing G-to-A hypermutations in the coding strand (127-131). These hypermutated viral genomes will be

destroyed by some cellular DNA degradation enzymes (132). In addition, some A3s inhibit virus replication by decreasing reverse transcription and integration via deaminase-independent mechanisms (133-139) (Fig. 1.7). One recent study demonstrated that human A3G directly interact with HIV-1 reverse transcriptase and inhibits its function (139).

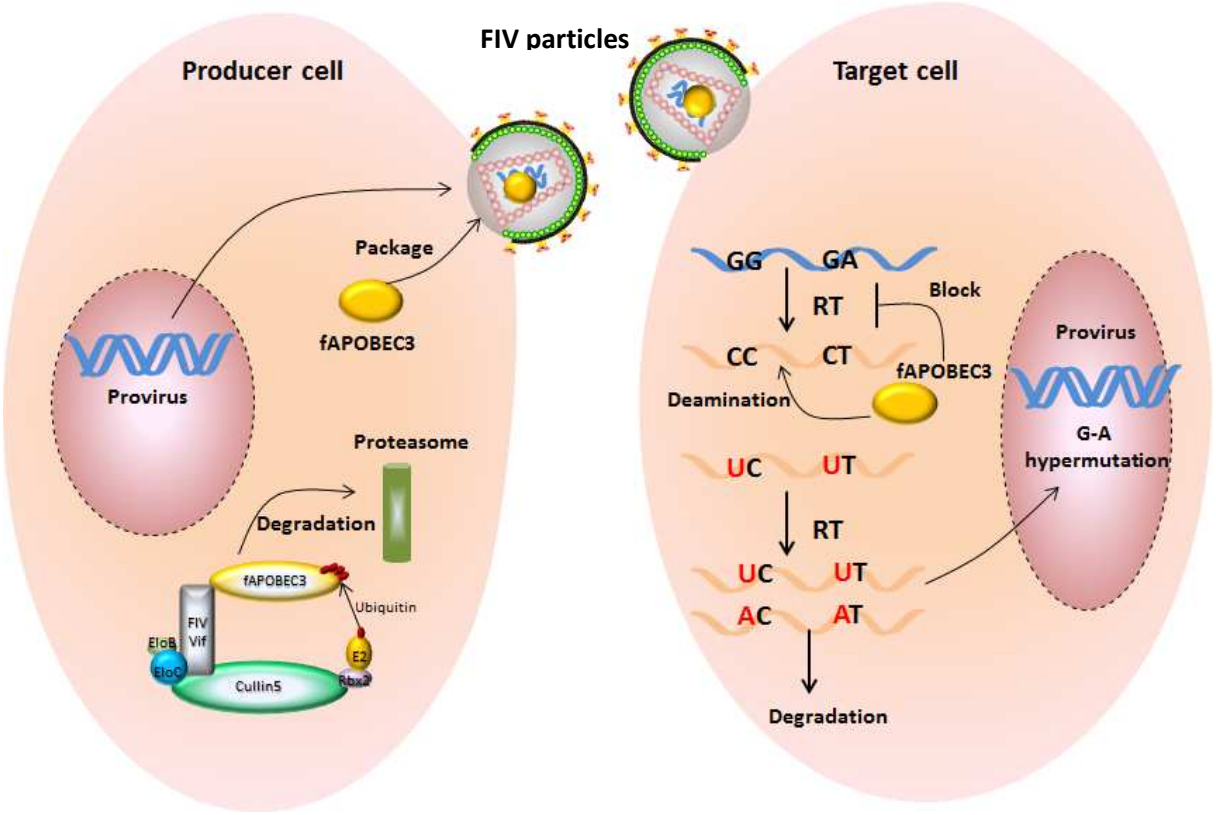

Fig. 1.7 Feline A3s inhibit the replication of FIV and are counteracted by FIV Vif. In producer cells, A3s can be incorporated into virus particles and be delivered into target cell in the absence of Vif. During viral reverse transcription, A3s are able to catalyze the cytidine-deamination to uridine in viral cDNA. In the synthesis of next strand virus DNA, lots of G-A hypermutations are produced. The highly mutated viral genomes are degraded by cellular enzymes. However, FIV Vif directly interacts with feline A3 and forms an A3-Vif-E3 ubiquitination complex, which induces A3 degradation by the proteasome pathway. In Vif expressing FIV infections, viral particels are produced that are free of A3 proteins.

1.5 Cullin 5-E3 ubiquitin complex

To achieve sufficient lentiviral replication, the lentivirus antagonizes some cellular restriction factors by hijacking Cullin-E3 unbiquitin complex to introduce their proteasomal degradation. Ubiquitin (Ub) is a small highly conserved regulatory protein that is expressed in most eukaryotic cells (140, 141). There are four ubiquitin genes in the human genome: *UBB*, *UBC*, *UBA52*, and *RPS27A* (141). Ubiquitination is thought to function as a "garbage disposal" for clearing away damaged proteins through an ATP-dependent reaction (142-146). Different types of poli-ubiquitination can induce protein degradation by the proteasome pathway, change protein enzyme activity or cellular localization, or inhibit the protein-protein interaction (144). Ubiquitination includes three main steps: activation, conjugation, and ligation and three kinds of enzymes are involved: ubiquitin-activating enzymes (known as E1s), ubiquitin-conjugating enzymes (known as E2s), and ubiquitin ligases (known as E3s). There is one major E1 enzyme, which is shared by all ubiquitin ligases. At the activation step, the E1 enzyme activates ubiquitin to form the Ub-S-E1 complex in the presence of ATP. The next step is conjugation: the E2 enzyme replaces the E1 enzyme and interacts with the activated ubiquitin. The last step is ligation: the E2 enzyme transfers the ubiquitin to the E3 enzyme, and then the E3 enzyme induces the ubiquitin to specific substrate proteins (147, 148). In humans and cats, there are four E3 ubiquitin ligase families: HECT, RING-finger, U-box, and PHD-finger (149) (Fig. 1.8). The RING-finger family is the largest. Normally, it is called the cullin-RING ubiquitin ligases (CRLs). CRLs include four members: cullins, RINGs, adaptor proteins, and substrate recognition receptors.

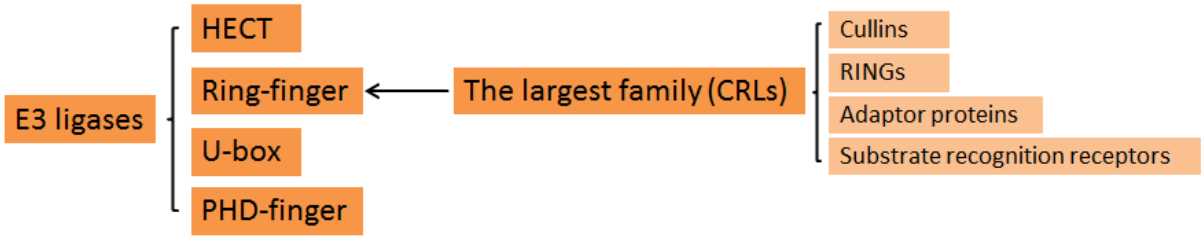

Fig. 1.8 Membership of E3 ubiquitin ligase. E3 ubiquitin ligase is classified into four families: HECT, RING-finger, U-box, and PHD-finger. The RING-finger E3 ligase is the largest family and named as Cullin-RING ubiquitin ligases (CRLs). Generally, CRLs consists of four components: cullins, RINGs, adaptor proteins and substrate recognition receptors.

Cullin (CUL) family proteins appear to be expressed in all eukaryotes and function as a scaffold for contact with the RING proteins to form the CRLs. There are eight cullin genes in the human genome: *CUL1, CUL2, CUL3, CUL4A, CUL4B, CUL7,* and *CUL9* (also called *PARC*) (150). All CUL members combine with different RING proteins, different adaptor proteins, and different substrate recognition receptors (Fig. 1.9). CUL5 can be found in many cells and organs, such as endothelial cells, kidney collecting tubule cells, vascular endothelial cells, and the brain (151-154). CUL5 binds the RING-box2 protein to form CRLs and in this CUL5-CRL complex, the adaptor proteins are Elongin B (ELOB) and Elongin C (ELOC) and the substrate recognition receptors are the SOCS-box containing proteins (150). Vif is an accessory protein for some lentiviruses and contains a SOCS-box domain. Vif acts as a substrate receptor for the CUL5 ubiquitin complex to induce proteasomal degradation of the APOBEC3 restriction factor (155-158).

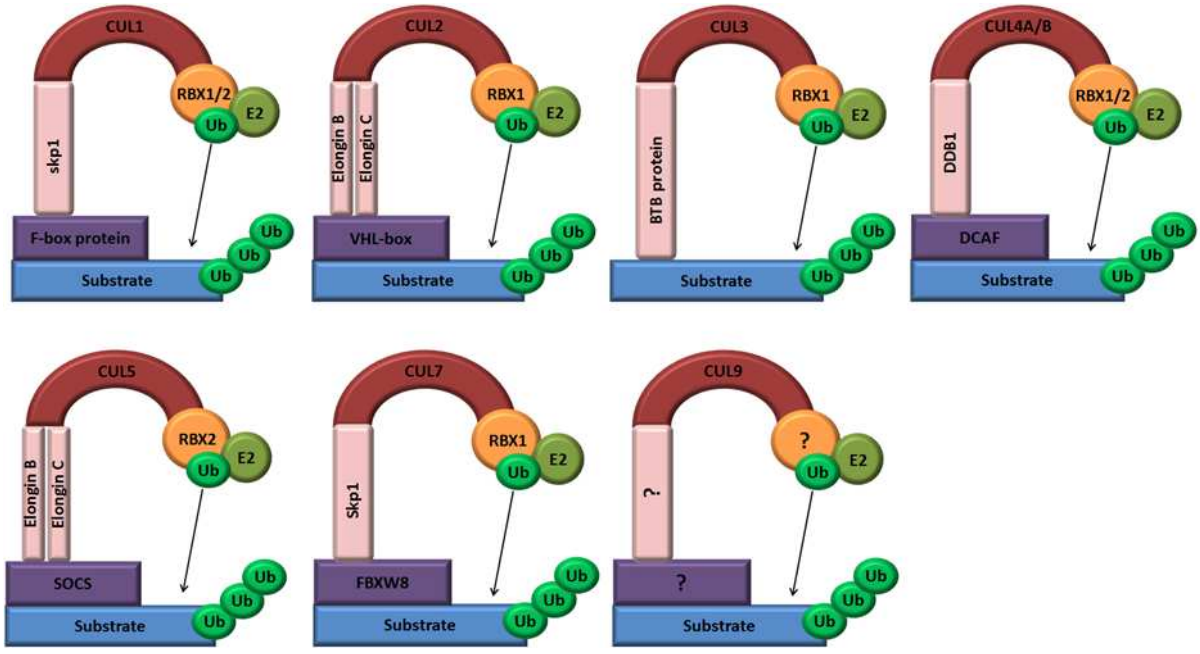

Fig. 1.9 Models of cullin-RING E3 ligases. CUL1 and CUL7 proteins recruit Skp1 as adaptor protein, CUL2 and CUL5 proteins recruit Elongin B/C as adaptor protein, CUL3 recruits BTB protein as adaptor protein, CUL4A and 4B recruit DDB1 as adaptor protein; Receptor proteins of CUL1, CUL2, CUL4A, CUL4B, CUL5, and CUL7 are F-box proteins, VHL-box proteins, DCAFs proteins, SOCS proteins, FBXW8 proteins, respectively; RING proteins (RBX1/2) interact with Cullins, which promotes ubiquitin transferring from RBX1/RBX2-

bound E2 to a substrates. The adaptor proteins, receptor proteins and RING proteins of CUL9 are unclear.

1.6 Feline APOBEC3 and FIV Vif

Human A3s include seven genes that contain either one (A3A, A3C, and A3H) or two (A3B, A3D, A3F, and A3G) zinc (Z)-binding domains with the conserved motifs of HXE(X)$_{23-28}$CXXC (X can be any residue) (159, 160). Similar to human A3-mediated restriction of HIV-1Δ*vif*, feline A3s are shown to inhibit FIVΔ*vif* (50, 52, 161-164). Moreover, natural polymorphisms of feline APOBEC3s correlate with the infection of FIV and FeLV in domestic cats (165). The domestic cat expresses three single domain of A3Z2s (A3Z2a - A3Z2c) and one A3Z3 protein as well as double domain A3Z2Z3 proteins by read-through transcription and mRNA alternative splicing (50, 161) (Fig. 1.10). Previous studies demonstrated that feline A3Z3 and A3Z2Z3, but not A3Z2s, inhibit FIVΔ*vif* (50, 161), while feline A3Z2s strongly restrict feline foamy virus (FFV) Δ*bet* and feline A3Z3 and A3Z2Z3 only slightly decrease FFV Δ*bet* infectivity (50, 166). In addition to feline retroviruses, feline A3s also show antiviral activity against HIV-1 (161, 163, 164, 167).

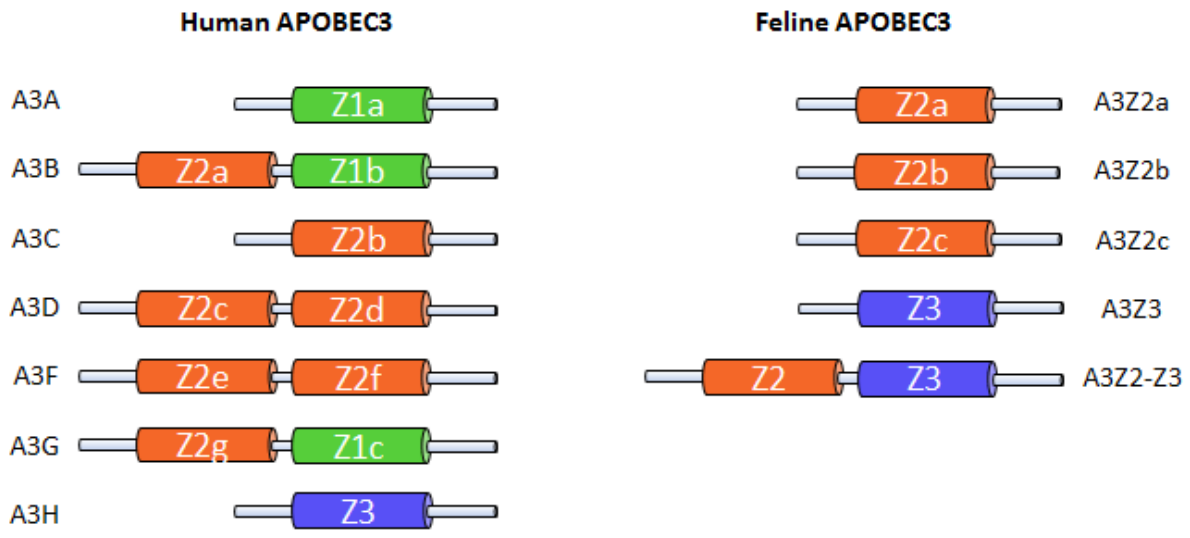

Fig. 1.10 Diagram of human APOBEC3 and feline APOBEC3. Human A3s include seven genes that contain either one (A3A, A3C, and A3H) or two (A3B, A3D, A3F, and A3G) zinc (Z)-binding domains. The domestic cat expresses three single domain of A3Z2s (A3Z2a - A3Z2c) and one

A3Z3 protein as well as double domain A3Z2Z3 proteins by read-through transcription and mRNA alternative splicing.

FIV Vif, similar to HIV-1 Vif, forms an E3 ubiquitin ligase complex, to induce feline A3 degradation (168) (Fig. 1.11). However, HIV-1 and SIV Vifs need the cofactor CBF-β to stabilize and form this complex (155, 169), whereas FIV and other non-primate lentiviruses (e.g. maedi-visna virus (MVV), caprine arthritis encephalitis virus (CAEV) and bovine immunodeficiency virus (BIV)) Vifs do not require CBF-β to induce A3s degradation (170-173). A recent study demonstrated that BIV Vif appears to operate independently of any cofactors, while MVV Vif hijacks cellular cyclophilin A (CYPA) as a cofactor to reconstitute the E3 ligase complex (170). Whether FIV Vif recruits any additional protein is unclear.

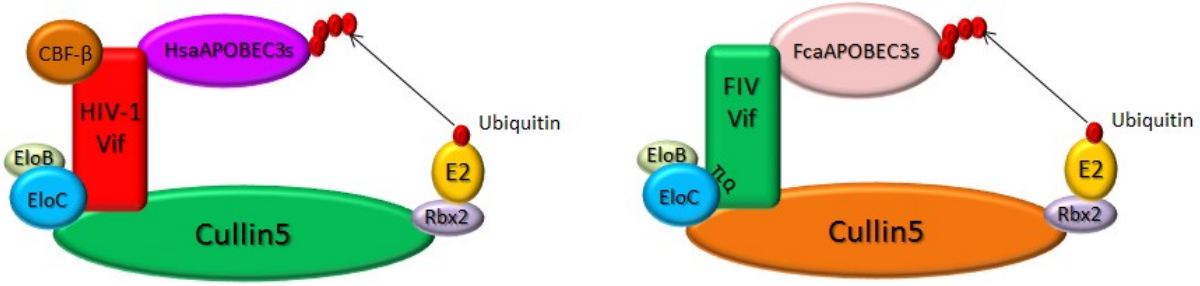

Fig. 1.11 Models of HIV-1/FIV Vif-E3 ligases. HIV-1 Vif forms Vif-E3 ligase together with Cullin 5, Elongin B/C, CBF-β, and RING box 2 proteins. FIV Vif forms Vif-E3 ligases together with Cullin 5, Elongin B/C, and RING box 2 proteins. Human A3s and feline A3s are the substrate for Vif-E3 ligases, respectively.

1.7 Molecular interaction of APOBEC3 with Vif

Human APOBEC3s, such as hA3G, hA3H hapII and hA3F, share a conserved Zinc-coordination motif, but HIV-1 Vif targets different sites in these A3 proteins for degradation. For example, the ^{128}DPDY^{131} motif in hA3G is involved in direct interaction with the ^{14}YRHHY^{17} domain of HIV-1 Vif (126, 174). The E121 residue in hA3H hapII determines its sensitivity to HIV-1 Vif derived from NL4-3 strain (175, 176). The hA3C and the C-terminal domain (CTD) of hA3F are conserved homologous Z2-typed A3s (159, 160), and 10 equivalent residues in these Z2-

typed A3s are identified as involving in HIV-1 Vif interaction (177, 178). Additionally, A3F.E289 and HIV-1 Vif.R15 show a strong interaction by applying molecular docking (179). The equivalent residue E106 in A3C also determines A3-Vif binding (180). In contrast to this conserved A3-Vif interaction, it was also demonstrated that E324 in A3F is essential for HIV-1 Vif interaction, but the equivalent residue E141 in A3C is not, which suggests that the Vif interaction interface might differ between A3C and A3F (177, 181). In addition, previous studies have proved that these two glutamic acids vary in primate A3Fs, and therefore determined the distinct sensitivities of primate A3F to HIV-1 Vif (182-184) (Fig. 1.12).

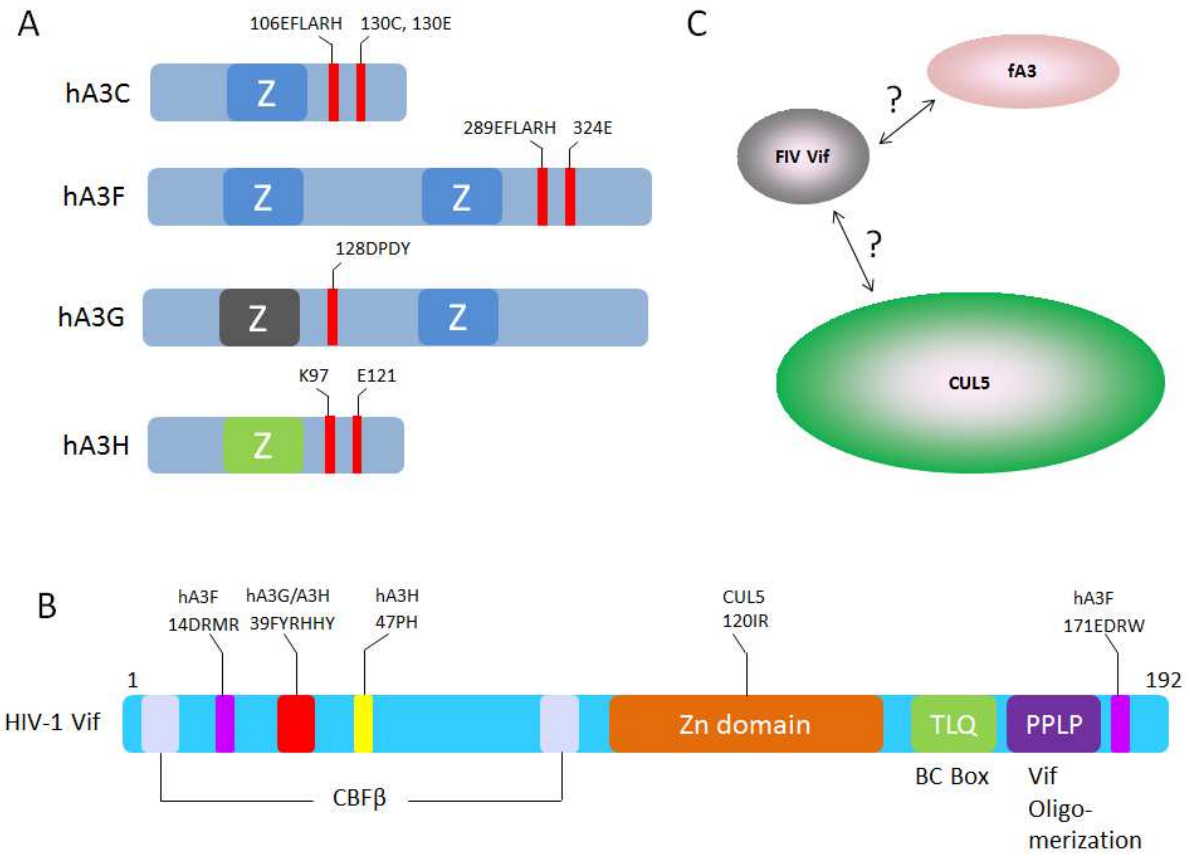

Fig. 1.12 Schematic representation of A3-Vif interaction sites. (A) It shows HIV-1 Vif binding sites in hA3C, hA3F, hA3G, and hA3H, respectively. (B) The hA3F, hA3G, hA3H, CUL5, CBF-β, and ElonginB/C binding sites in HIV-1 Vif are represented. (C) It is unclear how FIV Vif interacts with CUL5 and feline A3s.

The N-terminal part of HIV-1 Vif is mainly involved in interaction with human A3s. For example, the ^{40}YRHHY^{44} box is reported essential for A3G degradation, while the ^{14}DRMR^{17} motif determines A3F degradation (185). Vif derived from HIV-1 clone LAI, but not that of NL4-3, could induce the degradation of hA3H hapII, which is determined by residues F39 and H48 (186). The C-terminal of HIV-1 Vif consists of one Zinc coordination motif that interacts with CUL5, one SLQ BC box that binds to ELOB/C and one Vif dimerization domain (reviewed in (187)). Previously, it was also reported that the ^{171}EDRW^{175} motif in the C-terminus of Vif determines the degradation of A3F (181, 188). However, A3 interaction sites in SIV Vif have not yet been identified. Recently, it was reported that the ^{16}PXXME…PHXXV^{47} domain and G48 of HIV-2 Vif and SIVsmm Vif are involved in the interaction with A3F and A3G, respectively (189) (Fig. 1.12).

HIV-1 Vif cannot counteract the strong anti-HIV activity of feline A3Z2Z3, however binding of HIV-1 Vif and feline A3Z2Z3 was detectable by co-immunoprecipitation assays (162, 164). In contrast to HIV-1 Vif, Vifs from the HIV-2/SIV lineage counteract and induce degradation of feline A3Z2Z3 (162, 164). Residues in feline A3s that are functionally involved in the interaction with FIV Vif were identified by recent studies (162, 165, 190). In contrast, the determinants in FIV Vif important for inhibition of the antiviral activity of feline A3s are poorly understood (191), and which domain of FIV Vif interacts with cullin 5 is unclear (Fig. 1.12).

1.8 Objectives of current study

1. Identify the important domains of FIV Vif that interacts with feline APOBEC3s.

2. Identify the important domains of feline APOBEC3s that targeted by FIV Vif.

3. Find out the interaction surface between FIV Vif and CUL5.

4. Investigating how FIV escapes the restriction of feline SERINC.

2. Materials and Methods

2.1 Laboratory instruments

The following instruments were used in current study (Table 2.1).

Instruments	Company
Cell incubator BBD 6220	heraeus/ thermo scientific
Cell incubator KS4000-i	IKA
Centrifuge 4K15	Sigma
Centrifuge 5417R	Eppendorf
Centrifuge fresco 21	heraeus/ thermo scientific
Centrifuge PICO 21	heraeus/ thermo scientific
CO2 incubator	IBS
Film processor Curix 60	AGFA
Gel documentation system	Peqlab
Heating block	Bioblock scientific
Luminometer, Micro lumat plus	Berthold technologies
Microscope AE20	motic
Nano-drop NP-1000	Peqlab
OptimaTm MAX-XP ultracentrifuge	Beckmann coulter
PCR thermocycler T3	biometra
Photometer genesis 10Bio	thermo scientific
SDS-gelelectrophoresis apparatus	BioRad
Semi-dry blot apparatus	BioRad
Thermo shaker	biometra
Vortexer, top mix FB 15024	Fischer scientific

2.2 Chemicals

All chemicals in current study are listed in the following Table 2.2.

Chemicals	Company
Agar	applichem GmbH, Darmstadt
Agarose	Bio&Sell e.K, Nuernberg
Ampicillin	Sigma-aldrich, ST.Louis, USA
Casein peptone	Carl Roth GmbH, Karlsruhe
DMEM	GIBCO/BRL, Eggenstein
DMSO(Dimethylsulfoxid)	Merck, Darmstadt
Ethanol	Applichem GmbH, Darmstadt
Ethidiumbromide(EtBR)	Carl Roth GmbH, Karlsruhe
FBS	Biochrom KG, Berlin
Glycerin	Applichem GmbH, Darmstadt
Isopropanol	Carl Roth GmbH, Karlsruhe
Lipofectamine® LTX Reagent	Invitrogen Karlsruhe
L-glutamine	Biochrom KG, Berlin
Natriumchloride (NaCl)	Biomedicals, Heidelberg

Natriumhydroxide (NaOH)	Applichem GmbH, Darmstadt
Opti-MEM	Invitrogen, Karlsruhe
penicilllin	Biochrom KG, Berlin
Phosphate buffered saline (PBS) PAN	Biotech Gmbh, Aidenbach
6X sample buffer	Applichem GmbH, Darmstadt
Steady-glo® luciferase assay system	Promega GmbH, Mannheim
streptomycin	Biochrom KG, Berlin
Yeast extract	Carl Roth GmbH, Karlsruhe

2.3 Enzymes

All enzymes in current study are listed in the following table 2.3.

Enzymes	Company
DNA polymerases	fermentas
Restrictions endonucleasee (10U/ul)	Fermentas/biolabs
T4 DNA ligase (5U/ul)	fermentas

2.4 Kits

All kits in current study are listed in the following table 2.4.

Molecularbiology kits	Company
DNA T4 ligation kit	Fermentas, St. Leon-Rot
Plasmid miniprep TM-classic	Zymo research, Irvine, USA
Pure yieldTM plasmid maxiprep system	Promega GmbH, Mannheim
QIAquick®gel extraction kit	Qiagen GmbH, Hilden
QIAquick®PCR purification kit	Qiagen GmbH, Hilden

2.5 Buffers and solutions

2.5.1 Buffers for gel electrophoresis

20 x TAE buffer was used for gel electrophoresis and listed below (Table 2.5.1).

Compositions
0.8 M tris (hydroxymethyl)-aminomethan
0.8 M acetic acid
20mM EDTA
pH 8

2.5.2 6 x DNA loading dye

The 6 x DNA loading dye was used for DNA loading on agarose gels (Table 2.5.2).

Compositions	amounts
6X sample buffer	100µl
glycerine	150µl
add dH2O to final volume of 1250µl	

2.5.3 10 x SDS PAGE buffer (Table 2.5.3)

Compositions
25 mM tris
192 mM glycine
0.1% (v/v) SDS
pH 8.8

Table 2.5.3 The composition of 10 x SDS PAGE buffer.

2.5.4 20 x TBS

20 x TBS is basis for TBST (Table 2.5.4). Tween 20 was diluted in 1 x TBS buffer 0.2% (v/v). TBST was used for washing nitrocellulose membrane in western blotting.

Compositions
25 mM tris
150 mM NaCl
3 mM KCl
pH8

2.6 Bacterial strains (Competent cells)

The following bacterial strains belong to the genus *Escherichia coli* (E.coli) Table 2.6.

Name	Genotype
TopF 10	F-mcrA Δ(mrr-hsdRMS-mcrBC)Φ80lacZΔM15Δ lacX74 recA1 araD139Δ(araleu)7697 galU galK rpsL (StrR) endA1 nupG
Stab II	F-mcrAΔ(mcrBC-hsdRMS-mrr) recA1 endA1lon gyrA96 thi supE44 relA1 λ-Δ(lac-proAB)

2.7 Cells

Human embryonic kidney-HEK293T (293T, ATCC CRL-3216), human osteosarcoma-HOS (ATCC CRL-1543), feline kidney-CRFK (ATCC CCL-94) cell lines were maintained in Dulbecco's high-glucose modified Eagle's medium (DMEM, Biochrom, Berlin, Germany) supplemented with 10% fetal bovine serum (FBS), 2 mM L-glutamine, penicillin (100 U/ml), and streptomycin (100 µg/ml). CRFK-CD134 cell line was maintained in Dulbecco's high-glucose modified Eagle's medium (DMEM, Biochrom, Berlin, Germany) supplemented with 10% fetal bovine serum (FBS), 2 mM L-glutamine, penicillin (100 U/ml), streptomycin (100 µg/ml), and 800 µg/ml G418.

2.8 Vif and A3 plasmids.

Domestic cat A3s with a carboxy-terminal hemagglutinin (HA) tag were described previously (50, 161, 167). All the FcaA3s mutants were produced by fusion PCR (Primers are shown in Table 2.9 and 2.10). Human A3G with a C-terminal HA tag, a gift of Nathanial Landau, was previously described (131). FIV-34TF10 (codon-optimized), HIV-1, HIV-2, SIVmac and SIVsmm Vif genes were inserted into pcWPRE containing a C-terminal V5 tag (192). Codon-optimized Vif gene of FIV-34TF10 and Vif-TLQ-AAA were inserted into pcWPRE containing a C-terminal V5 tag (50, 162). All the FIV Vif mutants were produced by fusion PCR. FIV Vif-GST constructs were generated by inserting the full length FIV Vif or C-terminal truncated FIV Vif into pkGST (193) using HindIII and BamHI. The primers for all FIV Vif constructs are shown in Table 2.8. pcDNA3-DN-hCUL5-FLAG (15823) (194), pcDNA3-myc-CUL5 (19895) (195), pcDNA3-DN-hCUL2-FLAG (15819) (194), pcDNA3-myc3-CUL2 (19892) (195), T7-Elongin C-pcDNA3 (19998) (196) and HA-Elongin B-pcDNA3.1(+)-Zeo (20000) (197) were obtained from Addgene (Cambridge, USA). The CUL5 mutations were produced by fusion PCR and cloned into pcDNA3-myc-CUL5 by using *BamHI* and *XbaI* to replace wild type CUL5 (Table 2.11). Feline SERINC3/5 were cloned from CRFK cells by RT-PCR and then cloned into pcDNA3.1(+) or pBJ6 expression plasmid by using *EcoRI* and *NotI* (Table 2.12).

Name	Vector	Gene	Tag
pcDNA3.1 empty	pcDNA3.1 (+)	-	-

HIV-1 Vif	pcWPRE	HIV-1 Vif	V5
HIV-2 Vif	pcWPRE	HIV-2 Vif	V5
SIVagm Vif	pcWPRE	SIVagm Vif	V5
SIVmac Vif	pcWPRE	SIVmac Vif	V5
Feline A3Z2b	pcDNA3.1	Feline A3Z2b	HA
Feline A3Z3	pcDNA3.1	Feline A3Z3	HA
Feline A3Z2bZ3	pcDNA3.1	Feline A3Z2bZ3	HA
FIV Vif/mutants/T1-4	pcWPRE	FIV Vif /mutants/ N-terminal deletion constructs	V5
FIV Vif TLQ-AAA GST/ 50-160/110 mutants	pkGST	FIV Vif TLQ-AAA/ C-terminal deletion truncations/ 110 deletion mutants	GST
CUL5	pcDNA3-myc	Cullin 5	Myc3
CUL2	pcDNA3-myc	Cullin 2	Myc3
DN-CUL5	pcDNA3.1 (+)	Cullin 5 (dominant negative N441)	Flag
DN-CUL2	pcDNA3.1 (+)	Cullin 2 (dominant negative N427)	Flag
Elongin B	pcDNA3.1 (+)-Zeo	Elongin B	HA
Elongin C	pcDNA3	Elongin C	T7
Hu.SERINC5	pcDNA3.1 (+)	Human SERINC5	HA
Feline SERINC5	pcDNA3.1 (+)	Feline SERINC5	HA
Feline SERINC3	pcDNA3.1 (+)	Feline SERINC3	HA
pBJ6.Hu.SERINC5	pBJ6	Human SERINC5	HA
pBJ6.Feline SERINC5	pBJ6	Feline SERINC5	HA
pBJ6.Feline SERINC3	pBJ6	Feline SERINC3	HA
pMD.G (VSVG)	pMD.G	Envelope glycoprotein gene of vesicular stomatitis virus	-
pFP93	Helper construct CMV promoter	Gag, Pol, and Rev.	-
pLinSin	pGinSin	FIV Luciferase transfer vector Self inactivating	-
pEE14	vPGK	FIV Env 14	-

pPR	unknown	Full length virus FIV-PPR	-
C36	unknown	Full length virus FIV-C36	-

Table 2.7 Plasmids used in this study.

Primer name	Sequence (5' to 3')
FIVVif-EcoRI-F	atGAATTCGCCACCATGAGCGAAGAGGACTG
FIVVIF-V5NotI-R	atGCGGCCGCTCAGGTGCTGTCCAGGCC
FIVVifEcoRI24F	atGAATTCGCCACCatgctgtacatcagccgg
FIVVifEcoRI49F	atGAATTCGCCACCatggagaccggcttcatc
FIVVif-EcoRI73F	atGAATTCGCCACCatgatcggctacgtgcgg
FIVVifEcoRI103F	atGAATTCGCCACCatgcagtacagacccggc
FIVVifEcoRI144F	atGAATTCGCCACCatgccaggctggggccctg
FIVVifEEAAEcorI-F	atGAATTCGCCACCatgagcgcagcggactggcag
FIVVifQVAAEcorI-F	atGAATTCGCCACCatgagcgaagaggactgggcggcgtccag
FIVVifSRAAEcorI-F	atGAATTCGCCACCatgagcgaagaggactggcaggtggccgcgcggc
FIVVifLFAAEcorI-F	atGAATTCGCCACCatgagcgaagaggactggcaggtgtccaggcgggcggccgccgtgc
FIVVifGGAA-F	gtgctgcaggccgccgtgaacagcgcc
FIVVifGGAA-R	ggcgctgttcacggcggcctgcagcac
FIVVifYIAA-F	gcgccatgctggccgccagccggctgccc
FIVVifYIAA-R	gggcagccggctggcggccagcatggcgc
FIVVifERAA-F	cccccgacgcggcggagaagtacaagaagg
FIVVifERAA-R	ccttcttgtacttctccgccgcgtcggggg
FIVVifKDAA-F	gaagtacaaggcggccttcaagaagaggctg
FIVVifKDAA-R	cagcctcttcttgaaggccgccttgtacttc
FIVVifKKAA-F	caagaaggacttcgcggcgaggctgttcgac
FIVVifKKAA-R	gtcgaacagcctcgccgcgaagtccttcttg
FIVVifRLAA-F	gacttcaagaaggcggcgttcgacaccgag
FIVVifRLAA-R	ctcggtgtcgaacgccgccttcttgaagtc
FIVVif53FIAA-F	ccgagaccggcgccgccaagcggctgcgg
FIVVif53FIAA-R	ccgcagccgcttggcggcgccggtctcgg
FIVVif57LRAA-F	cttcatcaagcgggcggcgaaggccgaggg
FIVVif57LRAA-R	ccctcggccttcgccgcccgcttgatgaag
FIVVif61EGIAAA-F	ggctgcggaaggccgcggccgccaagtggagcttccacac
FIVVif61EGIAAA-R	gtgtggaagctccacttggcggccgcggccttccgcagcc
FIVVif65WSFAAA-F	gccgagggcatcaaggcggccgcccacacccgggactac
FIVVif65WSFAAA-R	gtagtcccgggtgtgggcggccgccttgatgccctcggc
FIVVif81VAGAAA-F	gcgggagatggcggccgccagcaccacc
FIVVif81VAGAAA-R	ggtggtgctggcggccgccatctcccgc
FIVVif95YIAA-F	gcggatgtacatcgccgccagcaaccccctgtgg
FIVVif95YIAA-R	ccacaggggttgctggcggcgatgtacatccgc
FIVVif119VNAA-F	gaatggcccttcgcggccatgtggatcaag
FIVVif119VNAA-R	cttgatccacatggccgcgaagggccattc

FIVVif126GFMAAA-F	gtggatcaagaccgccgctgcgtgggacgacatcgag
FIVVif126GFMAAA-R	ctcgatgtcgtcccacgcagcggcggtcttgatccac
FIVVif184CCSS-F	ccaagaagtggtccggcgactcctggaacc
FIVVif184CCSS-R	ggttccaggagtcgccggaccacttcttgg
Vif25L-A-F	gaacagcgccatggcgtacatcagcc
Vif25L-A-R	ggctgatgtacgccatggcgctgttc
Vif28SR-AA-F	ccatgctgtacatcgccgcgctgccccccg
Vif28SR-AA-R	cgggggggcagcgcggcgatgtacagcatgg
Vif30L-A-F	gtacatcagccgggcgcccccgacg
Vif30L-A-R	cgtcgggggggcgcccggctgatgtac
Vif47F-A-F	caagaagaggctggccgacaccgagac
Vif47F-A-R	gtctcggtgtcggccagcctcttcttg
Vif24M-A-F	gaacagcgccgcgctgtacatcagcc
Vif24M-A-R	ggctgatgtacagcgcggcgctgttc
Vif26Y-A-F	gaacagcgccatgctggccatcagccggc
Vif26Y-A-R	gccggctgatggccagcatggcgctgttc
Vif27I-A-F	gcgccatgctgtacgccagccggctg
Vif27I-A-R	cagccggctggcgtacagcatggcgc
FVif25L-S-F	gaacagcgccatgtcgtacatcagcc
FVif25L-S-R	ggctgatgtacgacatggcgctgttc
FVif25L-G-F	gaacagcgccatggggtacatcagcc
FVif25L-G-R	ggctgatgtaccccatggcgctgttc
FVif25L-V-F	gaacagcgccatggtgtacatcagcc
FVif25L-V-R	ggctgatgtacaccatggcgctgttc
FVif25L-I-F	gaacagcgccatgatttacatcagcc
FVif25L-I-R	ggctgatgtaaatcatggcgctgttc
FVif25L-F-F	gaacagcgccatgttttacatcagcc
FVif25L-F-R	ggctgatgtaaaacatggcgctgttc
FVif25L-Y-F	gaacagcgccatgtattacatcagcc
FVif25L-Y-R	ggctgatgtaatacatggcgctgttc
FVifHindIII-F	atAAGCTTGCCACCatgagcgaagaggactgg
FVifFullBamHI-R	atGGATCCcagctcgccgctccacag
FVif160BamHI-R	atGGATCCgctgaaggccttgatggc
FVif110BamHI-R	atGGATCCcttcaggccgggtctgtac
FVif80BamHI-R	atGGATCCcatctcccgcacgtagcc
FVif50BamHI-R	atGGATCCctcggtgtcgaacagcctc
FIV_vif PF	CTTCCTGAAGGGGATGAGTG
FIV_vif PR	ATCTCTTCCATTCATAGYTCTCC
Env_PR	CCTARTTCTTGCATAGCRAAAGC
A3H2F	TCATCCCCAATGGCACCCACAGC
A3H3R	TCAAACTCTGAGACGGAGGAGGAG
FIVVif.MI-AA-F	gaggccacccccgtggcggctatccggggcgag
FIVVif.MI-AA-R	ctcgccccggatagccgccacgggggtggcctc
FIVVif.IR-AA-F	cccccgtgatgattgccgcgggcgagatcgac
FIVVif.IR-AA-R	gtcgatctcgcccgcggcaatcatcacggggg

FIVVif.GE-AA-F	gattatccgggccgcgatcgaccccaag
FIVVif.GE-AA-R	cttggggtcgatcgcggcccggataatc
FVif.SLR-AAA-F	gcaccacctccctggccgcggcgatgtacatctac
FVif.SLR-AAA-R	gtagatgtacatcgccgcggccagggaggtggtgc
FVif.MY-AA-F	gagcctgcgggcggccatctacatcag
FVif.MY-AA-R	ctgatgtagatggccgcccgcaggctc
FVif.PLW-AAA-F	catcagcaacgccgcggcgcacagccag
FVif.PLW-AAA-R	ctggctgtgcgccgcggcgttgctgatg
FVif.YRP-AAA-F	gtggcacagccaggccgcagccggcctgaagaac
FVif.YRP-AAA-R	gttcttcaggccggctgcggcctggctgtgccac
Fvif.HTR-AAA-F	catcaagtggagcttcgccgccgcggactactacatc
Fvif.HTR-AAA-R	gatgtagtagtccgcggcggcgaagctccacttgatg
Fvif.DYY-AAA-F	cttccacacccgggccgccgccatcggctacgtg
Fvif.DYY-AAA-R	cacgtagccgatggcggcggcccgggtgtggaag
Fvif.IGY-AAA-F	cgggactactacgccgccgccgtgcgggagatgg
Fvif.IGY-AAA-R	ccatctcccgcacggcggcggcgtagtagtcccg
Fvif.VRE-AAA-F	catcggctacgcggcggcgatggtggccggcag
Fvif.VRE-AAA-R	ctgccggccaccatcgccgccgcgtagccgatg
Fvif.MWD-AAA-F	caagaccggctttgcggcggccgacatcgagaagc
Fvif.MWD-AAA-R	gcttctcgatgtcggccgccgcaaagccggtcttg
Fvif.IEK-AAA-F	ctttatgtgggacgacgccgcggcgcagaacatctg
Fvif.IEK-AAA-R	cagatgttctgcgccgcggcgtcgtcccacataaag
Fvif.I174-A-F	ccgtgatgattgcccggggcgagatc
Fvif.I174-A-R	gatctcgccccgggcaatcatcacgg
Fvif.R175-A-F	gtgatgattatcgcgggcgagatcgac
Fvif.R175-A-R	gtcgatctcgcccgcgataatcatcac
FIVVifK181A-F	cgagatcgaccccgcgaagtggtgcggcg
FIVVifK181A-R	cgccgcaccacttcgcggggtcgatctcg
FIVVifK182A-F	gatcgaccccaaggcgtggtgcggcgac
FIVVifK182A-R	gtcgccgcaccacgccttggggtcgatc
FIV Vif C138S-F	gaagcagaacatctccatcggcggcgag
FIV Vif C138S-R	ctcgccgccgatggagatgttctgcttc
FIV Vif C184S-F	cccaagaagtggtccggcgactgctggaac
FIV Vif C184S-R	gttccagcagtcgccggaccacttcttggg
FIV Vif C187S-F	gtggtgcggcgactcctggaacctgatg
FIV Vif C187S-R	catcaggttccaggagtcgccgcaccac
FIV Vif C192S-F	ctggaacctgatgtccctgcggaacagc
FIV Vif C192S-R	gctgttccgcagggacatcaggttccag
FIV VifC161S-F	ggccttcagctccggcgagcgg
FIV VifC161S-R	ccgctcgccggagctgaaggcc
FIV VifC209S-F	catgctggcctccggcgtgcc
FIV VifC209S-R	ggcacgccggaggccagcatg

Table 2.8 Primers used for introducing FIV Vif mutations.

Primer name	Sequence (5' to 3')
FcaZ3KL-TP.fw	gctaccagctgacgccgcccgaaggcacc
FcaZ3KL-TP.rv	ggtgccttcgggcggcgtcagctggtagc
FcaZ3PE-QN.fw	ccagctgaagctgcagaatggcaccctaattc
FcaZ3PE-QN.rv	gaattagggtgccattctgcagcttcagctgg
FcaZ3LI-TP.fw	gcccgaaggcaccacacctcacaaagactgcc
FcaZ3LI-TP.rv	ggcagtctttgtgaggtgtggtgccttcgggc
FcaZ3H-T.fw	cgaaggcaccctaattaccaaagactgcc
FcaZ3H-T.rv	ggcagtctttggtaattagggtgccttcg
FcaZ3DC-AA.fw	ctaattcacaaagccgcccttcgaaataag
FcaZ3DC-AA.rv	cttatttcgaagggcggctttgtgaattag
FcaZ3LR-AA.fw	cacaaagactgcgctgcaaataagaaaaag
FcaZ3LR-AA.rv	ctttttcttatttgcagcgcagtctttgtg
FcaZ3LI-AA.fw	gcccgaaggcaccgcagctcacaaagactgcc
FcaZ3LI-AA-rv	ggcagtctttgtgagctgcggtgccttcgggc
FcaZ3.fw	atgaattcgccaccatgaatccactacaggaag
HA-rv	agctcgagtcaagcgtaatctggaacatcgtatggataagcgtaatctggaacatcgtatg

Table 2.9 Primers used for introducing FcaA3Z3 mutations.

Primer name	Sequence (5' to 3')
FcaZ2bN18K.fw	gatagatcctaagaccttccgtttc
FcaZ2bN18K.rv	gaaacggaaggtcttaggatctatc
FcaZ2bT44R.fw	cttccaagtggagagagaagactacttc
FcaZ2bT44R.rv	gaagtagtcttctctctccacttggaag
FcaZ2bD165Y.fw	caactttgtgtaccacaagggaatgc
FcaZ2bD165Y.rv	gcattcccttgtggtacacaaagttg
FcaZ2bH166N.fw	caactttgtggacaacaagggaatgc
FcaZ2bH166N.rv	gcattcccttgttgtccacaaagttg
FcaZ2bDH-YN.fw	caactttgtgtacaacaagggaatgc
FcaZ2bDH-YN.rv	gcattcccttgttgtacacaaagttg
PtiY165D.fw	caactttgtggaccacaagggaatgc
PtiY165D.rv	gcattcccttgtggtccacaaagttg
FcaZ2bfeApo3.fw	tataagctttgaagaggaatggagccctggcgccccag
FcaZ2bHA-rv	agctcgagtcaagcgtaatctggaacatcgtatggataagcgtaatctggaacatcgtatg

Table 2.10 Primers used for introducing FcaA3Z2b mutations.

Primer name	Sequence (5' to 3')
CUL5-BamHI-F	atggatcccggcgacgtctaatctgttaaag
CUL5-XbaI-R	attctagatcatgccatatatatgaaagtgttg
CUL5_52LW-AA-F	gtgcatgcagtctgtgctgcggatgataaaggc
CUL5_52LW-AA-R	gcctttatcatccgcagcacagactgcatgcac
CUL5_54DD-AA-F	cagtctgtctttgggctgctaaaggcccagc

CUL5_54DD-AA-R	gctgggcctttagcagcccaaagacagactg

Table 2.11 Primers used for introducing CUL5 mutations.

Primer name	Sequence (5' to 3')
Hu+Fe SERINC5-F	atgtcagctcagtgctgtgcgg
Hu SERINC5-R	tcacacagagaactcccgg
Fe SERINC5-R	tcacacggagaactgccgag
Hu+Fe SERINC3-F	atgggggctgtgctgggtgtc
Hu SERINC3-R	tcagctgaagtcccgactgg
Fe SERINC3-R	tcagctgaagtcacgattgg
Hu+Fe SERINC5HindIII-F	ATAAGCTTGCCACCatgtcagctcagtgctgtgcgg
Hu SERINC5 XhoI-R	ATCTCGAGctaagcgtaatctggaacatcgtatggataCACAGAGAACTCCCGGGTG
Fe SERINC5 XhoI-R	ATCTCGAGctaagcgtaatctggaacatcgtatggatacacggagaactgccgagag
Hu+Fe SERINC3HindIII-F	ATAAGCTTGCCACCatgggggctgtgctgggtgtc
Hu SERINC3 XhoI-R	ATCTCGAGctaagcgtaatctggaacatcgtatggatagctgaagtcccgactgg
Fe SERINC3 XhoI-R	ATCTCGAGctaagcgtaatctggaacatcgtatggatagctgaagtcacgattgg
Hu+Fe SERINC5NotI-F	ATGCGGCCGCatgtcagctcagtgctgtgcgg
Hu SERINC5 EcoRI-R	ATGAATTCctaagcgtaatctggaacatcgtatggataCACAGAGAACTCCCGGGTG
Fe SERINC5 EcoRI -R	ATGAATTCctaagcgtaatctggaacatcgtatggatacacggagaactgccgagag
Hu+Fe SERINC3NotI-F	ATGCGGCCGCatgggggctgtgctgggtgtc
Hu SERINC3 EcoRI -R	ATCTCGAGctaagcgtaatctggaacatcgtatggatagctgaagtcccgactgg
Fe SERINC3 EcoRI -R	ATCTCGAGctaagcgtaatctggaacatcgtatggatagctgaagtcacgattgg

Table 2.12 Primers used for cloning human and feline SERINC genes.

2.9 Fusion PCR

In current study, I used fusion PCR to introduce point mutation in FIV Vif and FcaA3s expression plasmids. The fusion PCR step, reaction mixture and program are shown below (Fig. 2.1).

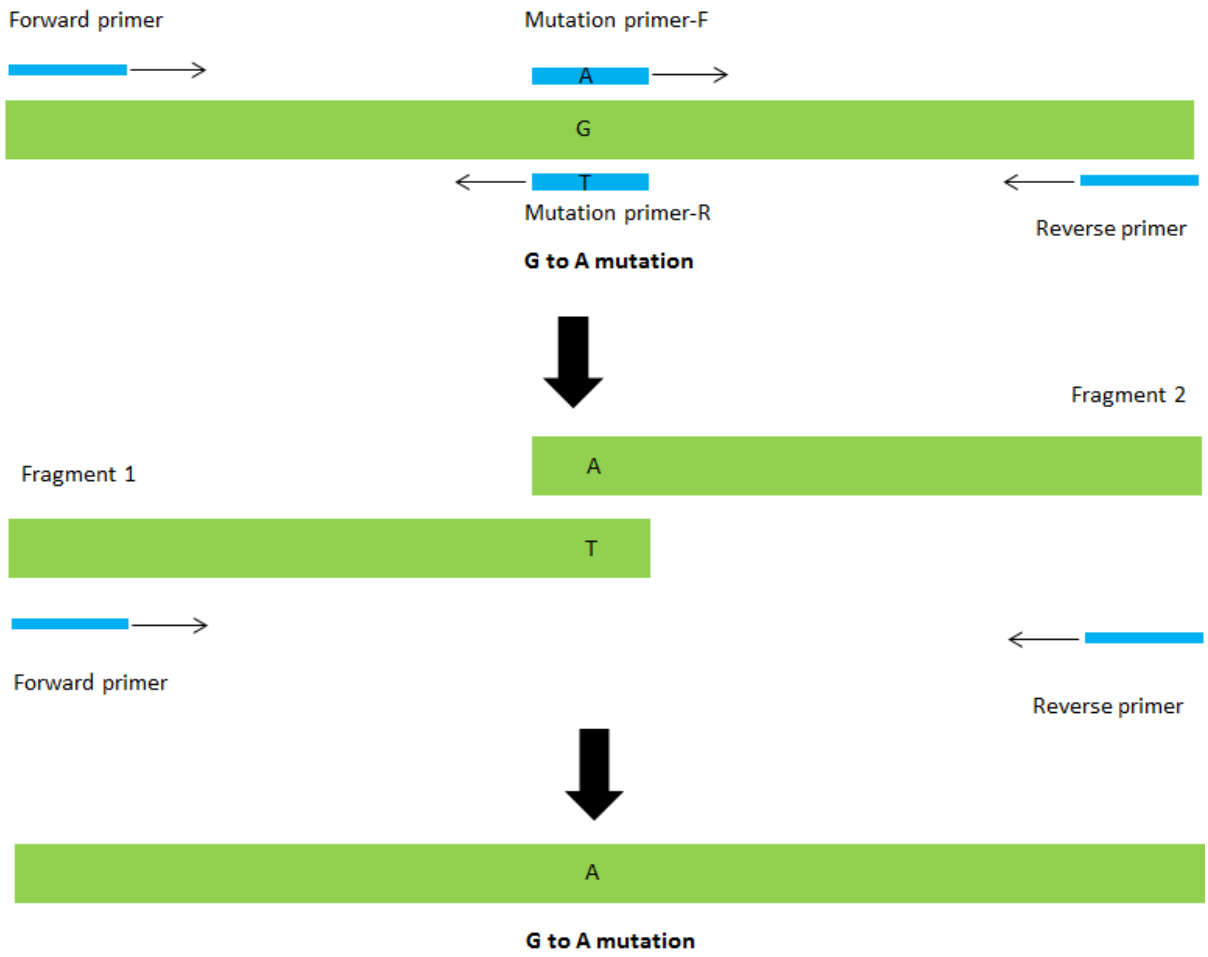

Fig. 2.1 **Steps of Fusion PCR.** Fusion PCR requires two steps of amplification. The primers of the first PCR are forward primer together with reverse mutation primer or forward mutation primer with reverse primer. After first round amplification, two PCR fragments are produced. Fragment 1 and fragment 2 from first round PCR are used as templates for PCR amplification with forward primer and reverse primer.

Step	Temperature (℃)	Time	
Initial denaturation	95	1-3 min	
denaturation	95	30 s	
Primer-annealing	X	30 s	30 cycles
elongation	72	2 min/kb	
Final elongation	72	5-15 min	
cooling	4	rest	

Table 2.13 The PCR program.

DNA template	20-50 ng
10X restriction buffer+MgSO4	5 µl
Upstream primer	5-50 pM
Downstream primer	5-50 pM
DNA polymerase (2.5 U/ul)	1 µl
dNTP mix (10 mM each)	1 µl
Nuclease-free water to final volume of 50ul	

Table 2.14 The composition of PCR mixture.

2.10 Transfection

A3 degradation experiments were performed in 24-well plates, 1×10^5 293T cells were transfected with 50 ng feline A3Z2 or 250 ng feline A3Z3 or A3Z2Z3 expression plasmids together with 30 ng codon-optimized FIV Vif expression plasmid, pcDNA3.1(+) (Thermo Fisher Scientific, Schwerte, Germany) was used as control. To produce FIV-luciferase viruses, 293T cells were co-transfected with 0.6 µg FIV packaging construct, 0.6 µg FIV-luciferase vector, 0.6 µg A3 expression plasmid, 0.2 µg VSV-G expression plasmid, 80 ng FIV Vif expression plasmid; in some experiments pcDNA3.1(+) was used instead of Vif or A3 expression plasmids. At 48 h post transfection, cells and supernatants were collected. The FcaA3Z2bZ3 degradation experiments were performed in 12-well plates, 2×10^5 293T cells were transfected with 300 ng feline A3Z2b or feline A3Z3 or A3Z2bZ3 expression plasmids together with 60 ng codon-optimized FIV Vif expression plasmid, pcDNA3.1(+) was used as control, and 700 ng pcDNA3-DN-hCUL5-FLAG or pcDNA3-DN-hCUL2-FLAG expression plasmids, pcDNA3.1(+) was used as control. The test of interaction between CUL5 and FIV Vif, 293T cells were co-transfected with 1000 ng pcDNA3-myc-CUL5 and 1000 ng FIV Vif-V5 or FIV Vif mutants in 6-well plates; pcDNA3.1(+) was used as control. For the interaction between ELOB, ELOC and FIV Vif, 293T cells were co-transfected with 700 ng T7-Elongin C-pcDNA3, 700 ng HA-Elongin B-pcDNA3.1(+)-Zeo and 700 ng FIV Vif-V5 or FIV Vif mutants in 6-well plates; pcDNA3.1(+) was used as control. For transfections in the presence of MG132 (474790, Calbiochem) and TPEN (16858-02-9, Calbiochem), the culture medium was replaced with fresh DMEM containing different concentrations of MG132 or TPEN, or dimethyl sulfoxide (DMSO). After the cells were treated for 16 h, the cell lysates were used for immunoprecipitation or immunoblotting as described below. All the transfections were

performed by using Lipofectamine LTX (Thermo Fisher Scientific) according to manufacturer's instruction.

2.11 Viruses and infection

To produce FIV single-cycle luciferase viruses (FIV-Luc), 293T cells were co-transfected with the replication deficient packaging construct pFP93 (198), a gift from Eric M. Poeschla, which only expresses *gag*, *pol*, and *rev*; the FIV luciferase vector pLinSin (50); a VSV-G expression plasmid pMD.G; FcaA3s expression plasmids; FIV Vif expression plasmid; or empty vector pcDNA3.1(+) (Fig. 2.2). To produce FIV Env pseudotyped FIV-Luc, 293T cells were co-transfected with the replication deficient packaging construct pFP93, the FIV luciferase vector pLinSin, FIV Env expression plasmid pEE14, FcaSERINC expression plasmids, or empty vector pcDNA3.1(+) (Fig. 2.3). The reverse transcriptase (RT) activity of FIV was quantified by using the Cavidi HS lenti RT kit (Cavidi Tech, Uppsala, Sweden). For reporter virus infection, 293T or CRFK-CD134 cells were seeded in 96-well plate one day before transduction. After normalizing for RT activity, the same amounts of viruses based on RT values were used for infection. Two days post transduction, firefly luciferase activity was measured with the Steadylite HTS reporter gene assay system (Perkin-Elmer, Cologne, Germany) according to the manufacturer's instructions on a MicroLumat Plus luminometer (Berthold Detection Systems, Pforzheim, Germany). Each transduction was done in triplicates; the error bar of each triplicate was shown.

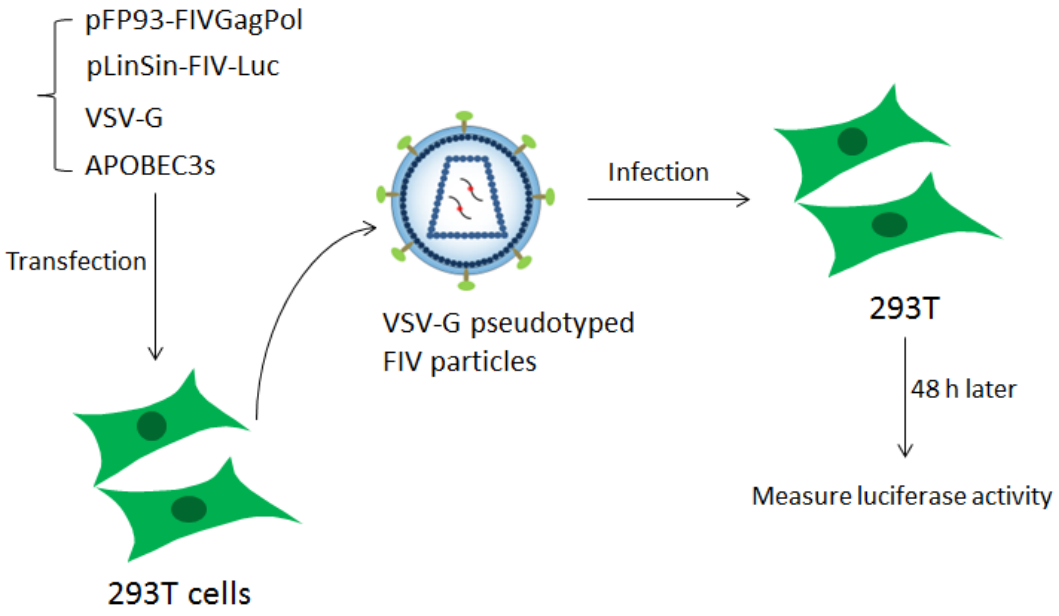

Fig. 2.2 **Schematic representation of VSV-G pseudotyped FIV single round infection assay.** Feline A3s expression plasmids together with FIV-based 3 plasmids system are cotransfected into 293T cells. 48 hours later, viral supernatant are collected, which contains VSV-G pseudotyped FIV particles. The supernatant are used for 293T cells infection. 48 hours later, viral infectivity is determined by detecting the luciferase activity.

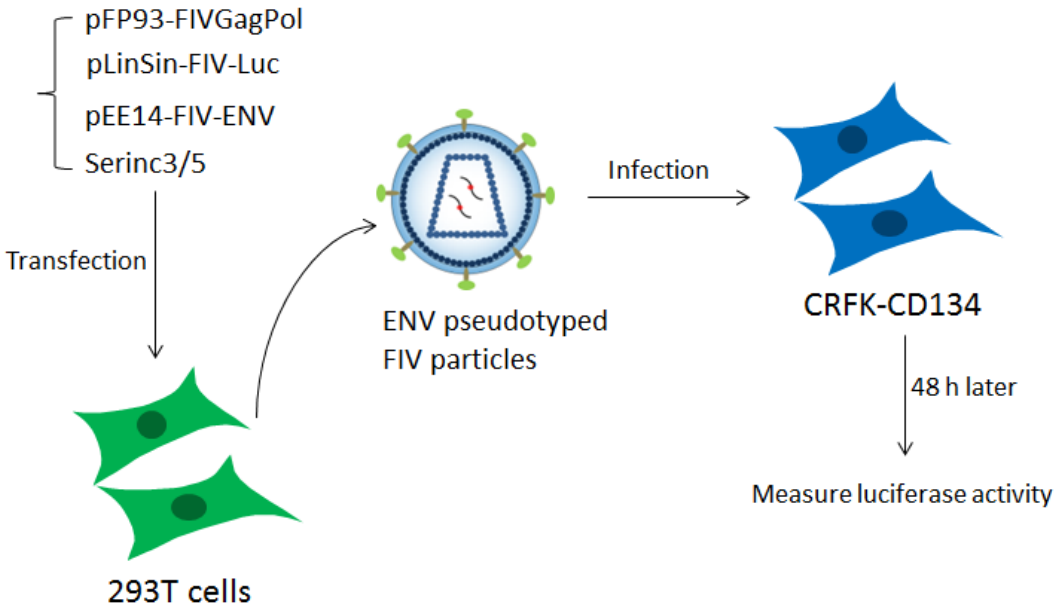

Fig. 2.3 **Schematic representation of Env pseudotyped FIV single round infection assay.** Feline SERINC3/5 expression plasmids together with FIV-based 3 plasmids system are cotransfected into 293T cells. 48 hours later, viral supernatant are collected, which contains

VSV-G pseudotyped FIV particles. The supernatant are used for CRFK-CD134 infection. 48 hours later, viral infectivity is determined by detecting the luciferase activity.

2.12 Immunoblot analysis

Transfected 293T cells were lysed in radioimmunoprecipitation assay (RIPA) buffer (25 mM Tris-HCl [pH7.6], 150 mM NaCl, 1% NP-40, 1% sodium deoxycholate, 0.1% sodium dodecyl sulfate [SDS], protease inhibitor cocktail set III [Calbiochem, Darmstadt, Germany]). The expression of A3s and Vif were detected by mouse anti-hemagglutinin (anti-HA) antibody (1:7,500 dilution, MMS-101P; Covance, Münster, Germany) and mouse anti-V5 antibody (1:4,500 dilution, MCA1360, ABDserotec, Düsseldorf, Germany) separately, tubulin was detected using mouse anti-α-tubulin antibody (1:4,000, dilution, clone B5-1-2; Sigma-Aldrich, Taufkirchen, Germany), followed by horseradish peroxidase-conjugated rabbit anti-mouse antibody (α-mouse-IgG-HRP; GE Healthcare, Munich, Germany), and developed with ECL chemiluminescence reagents (GE Healthcare). For test of encapsidation of FcaA3 proteins into FIV particles, HEK293T cells were transfected with 600 ng pFP93, 600 ng of pLinSin, 200 ng pMD.G, 600 ng of A3 constructs, and 80 ng FIV Vif or empty vector pcDNA3.1(+). Viral supernatants were collected 48 h later, overlaid on 20% sucrose and centrifuged for 4 h at 14,800 rpm in a table top centrifuge. Viral pellet was resuspended in RIPA buffer, boiled at 95^{o}C for 5 min with Roti load reducing loading buffer (Carl Roth, Karlsruhe, Germany) and resolved on a SDS-PAGE gel. The A3s and tubulin proteins were detected as described above. VSV-G and FIV p24 proteins were detected using mouse anti-VSV-G antibody (1: 10,000 dilution; clone P5D4; Sigma-Aldrich) and mouse anti-FIV p24 antibody (1: 2,000 dilution; clone PAK3-2C1; NIH AIDS REPOSITORY) separately, followed by horseradish peroxidase-conjugated rabbit anti-mouse antibody (α-mouse-IgG-HRP; GE Healthcare), and developed with ECL chemiluminescence reagents (GE Healthcare). The following antibodies were used for FIV-CUL5 study: mouse anti-T7-tag monoclonal antibody (1:1000 dilution, 69522, mouse monoclonal IgG2b, Merck, Germany), mouse anti-CUL-5 monoclonal antibody (1:1000 dilution, sc-373822, Santa Cruz, USA), mouse anti-myc monoclonal antibody (1:100 dilution, MCA2200, MbD Serotec, Canada), mouse anti-flag M2 monoclonal antibody (1:1000 dilution,

F1804, Sigma, USA). The second antibody was horseradish peroxidase-conjugated rabbit anti-mouse antibody (1:10,000 α-mouse-IgG-HRP; GE Healthcare, Munich, Germany).

Name	Number	Company	Host	Dilution
anti-HA	MMS-101P	Covance, Münster, Germany	mouse	1:7,500
anti-V5	MCA1360	ABDserotec, Düsseldorf, Germany	mouse	1:4,500
anti-α-tubulin	clone B5-1-2	Sigma-Aldrich, Taufkirchen, Germany	mouse	1:4,000
anti-VSV-G	P5D4	Sigma-Aldrich	mouse	1:10,000
anti-FIV p24	PAK3-2C1	NIH AIDS REPOSITORY	mouse	1: 2,000
anti-T7	69522	Merck, Germany	mouse	1:1000
anti-CUL-5	sc-373822	Santa Cruz, USA	mouse	1:1000
anti-myc	MCA2200	MbD Serotec, Canada	mouse	1:1000
anti-flag M2	F1804	Sigma, USA	mouse	1:1000

Table 2.15 The list of antibodies used in this study.

2.13 Immunofluorescence

HOS cells grown on polystyrene coverslips (Thermo Fisher Scientific) were transfected with expression plasmids for wild type FIV Vif or mutants using Lipofectamine LTX (Thermo Fisher Scientific). At day two post transfection, cells were fixed in 4% paraformaldehyde in PBS for 30 min, permeabilized in 0.1% Triton X-100 in PBS for 15 min, incubated in blocking buffer (10% FBS in PBS) for 1 h, and then cells were stained by mouse anti-V5 antibody in a 1:1,000 dilution in blocking solution for 1 h. Donkey anti-mouse Alexa Fluor 488 (Thermo Fisher Scientific) was used as a secondary antibody in a 1:300 dilution in blocking solution for 1 h. Finally, DAPI was used to stain nuclei for 2 min. The images were captured by using a 60 × objective on a Zeiss LSM 510 Meta laser scanning confocal microscope (Carl Zeiss, Cologne, Germany). The images were analyzed by ZEN 2.1 (blue edition) software (Carl Zeiss).

2.14 GST-pull down

To determine Vif and A3 binding, 293T cells were co-transfected with 1 µg FcaA3 and 1 µg FIV Vif constructs that expressed a C-terminal GST tag or pkGST empty vector. 48 h later, the cells were lysed in IP-lysis buffer (50 mM Tris/HCl pH 8, 1 mM PMSF, 10% Glycerol, 0.8% NP-40, 150 mM NaCl, and protease inhibitor cocktail set III (Calbiochem)). The lysates were cleared by centrifugation. The supernatants were incubated with 50 µl pre-equilibrated glutathione sepharose beads. After 2 h incubation at 4˚C in end-over-end rotation, the samples were washed 4 times with lysis buffer on ice. Bound proteins were eluted by boiling the beads for 5 min at 95°C in SDS loading buffer. FcaA3 was detected by immunoblot using anti-HA antibody. The GST or Vif-GST proteins were observed by coomassie brilliant blue staining.

2.15 Immunoprecipitation

293T cells were transfected with FIV Vif-V5 together with pcDNA3-myc-CUL5 or T7-Elongin C-pcDNA3, HA-Elongin B-pcDNA3.1(+)-Zeo or FcaA3Z2bZ3-HA expression plasmids. At 48h post-transfection, the cells were harvested and lysed in IP-lysis buffer (50 mM Tris/HCl pH 8, 10% Glycerol, 0.8% NP-40, 150 mM NaCl) with protease inhibitor cocktail set III (Calbiochem, Darmstadt, Germany) on ice for 20 min. Cell lysates were clarified by centrifugation at 10,000g for 30 min at 4°C. The supernatant were incubated with 15 µl rabbit anti-c-myc agarose affinity gel antibody beads (A7470, Sigma, USA) or 15 µl rat anti-HA affinity matrix beads (16598600, Roche, USA). After 2 h incubation at 4˚C in end-over-end rotation, the samples were washed 4 times with lysate buffer on ice. Bound proteins were eluted by boiling the beads for 5 min at 95°C in SDS loading buffer. The eluted materials were subsequently analyzed by immunoblotting. To detect the interaction of FIV Vif with endogenous CUL5, 5 x 10^5 293T cells in 6-well plates were transfected with wild type FIV Vif or indicated mutant expression plasmids. The cells were harvested like above, and 500 µl cell lysis were incubated with 2 µg mouse anti-V5 antibody (MCA1360, ABDserotec, Düsseldorf, Germany) and 20 µl protein A/G plus agarose (Santa Cruz, Heidelberg, Germany) for 4 h at 4°C in end-over-end rotation. The samples were washed 4 times after 4 h incubation, and bound proteins were analyzed by immunoblotting.

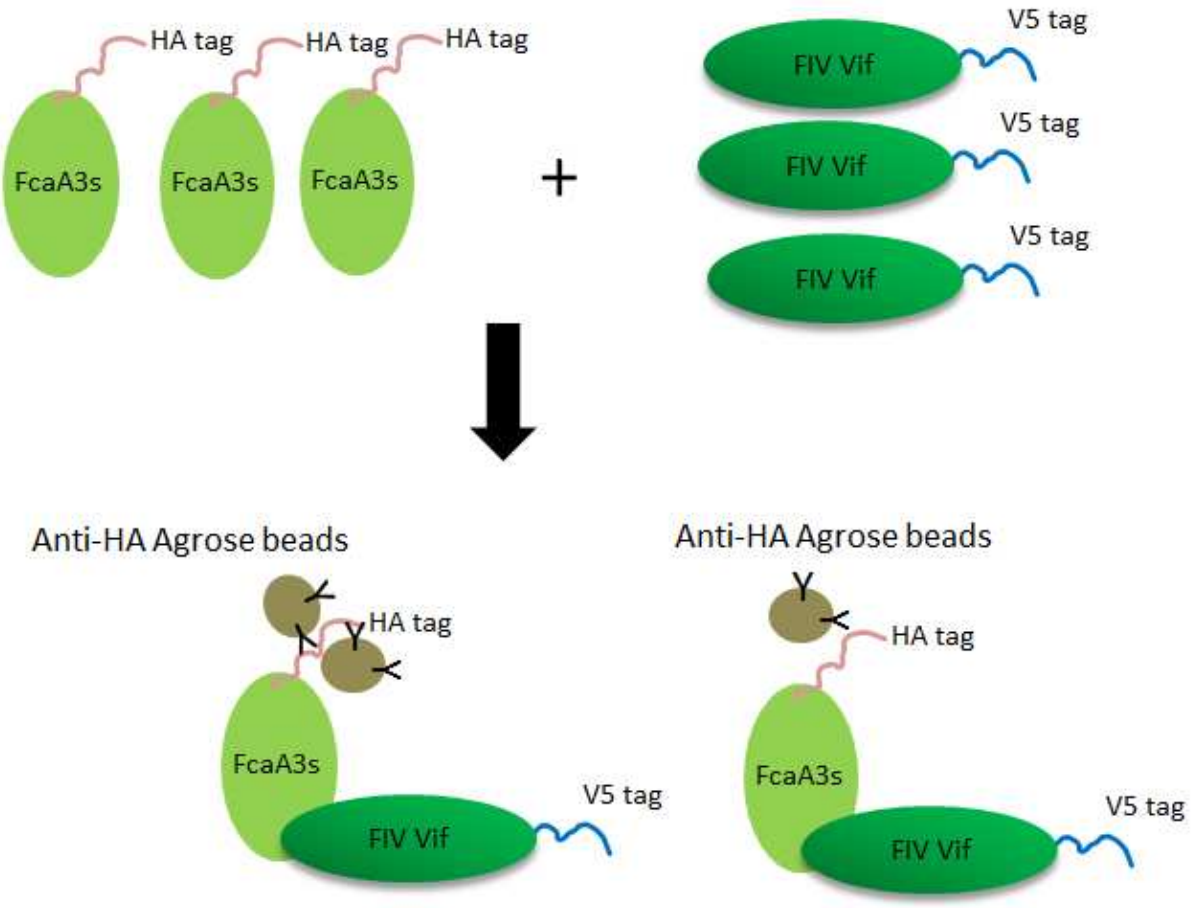

Fig. 2.4 **The Scheme of Co-IP for detecting FcaA3s-FIV Vif interaction.** Feline APOBEC3s (HA tag) and FIV Vif (V5 tag) expression plasmids are cotransfected into 293T cells. 48 hours later, 293T cells are harvested. Cell lysis is incubated with anti-HA agarose beads at 4°C for 2 hours. Then the interacted proteins are detected by western blotting.

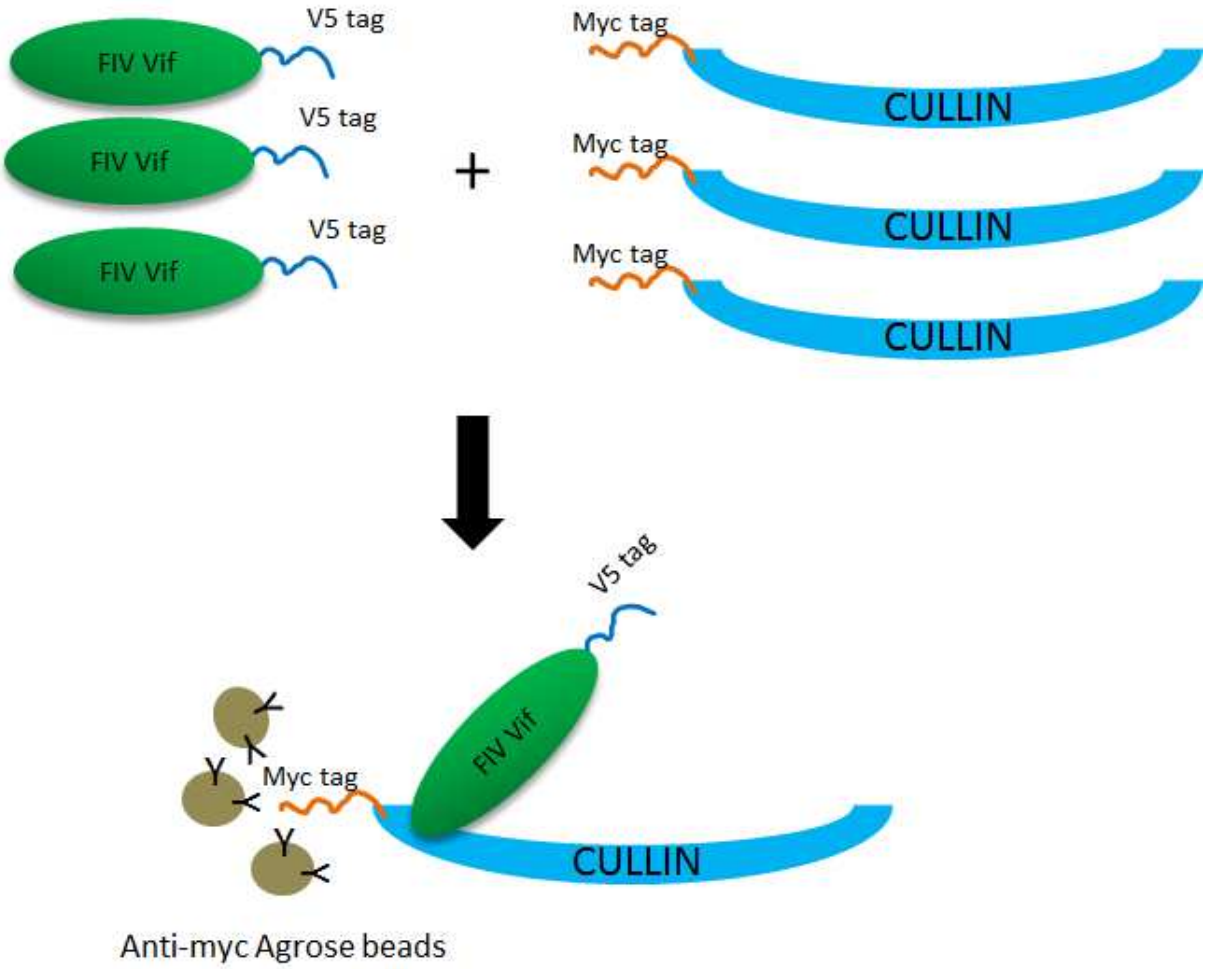

Fig. 2.5 **The Scheme of Co-IP for detecting Cullin-FIV Vif interaction.** Cullin (myc tag) and FIV Vif (V5 tag) expression plasmids are cotransfected into 293T cells. 48 hours later, 293T cells are harvested. Cell lysis is incubated with anti-myc agarose beads at 4°C for 2 hours. Then the interacted proteins are detected by western blotting.

2.16 *Vif* sequences from naturally infected cats

Fifteen samples of peripheral blood of domestic cats naturally infected with FIV were submitted to DNA extraction. DNA was extracted using buffer saturated phenol and submitted to three PCRs to detect proviral and genomic DNA. In order to amplify the *vif* genes, a semi-nested PCR was developed. In the first round of amplification the primers FIV_vif_PF and Env_PR were used to obtain a 3 kb amplicon using the Phusion High-Fidelity DNA Polymerase (New England Biolabs, Ipswich, USA). In the second round of amplification

the primers FIV_vif_PF and FIV_vif_PR were used and the PCR product was obtained with Taq DNA Polymerase (Thermo Fisher Scientific). The product was cloned into pCR2.1 vector using TOPO TA Cloning kit (Thermo Fisher Scientific) and submitted to sequencing. The A3Z3 haplotype of each sample was determined using a previously described protocol (165) using primers A3H2F and A3H3R, and named (see recent report (190)). Sequences were analysed with the Geneiuos software (Biomatters, Auckland, New Zealand). More information about A3Z3 haplotype and the corresponding FIV Vif sequence are shown in table 2. This part of work was performed by my project cooperators, Lucía Cano Ortiz and Ana Cláudia Franco from laboratory of Virology, Federal University of Rio Grande do Sul, Porto Alegre, Brazil.

2.17 Homology Modeling

We modeled the complex of FIV Vif and Cul5 based on the X-ray crystal structure of the HIV-1 Vif and Cul5 complex as a template (158). Owing to the low sequence identity between FIV and HIV-1 Vif, we performed the modeling in an iterative fashion. We used ClustalW2 (158) to align the sequences, using the (T/S)LQ-BC box and the conserved 174IR175 motif as anchor points to guide the alignment. Next, we modeled the complex employing Modeler v9.10 (199) and, subsequently, manually curated the sequence alignment based on the resulting models: Accounting for a possible zinc dependency of FIV Vif, cysteines in the FIV Vif sequence, which in the models were structurally close to zinc binding cysteine and histidine residues in HIV-1 Vif, were aligned to these zinc binding residues in the HIV-1 sequence (C113, C114, H108, and H139). Furthermore, we used information on the secondary structure of FIV Vif, predicted by PSIPRED (200) to guide the manual curation of the sequence alignment. The final model was then used to predict interacting residues. The model is accessible at the Protein Model Data Base (PMDB; https://bioinformatics.cineca.it/PMDB/main.php) with accession code: PM0081296. This part of work was performed by my project cooperators, Christoph G. W. Gertzen and Holger Gohlke from Institute of Pharmaceutical and Medicinal Chemistry, Heinrich Heine University Düsseldorf, Düsseldorf, Germany

2.18 Nucleotide sequence accession numbers

The GenBank accession numbers for FIV Vif are: FIV C36 (AY600517.1); FIV 34TF10 (M25381.1); FIV PRR (M36968.1); FIV TM-2 (M59418.1); FIV Shizuoka (LC079040.1); FIV Oma (AY713445); FIV Lion B (EU117991); FIV Lion E (EU117992); FIV puma A (U03982); FIV bobcat A (KF906143); FIV puma B.1 (DQ192583); FIV puma B.2 (KF906194); Vif_FIV_RS09 (KX668638); Vif_FIV_RS11 (KX668640); Vif_FIV_RS13 (KX668642); Vif_FIV_RS02 (KX668631); Vif_FIV_RS04 (KX668633); Vif_FIV_RS08 (KX668637); Vif_FIV_RS14 (KX668643); Vif_FIV_RS06 (KX668635); Vif_FIV_RS12 (KX668641); Vif_FIV_RS03 (KX668632); Vif_FIV_RS05 (KX668634); Vif_FIV_RS07 (KX668636); Vif_FIV_RS10 (KX668639); Vif_FIV_RS01 (KX668630); Vif_FIV_RS15 (KX668644). The feline APOBEC3 and human APOBEC3G GenBank accession numbers are: FcaA3Z2b (AY971954), FcaA3Z3 (EU109281), FcaA3Z2bZ3 (EU109281) and HsaA3G (NM_021822). Human SERINC5 (NM_178276.6); Chimpanzee SERINC5 (XM_016953076.1); African green monkey SERINC5 (XM_007976640.1); Rhesus Macaque SERINC5 (XM_015140335.1); Feline SERINC5 (XM_011284262.3); Equine SERINC5 (XM_001503874.4); Rabbit SERINC5 (XM_017344548.1); Mouse SERINC5 (NM_172588.2). Human SERINC3 (NM_006811.3); Chimpanzee SERINC3 (NM_001280388.1); African green monkey SERINC3 (XM_008016564.1); Rhesus Macaque SERINC3 (NM_001260972.1); Feline SERINC3 (XM_011280708.3); Equine SERINC3 (XM_001917430.4); Rabbit SERINC3 (XM_008274475.2); Mouse SERINC3 (NM_012032.4).

2.19 Statistical analysis

Data are represented as the mean with SD in all bar diagrams. Statistically significant differences between two groups were analyzed using the unpaired Student's t-test with GraphPad Prism version 5 (GraphPad software, San Diego, CA, USA). A p value ≤ 0.05 was considered statistically significant: P value < 0.001 extremely significant (***), 0.001 to 0.01 very significant (**), 0.01 to 0.05 significant (*), > 0.05 not significant (ns).

3. Results

3.1 Identification of FIV Vif domains responsible for feline A3 degradation

3.1.1 Identification of FIV Vif determinants specific for feline A3Z2 degradation.

Previous studies have described that feline A3 cytidine deaminases can act as restriction factors for FIV, which are counteracted by the FIV Vif protein (50, 52, 161, 164). However, the molecular interaction between FIV Vif and feline A3s is poorly understood. In order to identify determinants in the FIV Vif protein that are specific to the degradation of different feline A3 proteins, I used a FIV from domestic cats (*Felis catus*, Fca), hereafter referred to as FIV. First several FIV Vif constructs were generated that had N-terminal deletions. The amino acids 1-24, 1-49, 1-73, or 1-103 of FIV Vif were deleted, respectively, termed FIV Vif T1, FIV Vif T2, FIV Vif T3 and FIV Vif T4 (Fig. 3.1A). Co-transfection experiments of cat-derived A3s and FIV Vif expression plasmids were performed in 293T cells. All A3 constructs expressed the corresponding A3 protein with a C-terminal HA-tag, whereas Vif was expressed as a C-terminal V5-tag fusion protein (Materials and Methods 2.8). Immunoblots of protein extracts from cells co-expressing both A3 and Vif were used as readout for the degradation of the respective A3 protein (Materials and Methods 2.12). The results showed that wild type FIV Vif induced degradation of single-domain feline A3Z2b, A3Z3 and double-domain A3Z2bZ3 in agreement with previous reports (161, 162). FIV Vif T1 induced degradation of single-domain feline A3Z3 and double-domain A3Z2bZ3, but could not mediate the degradation of feline A3Z2b, which suggested the possibility that amino acids 1-24 of FIV Vif are specific for interaction with feline A3Z2b (Fig. 3.1B). FIV Vif T2 failed to deplete feline A3Z3 and A3Z2b, but moderately induced degradation of feline A3Z2bZ3 (Fig. 3.1B). All three feline A3 proteins showed resistance to FIV Vif T3 and T4 (Fig. 3.1B). Taken together, these results implied that amino acids 1-24 of FIV Vif are specific to feline A3Z2b degradation, while the feline A3Z3 interaction site may localize to residues 24-49 of FIV Vif.

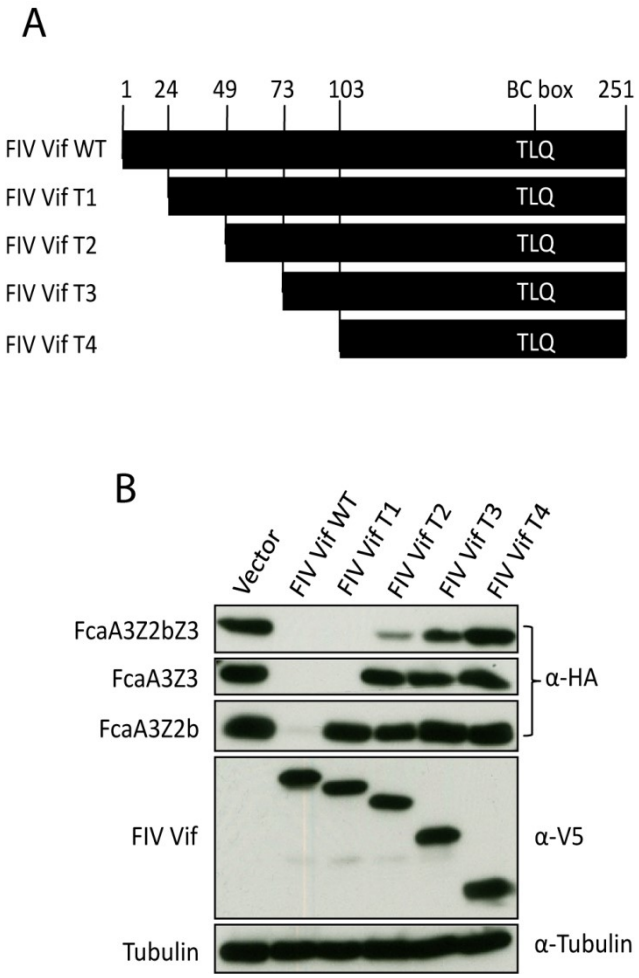

Fig. 3.1 The N-terminal region of FIV Vif determines specific A3 degradation. (A) Schematic structure of FIV Vif N-terminal deletion constructs (T1, T2, T3, T4). The C-terminal amino acids TLQ that interact with Elongin B and Elongin C (BC box) of the E3 complex are shown. The numbers represent the amino acids position in FIV Vif. (B) FIV Vif wild type, FIV Vif T1, FIV Vif T2, FIV Vif T3 or FIV Vif T4 were co-expressed with FcaA3Z2bZ3, FcaA3Z3 and FcaA3Z2b. A3s, FIV Vifs and tubulin proteins were detected by using anti-HA, anti-V5 and anti-tubulin antibodies, respectively.

A previous study demonstrated that FIV Vif from lions also counteracted feline A3s from the domestic cat (162). Thus, I analyzed sequences of domestic cat FIV Vif and lion FIV Vif, and identified conserved amino acids that localized at residues 1-24 of domestic cat FIV Vif as potential feline A3Z2b interaction sites (Fig. 3.2A). Next, these conserved residues were mutated in cat FIV Vif to alanines and tested for their degradation activity of feline A3Z2b

(Materials and Methods 2.9). Filippis *et al.* showed that mutations of a big residue into alanine or glycine rarely lead to major rearrangements in the direct 3-D environment (201). The results showed that alanine mutations in residues 3EE4, 7QV8 and 9SR10 did not alter the FIV Vif activity to degrade feline A3Z2b, whereas replacing 12LF13 and 18GG19 by alanines abolished FIV Vif mediated A3Z2b degradation (Fig. 3.2B). In addition, it was found that mutations in the 12LF13 and 18GG19 motifs had no influence on FIV Vif-induced degradation of feline A3Z3 and A3Z2bZ3 (Fig. 3.2C). These results demonstrated that residues of 12LF13 and 18GG19 of FIV Vif selectively determine degradation of feline A3Z2b.

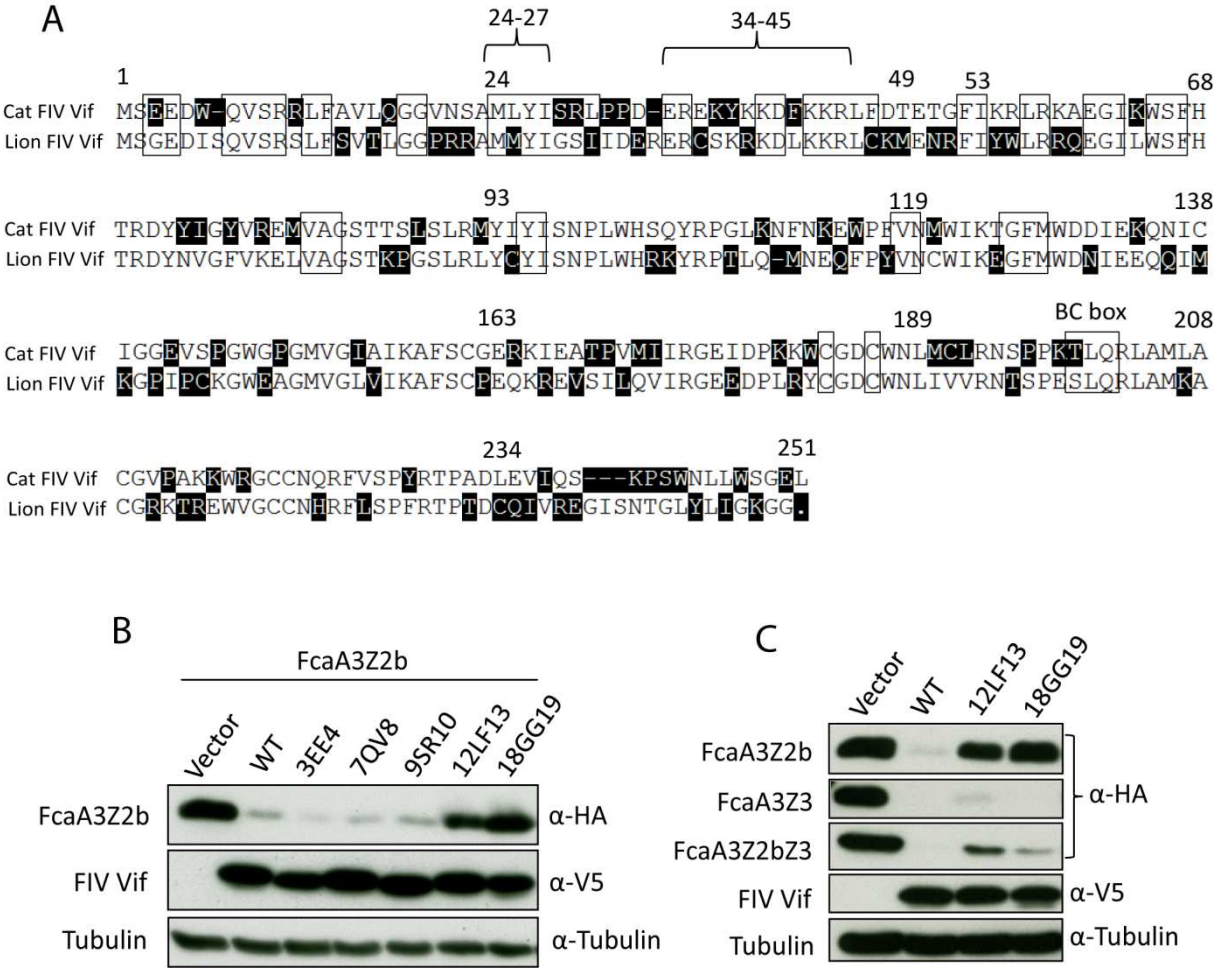

Fig. 3.2 Identification of determinants in FIV Vif important for degradation of feline A3Z2b. (A) Sequence alignment of domestic cat FIV and lion FIV Vif. The numbers represent amino acids position in domestic cat FIV Vif; the boxes represent the conserved regions between domestic FIV Vif and lion FIV Vif. The distinct amino acids between two Vif proteins are shown in black. Two extra regions of 24-27 and 34-45 are additionally indicated. (B) FcaA3Z2b was co-expressed with FIV Vif wild type or Vif alanine mutants of the indicated

residues. A3, FIV Vif and tubulin proteins were detected by using anti-HA, anti-V5 and anti-tubulin antibodies, respectively. (C) FcaA3Z2b, FcaA3Z3 or FcaA3Z2bZ3 were co-expressed with FIV Vif wild type and alanine Vif mutants of residues 12LF13 or 18GG19. A3, FIV Vif and tubulin proteins were detected by using anti-HA, anti-V5 and anti-tubulin antibodies, respectively.

3.1.2 Identification of feline A3Z3 interaction sites of FIV Vif.

Figure 3.1 suggested that the amino acids from 24 to 49 of FIV Vif interacted with feline A3Z3. To identify the specific feline A3Z3 interaction residues in this region, I analyzed the sequences of cat FIV Vif and lion FIV Vif. I found that residues 24-27 and 34-45 were conserved, while amino acids 27-34 of Vif were more variable (Fig. 3.2A). Then, I replaced the conserved residues (26YI27, 34ER35, 40KD41, 43KK44 and 45RL46) in cat FIV Vif by alanines (Materials and Methods 2.9; Fig. 3.3A). Additionally, I chose nine conserved motifs in the region between residues 53 and 184 for alanine mutations (53FI54, 57LR58, 61EGI63, 65WSF67, 81VAG83, 95YI96, 119VN120, 126GFM128 and 184C187C) (Materials and Methods 2.9; Fig. 3.3A). All FIV Vif mutants were co-expressed with either one of the three feline A3 proteins (A3Z2b, A3Z3 and A3Z2bZ3) and immunoblots were used to evaluate the expression of A3 proteins and FIV Vif mutants (Materials and Methods 2.10 and 2.12). The result showed that all FIV Vif mutants displayed similar expression levels (Fig. 3.3B). The alanine mutant of 26YI27 showed no degradation activity of any feline A3 protein, while FIV Vif mutants of 34ER35, 40KD41 and 43KK44 diminished feline A3Z2b, A3Z3 and A3Z2bZ3 levels as efficient as wild type FIV Vif (Fig. 3.3B). Alanine mutations introduced in position 45RL46 of FIV Vif had a minor influence on feline A3 degradation (Fig. 3.3B). Mutants of residues 53FI54, 57LR58, 61EGI63 and 65WSF67 slightly induced degradation of feline A3Z2b, not much of A3Z3, and triggered quite efficient degradation of feline A3Z2bZ3 (Fig. 3.3B). All three feline A3 proteins were mostly resistant to alanine mutants of Vif residues 81VAG83, 95YI96, 119VN120, 126GFM128 and 184C187C (Fig. 3.3B). Next, I focused on the motif of residues 26YI27 in FIV Vif. Single mutations around this motif in FIV Vif were generated (M24A, L25A, Y26A, I27A and L30A), and additionally residues 28SR29 and F47 replaced by alanines (Materials and Methods 2.9; Fig. 3.3A and C). The immunoblotting

results of the A3 degradation test revealed that mutations M24A, L25A and I27A of FIV Vif specifically blocked the capacity to induce degradation of feline A3Z3, but had no influence on degradation of feline A3Z2b and A3Z2bZ3 (Fig. 3.3C). Interestingly, the mutation Y26A impaired FIV Vif degradation for all three feline A3 proteins. In contrast, mutations in residues 28SR29, L30 and F47 of FIV Vif had no effect on feline A3 degradation (Fig. 3.3C).

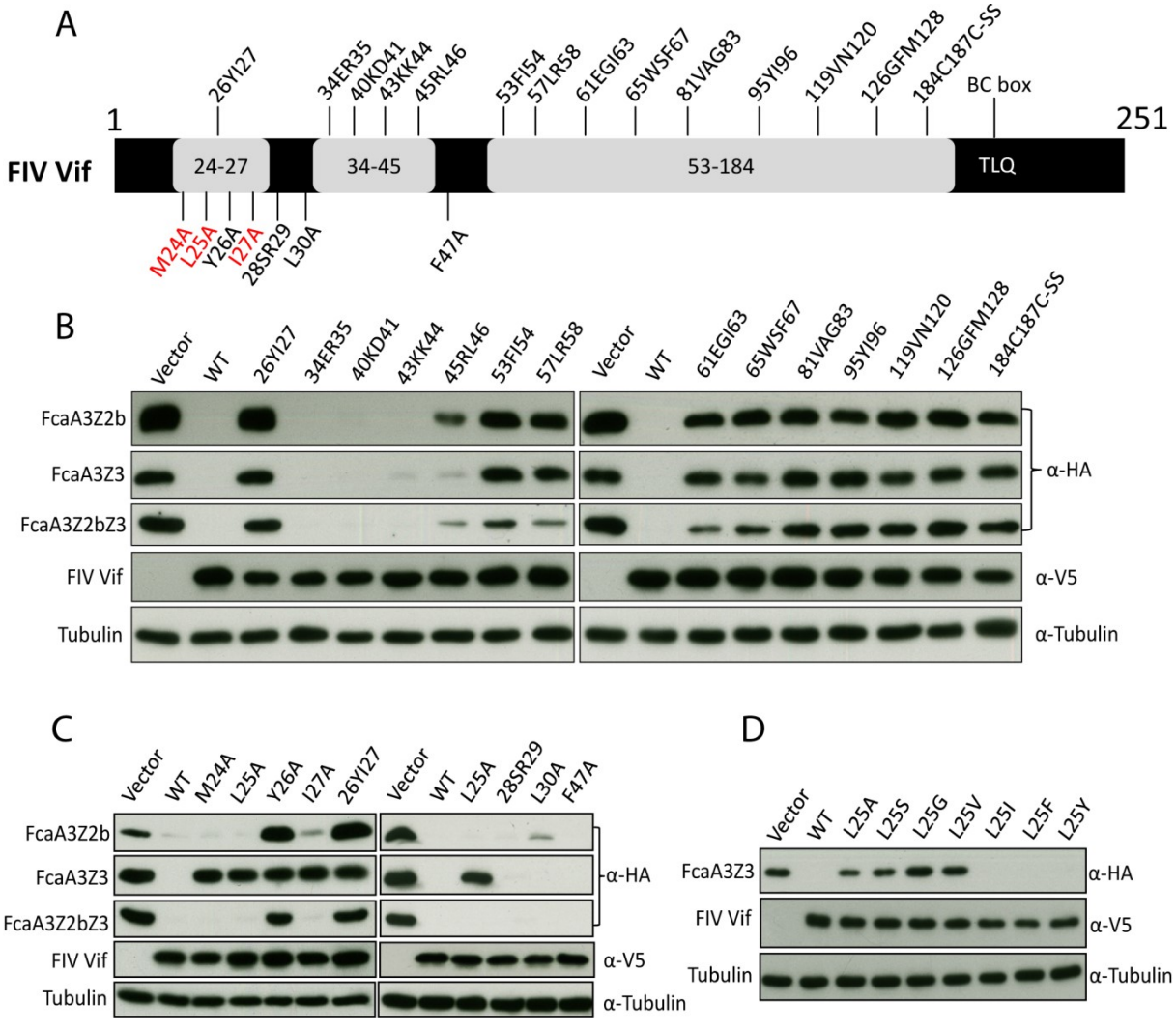

Fig. 3.3 Identification of determinants in FIV VIF that confer degradation of feline A3Z3. (A) FIV Vif schematic structure, locations of tested mutations indicated. The numbers are the position of amino acids, all these amino acids were mutated to alanines, and additionally some residues were mutated to other amino acids. The residues that determine FIV Vif degradation activity against FcaA3Z3 are shown in red. (B, C) FcaA3Z2b, FcaA3Z3 or FcaA3Z2bZ3 were co-expressed with FIV Vif wild type and Vif mutants. A3, FIV Vif and tubulin proteins were detected by using anti-HA, anti-V5 and anti-tubulin antibodies,

respectively. (D) Leucine 25 of FIV Vif was replaced by several amino acids: alanine-A, serine-S, glycine-G, valine-V, isoleucine-I, phenylalanine-F and tyrosine-Y. FcaA3Z3 was co-expressed with FIV Vif wild type and Vif mutants. A3, FIV Vif and tubulin proteins were detected by using anti-HA, anti-V5 and anti-tubulin antibodies, respectively.

Next, I constructed several derivatives of FIV Vif in which residue 25 was replaced by different amino acids (Materials and Methods 2.9; Fig. 3.3D). However, L25A, L25S, L25G and L25V mutants could not degrade feline A3Z3, whereas L25I, L25F as well as L25Y mutants degraded feline A3Z3 as efficiently as wild type FIV Vif (Fig. 3.3D). Compared with amino acids alanine, serine, glycine and valine, the residues isoleucine, phenylalanine and tyrosine have a more complex side-chain. These results may suggest that the specific spatial distance of the FIV Vif-A3Z3 interaction area determines the FIV Vif induced degradation of feline A3Z3.

3.1.3 FIV Vif mutants fail to counteract the anti-viral activity of feline A3s.

Previous studies reported that FIV Vif inhibited feline A3s by E3-complex induced degradation, and thus prevented A3 incorporation into FIV particles (161, 168). Thus, I analyzed the anti-FIV activity of feline A3Z3 in the presence of wild type or mutant FIV Vifs by using a single round FIV-luciferase reporter virus (Materials and Methods 2.11). As previously reported (162), feline A3Z3 inhibited FIVΔ*vif* 5-7-fold, which could be counteracted by wild type FIV Vif (Fig. 3.4A). However, the presence of defined FIV Vif mutants (M24A, L25A, L25S, L25G, L25V and I27A) destroyed this FIV Vif activity (Fig. 3.4A). The immunoblots of virus-producing cells indicated that FIV wild type Vif decreased the protein level of feline A3Z3 and prevented feline A3Z3 incorporation into FIV viral particles (Fig. 3.4B). However, the tested FIV Vif mutants had no effect on the protein level of feline A3Z3 in cells and failed to generate A3-free virions (Fig. 3.4B).

FIV Vif counteracts feline A3s by interacting with both single Z2 and Z3 domains (161, 162). Hence, I generated a FIV Vif mutant in which the A3Z2 interaction sites 18GG19 and the A3Z3 interaction site L25 were replaced by alanines, termed FIV Vif.18GG19+L25A (Materials and Methods 2.9). Testing this Vif mutant, I found that it did not neutralize the anti-viral activity of feline A3Z2bZ3. The Vif mutants of residues 18GG19 and L25 rescued most of the

infectivity of FIVΔ*vif* compared to infections without Vif (vector) (Fig. 3.4C). The corresponding immunoblots from virus producing cells and viral particles demonstrated that FIV Vif.18GG19+L25A did not influence feline A3Z2bZ3 protein levels and its viral incorporation (Fig. 3.4D).

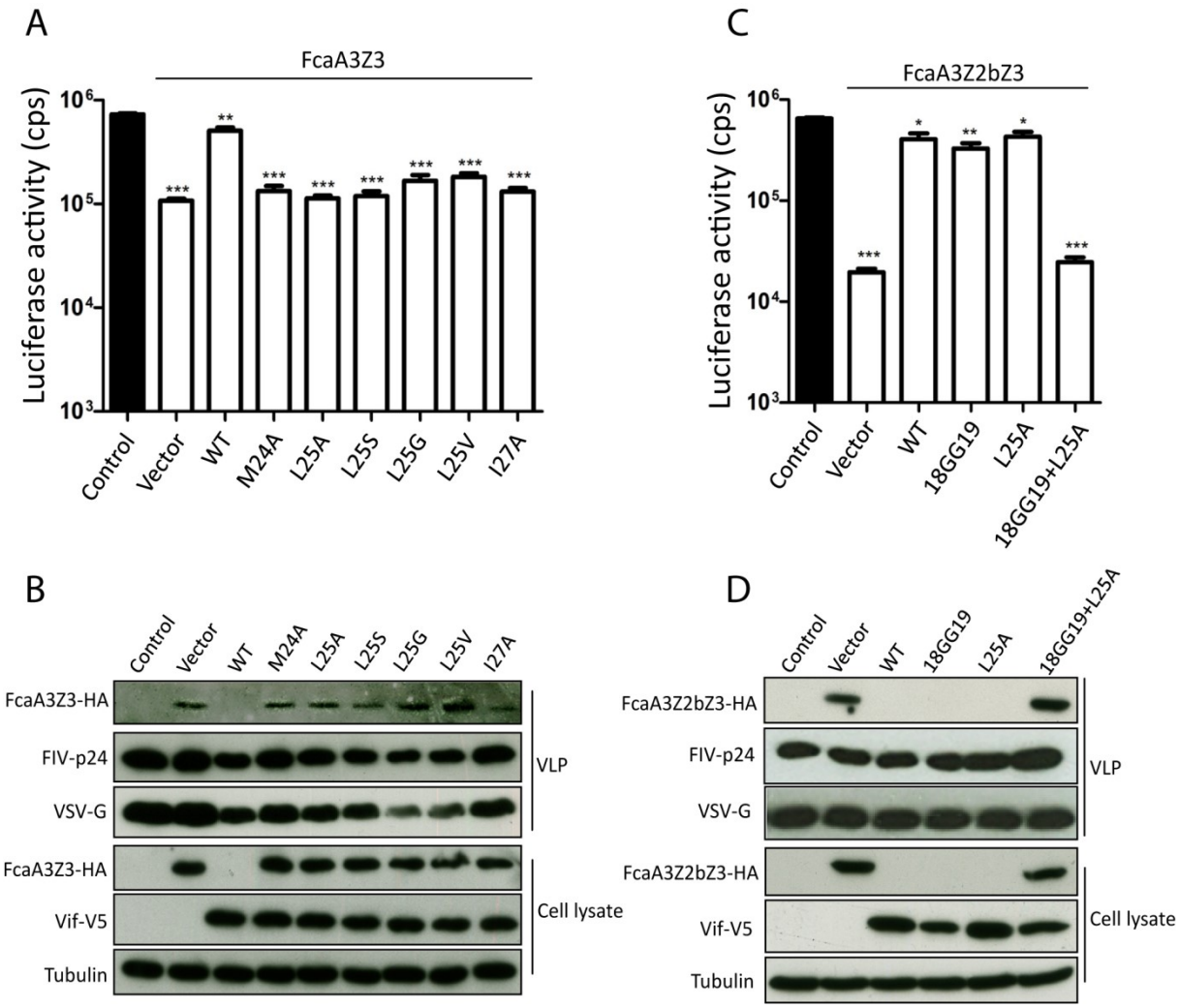

Fig. 3.4 FIV Vif mutants cannot counteract the anti-viral activity of feline A3s. (A, C) Single-round FIVΔ*vif* luciferase reporter virions were produced in the presence of feline A3 expression plasmids (FcaA3Z3 or FcaA3Z2bZ3) with FIV Vif wild type or Vif mutants, pcDNA3.1(+) was added as a control (vector). Infectivity of reporter vectors was determined by quantification of luciferase activity in 293T cells transduced with vector particles. (B, D) Cell lysates of FIV producer cells examined in (A, C) were used to detect the expression of feline A3s and FIV Vif by anti-HA and anti-V5 antibodies, respectively. Cell lysates were also analyzed for equal amounts of total proteins using anti-tubulin antibody. Feline A3s encapsidated into FIV virus like particles (VLPs) were detected by anti-HA antibody. VSV-G

and FIV p24 proteins in VLPs were also detected by anti-VSV-G and anti-FIV p24 antibodies separately. Asterisks represent statistically significant differences: ***, $p < 0.001$; **, $0.001 < p < 0.01$; *, $0.01 < p < 0.05$ [Dunnett's *t* test].

3.1.4 FIV Vif mutants failing to degrade A3s still can bind to A3.

The results above demonstrated that FIV Vif residues 12LF13, 18GG19, M24, L25 and I27 determine the specific degradation of either feline A3Z2 or A3Z3. To determine whether mutations in these Vif sites alter the cellular localization of Vif, wild type and mutant FIV Vif were expressed in HOS cells. The cellular localization was determined by confocal microscopy (Materials and Methods 2.13). The results showed that wild type FIV Vif was mainly localized to the cytoplasm. I also observed some small levels of wild type FIV Vif localizing to the nucleus (Fig. 3.5), which was consistent with a previous study (202). The cellular localizations of the FIV Vif mutants were found to be identical to wild type FIV Vif (Fig. 3.5). These results suggest that mutations in 12LF13, 18GG19, M24, L25 and I27 of FIV Vif impair the degradation of selective feline A3s, but do not alter the subcellular localization of FIV Vif.

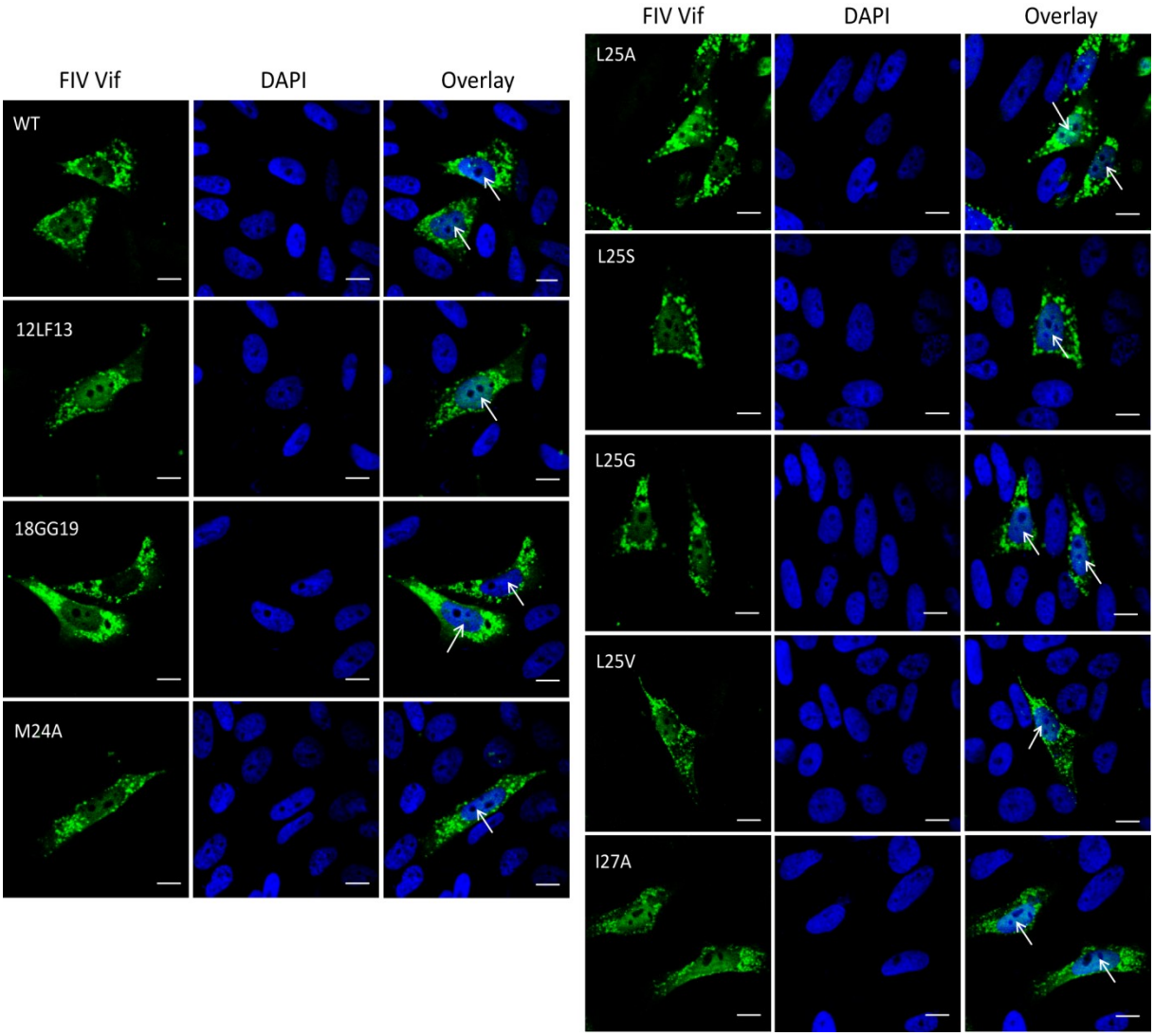

Fig. 3.5 Cellular localization of FIV Vif and Vif mutants. HOS cells were transfected with FIV Vif wild type and Vif mutants. All Vif mutants were generated by replacing the indicated residues by alanines. The numbers represent the amino acids position. To detect FIV Vif and Vif mutants (green) immunofluorescence, staining was performed with an anti-V5 antibody. Nuclei (blue) were visualized by DAPI staining. The white bar indicates 10 µm. The white arrows indicate Vif protein in the nucleus.

To characterize the determinants of binding of FIV Vif to feline A3, GST-pull down assays were performed (Materials and Methods 2.14). I tested FIV Vif constructs with a GST-tag, which had a C-terminal deletion, expressing the first 160 (Vif 1-160), 110 (Vif 1-110), 80 (Vif 1-80) or 50 (Vif 1-50) amino acids of Vif (Fig. 3.6A). For the full length of the FIV Vif, I inactivated the BC box (TLQ-AAA) to prevent A3 degradation activity. These five Vif

constructs were co-transfected with a feline A3Z2bZ3 expression plasmid into 293T cells. 48 h later, cells were harvested, and Vif was pulled down by glutathione sepharose beads. The binding between FIV Vif and feline A3Z2bZ3 was evaluated by detecting the A3Z2bZ3 protein in the pull-down complex. It was found that GST alone could not pull down feline A3Z2bZ3, while it was detected in the pull-down complex of Vif.TLQ-AAA, Vif.1-160, Vif.1-110 and Vif.1-80 (Fig. 3.6B). Vif.1-50 displayed very weak binding to feline A3Z2bZ3, compared to the GST control (Fig. 3.6B). These results may suggest that residues 50 to 80 of FIV Vif confer binding to feline A3Z2bZ3. However, the specific A3Z2 and A3Z3 degradation determinants locate at residues 1-50 of FIV Vif (Fig. 3.2 and 3.3). To test whether these determinants were involved in the binding of A3Z2 and A3Z3, I generated several derivatives of Vif.1-110 in which residues 12LF13, 18GG19, M24, L25 or I27 were replaced by alanines separately (Fig. 3.6A). The binding to A3Z2 or A3Z3 of these mutants was detected by GST-pull-down assays. It was found that Vif.1-110, Vif.1-110-12LF13 and Vif.1-110-18GG19 had identical protein level in the pull-down complex, and immunoprecipitated similar amounts of feline A3Z2b protein (Fig. 3.6C). Vif.1-110 could also bind to feline A3Z3, and introducing M24A and L25A into Vif.1-110 did not alter its binding affinity to feline A3Z3 (Fig. 3.6D). Compared with Vif.1-110, I detected less Vif.1-110-I27A and feline A3Z3 proteins in immunoprecipitated complexes (Fig. 3.6D). Taken together, these results suggest that the specific A3Z2 and A3Z3 degradation determinants in FIV Vif (12LF13 and 18GG19 for A3Z2; M24, L25 and I27 for A3Z3) do not determine to any great extent the Vif-A3 binding, which, however, is regulated by the region from residue 50 to 80 of the FIV Vif.

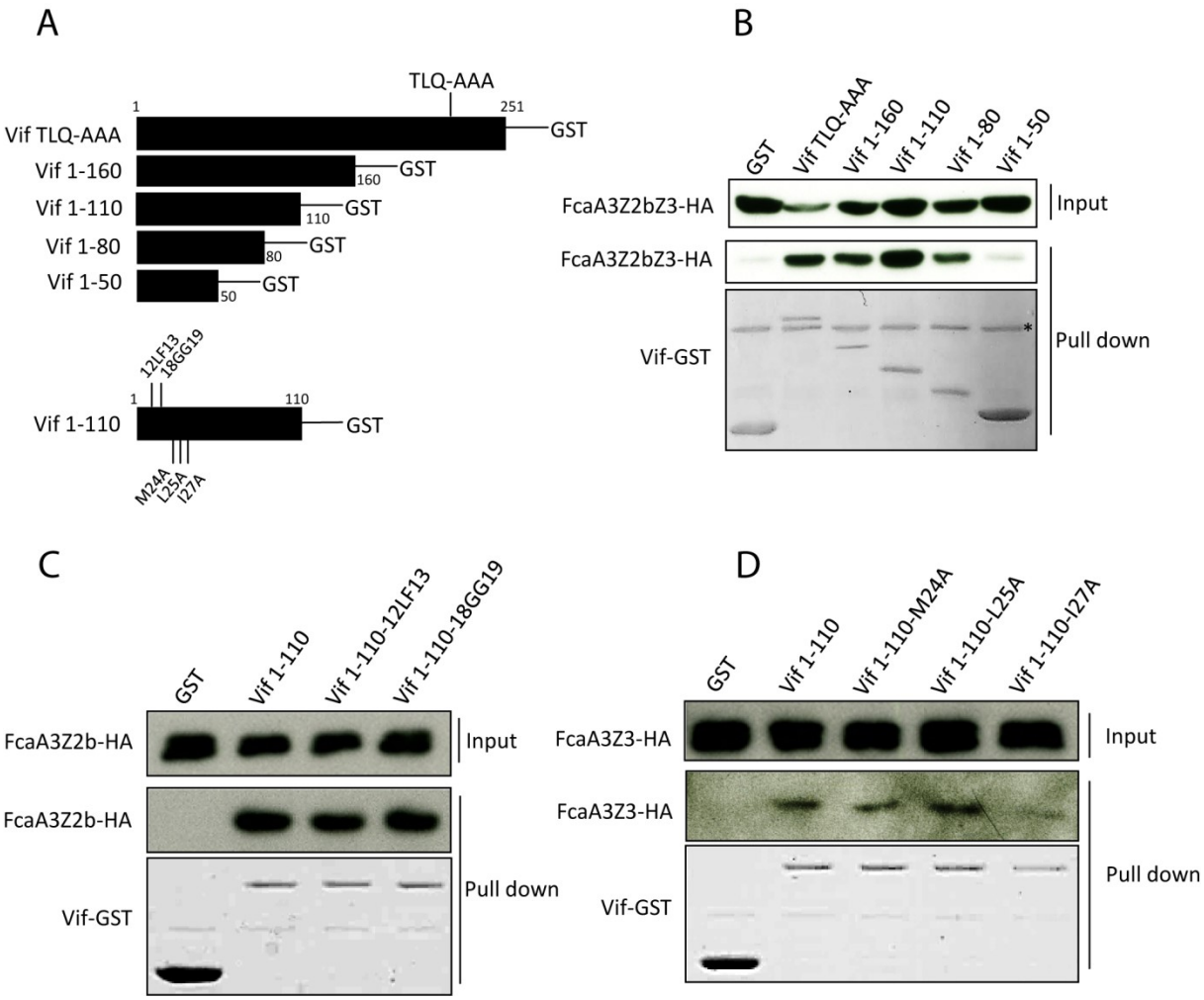

Fig. 3.6 Binding of FIV Vif to feline A3s. (A) Schematic structure of C-terminal truncations of FIV Vifs. TLQ-AAA represents the inactive BC box of FIV Vif. FIV Vif TLQ-AAA, FIV Vif 1-50, FIV Vif 1-80, FIV Vif 1-110 and FIV Vif 1-160 constructs were fused with a C-terminal GST tag. (B, C, D) 293T cells were co-transfected with an expression plasmid encoding GST or different FIV Vif constructs fused with a C-terminal GST, as indicated. At 48 h, the transfected cells were lysed and incubated with glutathione-sepharose beads. The feline A3s of input and bound fractions were detected by immuno blots using anti-HA antibody. The pull-down fractions were also used for coomassie staining to show the GST or Vif-GST. * indicates unspecific bands.

3.1.5 The specific A3Z2 and A3Z3 interaction sites are conserved in FIV Vif variants except puma FIV_{Pco} Vif.

After the identification of the selective A3Z2 and A3Z3 interaction sites of domestic cat FIV Vif (isolate FIV-34TF10), 15 Vif sequences that belong to naturally FIV infected cats, and their respective A3Z3 haplotypes, were analyzed. Our collaboration partner, Lucía Cano Ortiz and Ana Cláudia Franco identified three animals with haplotype I, four with haplotype II, two with III, four with IV and one animal displayed haplotype V (165). A3Z3 haplotype of one sample was not determined. All 15 Vifs isolated showed that the A3Z2 and A3Z3 interaction sites are highly conserved (Fig. 3.7A and Table 3.1). It was described that FIV from several felid species showed genetic divergence, which suggests virus-host adaptations and rare cross-species transmissions in the wild (39, 40). Thus, I analyzed Vif sequences of additional domestic cat FIV strains and Vif from several non-domestic cat FIVs. I identified that the feline A3Z2 and A3Z3 interaction sites are conserved in domestic cat FIV Vif from subtype A, B and D (Fig. 3.7B). FIV Vif from pallas cats (*Otocolobus manul*) had one substitution (F13Y) at the feline A3Z2 interaction sites (Fig. 3.7B). The A3Z2 and A3Z3 interaction sites in lion FIV Vif from subtype B and E were identical to domestic cat FIV Vif except one substitution (L25M) in FIV lion (*Panthera leo*) subtype E Vif (Fig. 3.7B). Interestingly, Vif from three FIV_{Pco} strains of puma (*Puma concolor*) and one FIV_{Pco} strain of bobcat (*Lynx rufus*) had an evident difference compared to the other FIV Vifs, especially the Vif from the FIV subtype B of puma had two discontinuous deletions at the N-terminal region (Fig. 3.7B) (41). Taken together, the sequence analysis suggests that the A3Z2 and A3Z3 interaction sites of the FIV Vif protein are highly conserved in different domestic cat FIV Vifs in agreement with its importance in counteracting A3 restriction of the host and interestingly conserved as well in some FIVs from non-domestic cats.

Sequence Name Vif	Haplotype A3Z3	Alleles A3Z3
Vif_FIV_RS09	I	Homozygous
Vif_FIV_RS11	I	Homozygous
Vif_FIV_RS13	I	Homozygous
Vif_FIV_RS02	II	Heterozygous Codon 65: S or A
Vif_FIV_RS04	II	Heterozygous Codon 65: S or A
Vif_FIV_RS08	II	Heterozygous Codon 65: S or A
Vif_FIV_RS14	II	Homozygous Codon 65: S
Vif_FIV_RS06	III	Heterozygous Codon 65: S or A Codon 68: Q or R Codon 96: I or V
Vif_FIV_RS12	III	Homozygous Codon 65: S Heterozygous Codon 68: R or Q Codon 94: T or A
Vif_FIV_RS03	IV	Heterozygous Codon 65: S or A Codon 96: I or V
Vif_FIV_RS05	IV	Heterozygous Codon 65: S or A Codon 96: I or V
Vif_FIV_RS07	IV	Heterozygous Codon 65: S or A Codon 96: I or V
Vif_FIV_RS10	IV	Heterozygous Codon 65: S or A Codon 96: I or V
Vif_FIV_RS01	V	Heterozygous Codon 65: I or V
Vif_FIV_RS15	not characterized	

Table 3.1 Haplotypes of feline A3Z3 in FIV infected cats. This table was provided by Lucía Cano Ortiz and Ana Cláudia Franco from laboratory of Virology, Federal University of Rio Grande do Sul, Porto Alegre, Brazil.

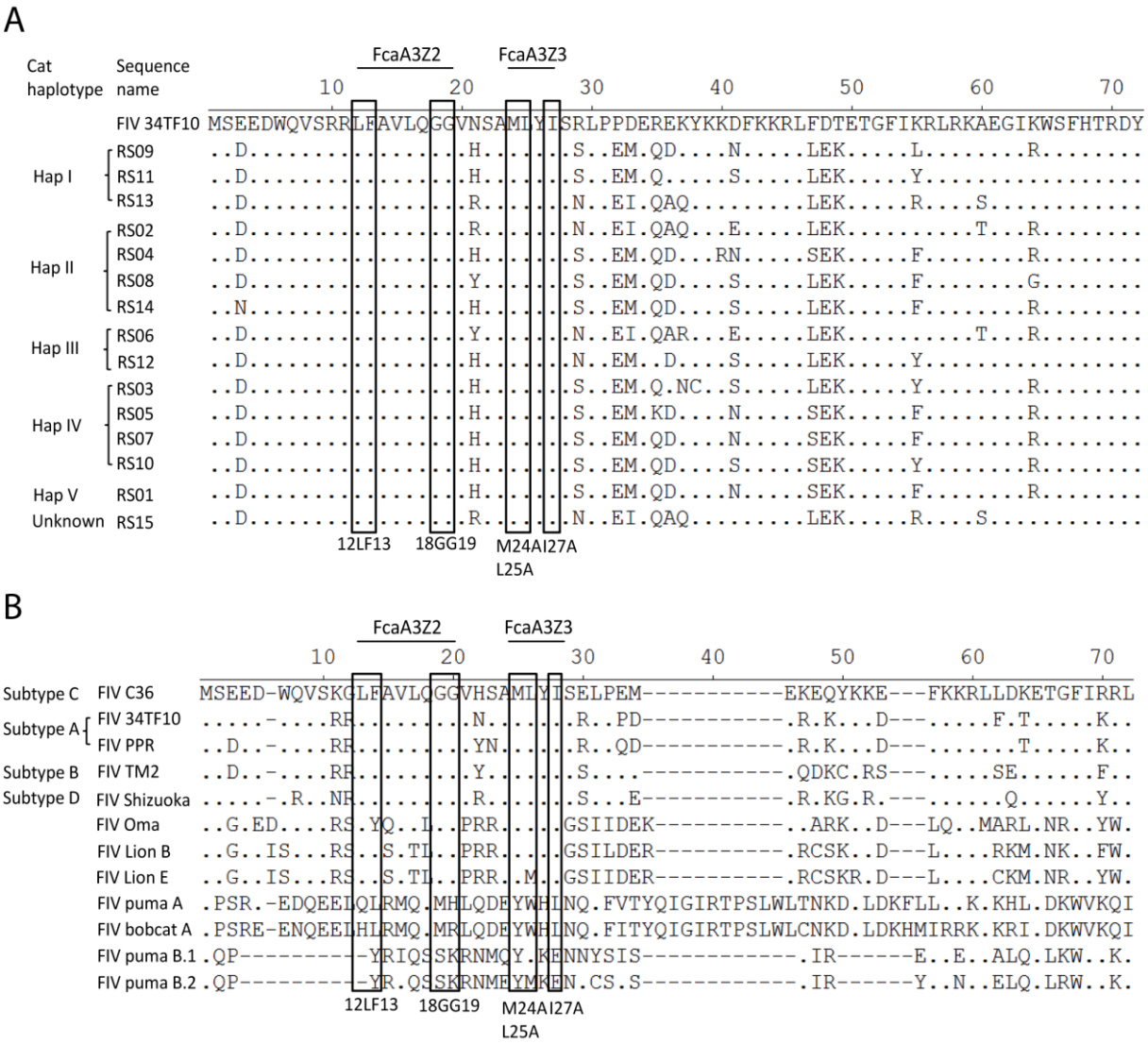

Fig. 3.7 Sequence alignment of Vif from different FIV stains. (A) Sequence alignment of Vif (N-terminus) naturally isolated from cats infected with subtype B FIV in Brazil with known A3Z3 haplotypes. (B) Subtype A of FIV includes FIV C36, FIV 34TF10 and FIV PRR. Subtype B includes FIV TM2. FIV Shizuoka belongs to subtype D. Other FIV Vifs sequence are from non-domestic cats of FIV Oma (pallas cats), FIV lion B, FIV lion E, FIV puma A, FIV bobcat Aand FIV puma B. The different residues between these FIV Vifs are shown. Dots represent identical residues with Vif of FIV C36. Hyphens indicate sequence deletion. The feline A3Z2 and A3Z3 interaction sites are boxed.

3.2 Identification of feline A3s domains targeted by FIV Vif and HIV-2/SIVmac Vif

3.2.1 FIV and HIV-2/SIVmac/smm Vif induced degradation of felines A3s.

In order to identify the molecular interaction of the FIV Vif protein and feline A3 proteins, co-transfection experiments of cat-derived A3s and FIV Vif expression plasmids were performed in 293T cells (Materials and Methods 2.10). All A3 constructs expressed the corresponding A3 protein as a C-terminal HA-tag, whereas Vif was expressed as a C-terminal V5-tag fusion protein (Materials and Methods 2.8). In addition, I also studied Vifs derived from HIV-1, HIV-2, SIVmac, and SIVsmm. Immunoblots of protein extracts from cells co-expressing both A3 and Vif were used as a read-out for degradation of the respective A3 protein. Results in Fig. 3.8 show that FIV Vif induces degradation of single-domain feline A3Z2a, A3Z2b, A3Z2c, A3Z3, and double-domain A3Z2bZ3 and A3Z2cZ3 in agreement with previous reports (168, 192, 203, 204). The double-domain feline A3Z2bZ3 and A3Z2cZ3 were degraded by SIVmac Vif as seen before (173, 203), as well by the Vifs of SIVsmm and HIV-2. For subsequent experiments I used the expression plasmid FcaA3Z2bZ3, hereafter referred to as feline A3Z2Z3 for simplicity.

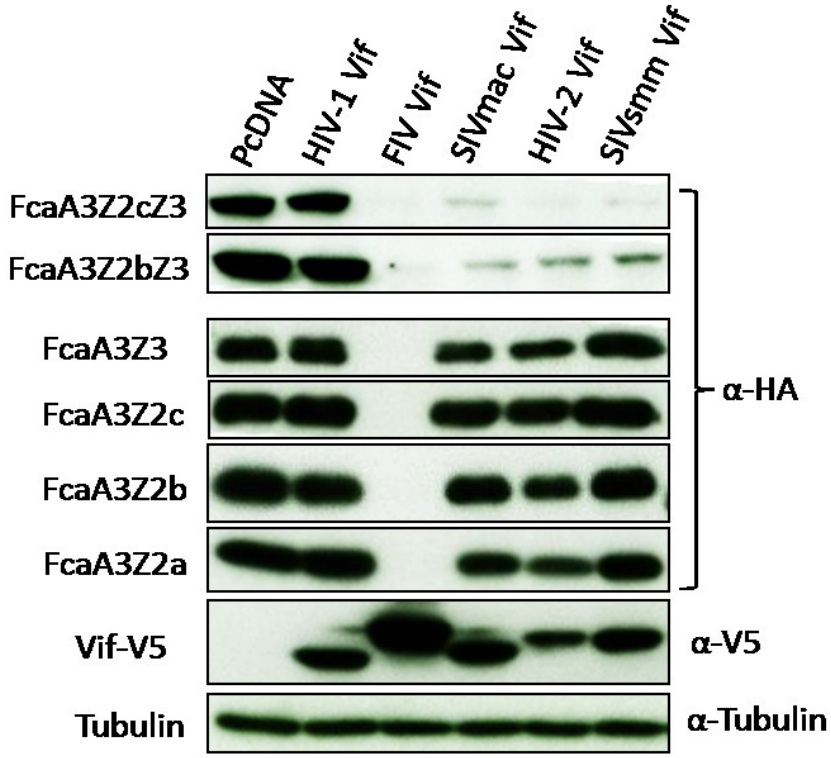

Fig. 3.8 The interaction of feline APOBEC3s with FIV Vif. 293T cells were transfected with expression plasmids for FcaA3Z2a, FcaA3Z2b, FcaA3Z2c, FcaA3Z3, FcaA3Z2bZ3 and FcaA3Z2cZ3 together with HIV-1, SIVmac, HIV-2 and SIVsmm or FIV Vif or no Vif (replaced by pcDNA3.1). Cells were harvested 48 h later. FcaA3s, Vifs and tubulin were visualized by immunoblot using anti-HA, anti-V5 and anti-tubulin antibodies.

3.2.2 Identification of feline A3Z3 residues important for FIV Vif induced degradation.

The A3Z3 region position 23 to 50 differs in 16 amino acids between human and feline A3Z3s, and contains highly conserved amino acid positions. I mutated thus most feline-specific residues in feline A3Z3, in positions 35 to 38 and 40 to 48 (Materials and Methods 2.9; Fig. 3.9A). These mutated A3s were characterized for resistance to degradation by co-expression with FIV Vif (Materials and Methods 2.10). I found that only A3Z3s mutated at position 41+42 (LI>>TP and LI>>AA) showed partial resistance to degradation by Vif (Fig. 3.9B). The A65I in feline A3Z3 has been described in Brazilian cats and discussed to be a relevant resistance mutation against FIV (165, 205). Under our experimental conditions, A3Z3 mutated in position 65 (A65I) displayed only little resistance to Vif-mediated degradation (Fig. 3.9B). However, very important, the combination of mutations, A65I and L41A-I42A, resulted in an A3Z3 variant that showed complete resistance to FIV Vif degradation (Fig. 3.9B).

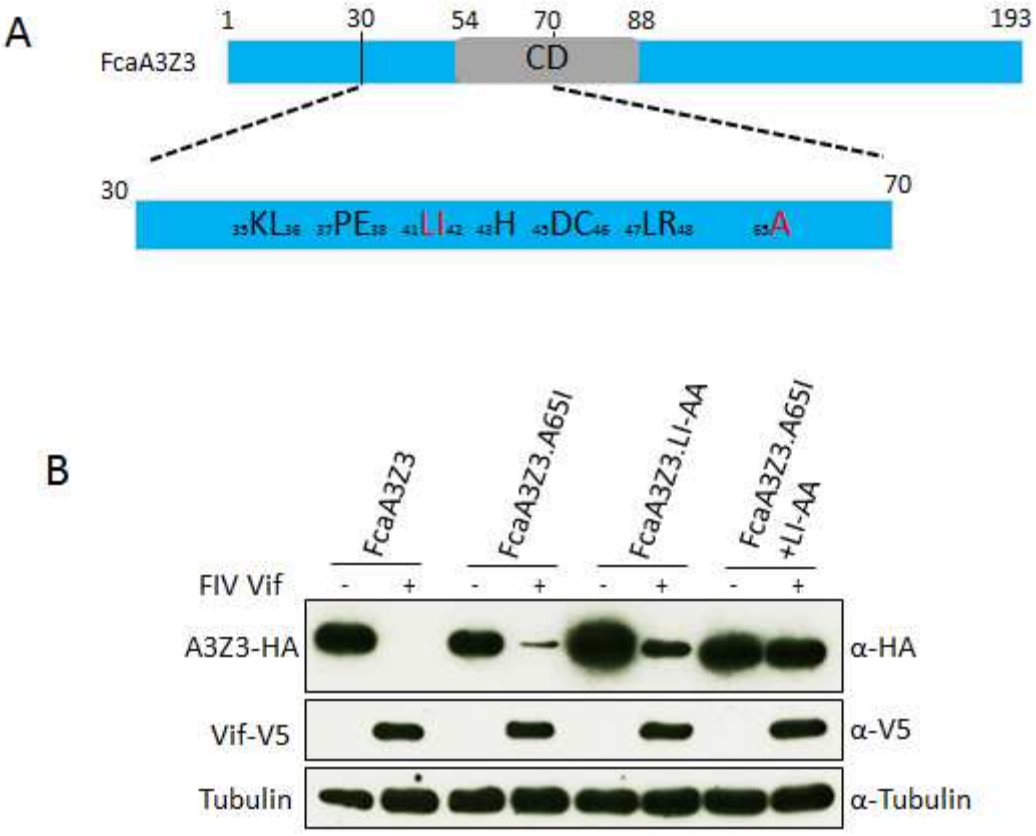

Fig. 3.9 Generation of FIV Vif resistant FcaA3Z3. (A) Representation of FcaA3Z3 protein. Residues investigated are shown. CD: cytidine deaminase domain. (B) Several mutants at N-terminal region of FcaA3Z3 were generated. To analyze the sensitivity of FcaA3Z3 mutants to FIV Vif, 293T cells were co-transfected with expression plasmids for FcaA3Z3 wild type (FcaA3Z3) or indicated mutants and FIV Vif. 48 h later, FcaA3Z3, Vif and tubulin proteins were detected by immunoblot.

3.2.3 Identification of feline A3Z2 residues important for FIV Vif induced degradation.

The felid A3Z2s (puma A3Z2, Lynx A3Z2 and Tiger A3Z2) are very similar to FcaA3Z2 as they share 89% - 93% identically conserved residues, whereas cat A3Z2 and human A3C are much more diverse and share only 47% identical amino acids. Thus, it was identified that four positions in which all big cat A3Z2s differed from FcaA3Z2, in positions N18, T44, D165 and H166 (Fig. 3.10A). Accordingly, the positions 18 and 44 were replaced in the cat sequence with the corresponding residues from big cat, but found both mutants to be efficiently degraded by FIV Vif (Materials and Methods 2.9; Fig. 3.10B). Very similar, A3Z2.D165Y was

depleted when co-expressed with FIV Vif. Interestingly, mutation of residue 166 (H166N) generated a partially Vif-resistant A3Z2 protein. I speculated that the adjacent D165 might enhance the Vif-resistance seen in the H166N variant. Indeed, the A3Z2.DH-YN mutant showed complete resistance to FIV Vif (Fig. 3.10B). I also analyzed tiger A3Z2.Y165D but could not reverse the resistance to degradation by FIV Vif (Fig. 3.10B). I conclude that D165-H166 in the C-terminal region of cat A3Z2 are important for Vif-mediated degradation together with other residues that remain to be characterized.

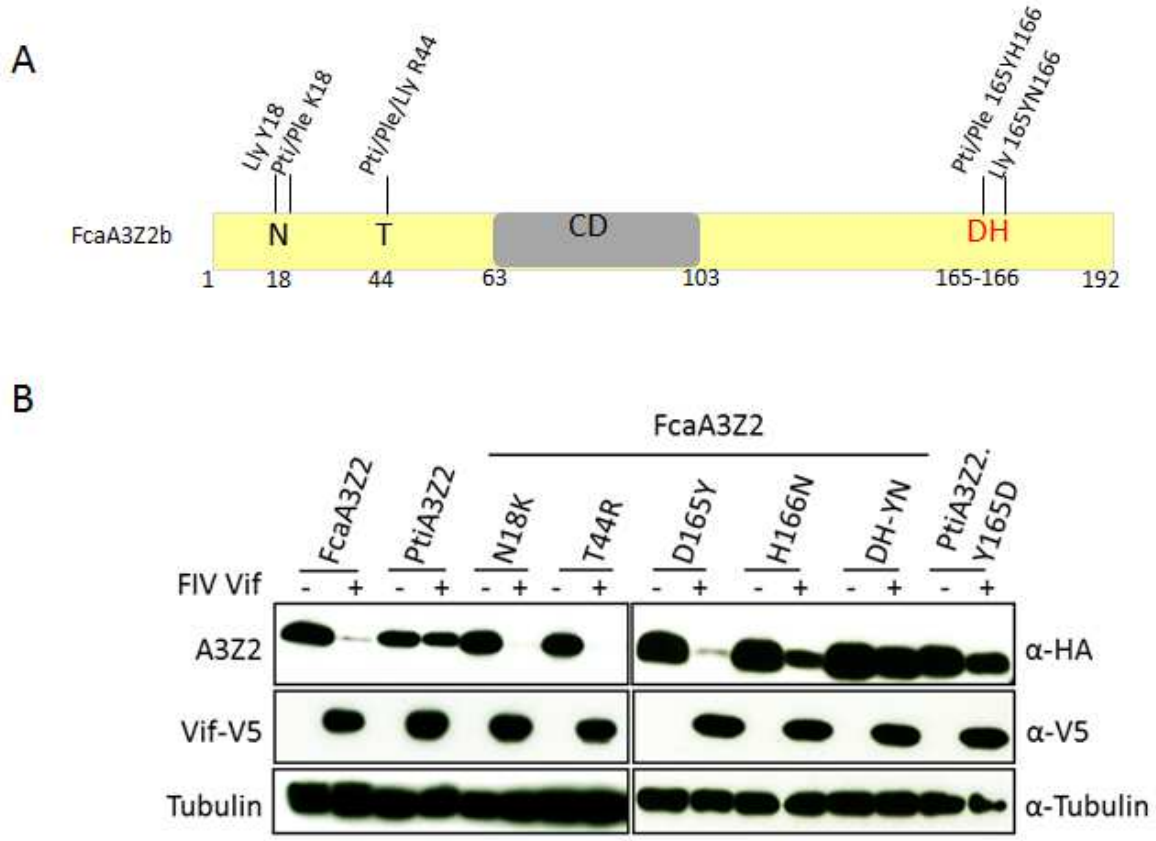

Fig. 3.10 FcaA3Z2 and FcaA3Z2Z3 mutations block degradation by feline Vifs. (A) Representation of FcaA3Z2b protein. Residues investigated are shown. CD: cytidine deaminase domain. Residues different found in A3Z2 of the domestic cat and big cats indicated. Pti, Ple, and Lly represent *Panthera tigris corbetti*; *Panthera leo bleyenberghi*; *Lynx lynx.* (B) Expression plasmids for FIV Vif and FcaA3Z2, PtiA3Z2 or several mutants of feline A3Z2 were co-transfected into 293T cells. The expression of A3 and Vif proteins were detected by using anti-HA and anti-V5 antibodies 48 h later.

3.2.4 The Linker of feline A3Z2Z3 is important for HIV-2/SIVmac induced degradation.

Under some conditions, APOBEC3s act as restriction factors for cross-species transmission of lentiviruses. To obtain an animal model for HIV based on cats, it is required to eliminate the restriction of cat A3s. Thus, the interaction between cat A3s and HIV or SIV Vif was also investigated in this study.

The Vif-mediated degradation profile exclusive to A3Z2Z3s may indicate that the HIV-2/SIVmac/smm Vifs require for interaction with the feline A3Z2Z3 a protein domain that is absent in the single-domain A3Z2 or A3Z3. It was speculated that the homeo-box domain insertion (linker region) could play a central role in these Vif interactions. To test our hypothesis, three constructs were assayed: an A3Z2Z3 in which the linker was deleted (ΔLinker); and two versions of A3Z2Z3 in which either residues 223 to 240 (Δ222) or residues 211 to 240 (Δ210) in the linker were removed (Materials and Methods 2.9; Fig. 3.11A). All these constructs successfully expressed protein upon transfection, and FIV Vif was able to degrade all of them (Materials and Methods 2.10). Only the linker truncations Δ222 and Δ210 were efficiently degraded by Vif of HIV-2/SIVmac/smm, whereas the ΔLinker construct showed very little degradation (Fig. 3.11B and C). Interestingly, the A3Z2Z3 lacking the linker domain (ΔLinker) showed dose-dependent moderate degradation, while mutants Δ222 and Δ210 showed a HIV-2/SIV Vif-dependent degradation similar as the wild type A3Z2Z3 protein (Fig. 3.11B and C).

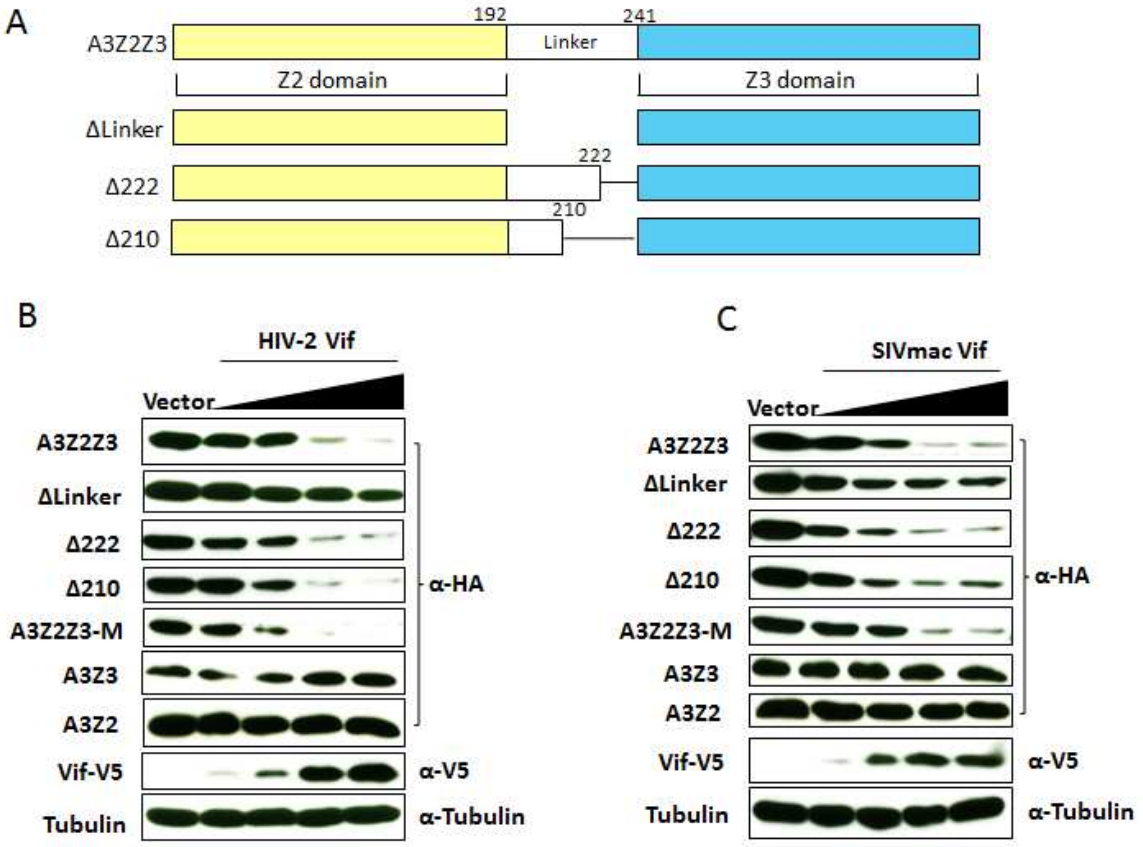

Fig. 3.11 The linker region in FcaA3Z2Z3 is important for HIV-2/SIVmac/smm Vif induced degradation. (A) Schematic representation of FcaA3Z2Z3 mutants (ΔLinker, Δ222, Δ210). Z2 and Z3 domains are shown as yellow and blue rectangle. The linker from amino acid 192 - 241 is shown as white rectangle. (B and C) Co-transfection of increasing amounts of expression plasmids for (B) HIV-2 Vif and (C) SIVmac Vif with constant amounts of the indicated A3 expression plasmids. The expression of FcaA3s and Vifs were analyzed by anti-HA and anti-V5 antibodies, respectively. Cell lysates were also analyzed for equal amounts of total proteins using anti-tubulin antibody.

3.3 Identification of a conserved interface of HIV-1 and FIV Vifs with Cullin 5

3.3.1 CUL5 and not CUL2 is required for FIV Vif degradation of feline A3s.

A previous study reported that FIV Vif interacts with Cullin 5 (CUL5) to form an E3 ubiquitin ligase complex that can induce the degradation of feline A3 proteins by the proteasome (168). However, the mechanism by which FIV Vif binds to CUL5 remains unclear and whether

FIV Vif binds to other Cullin family proteins is not known. Thus, the interaction of FIV Vif with CUL5 and CUL2 were firstly investigated. 293T cells were transfected with expression plasmids for FIV Vif-V5, CUL2-myc, or CUL5-myc, then the lysates were used for co-immunoprecipitation (co-IP) (Materials and Methods 2.10 and 2.15). The results indicated that FIV Vif was found in the CUL5-immunoprecipitated complex, while no FIV Vif was observed in the CUL2 immunoprecipitation (Fig. 3.12A). CUL2 and CUL5 interact with Rbx by using their C terminus that is critical for E3 ubiquitin ligase activity (See recent review (150)). Dominant-negative (DN) CUL5 or DNCUL2 has a C terminal deletion, which can inhibit SOCS box protein induced substrate degradation (194). Thus, I expressed the indicated feline A3s together with FIV Vif and DNCUL5 or DNCUL2 (Materials and Methods 2.10). Immunoblots of protein extracts from transfected 293T cells were used as a readout for the degradation of the respective A3 protein (Materials and Methods 2.12). The results showed that FIV Vif efficiently degraded all three tested feline A3s (FcaA3Z2b, FcaA3Z3, and FcaA3Z2bZ3) in the absence of DNCUL5 (Fig. 3.12B), which is consistent with previous studies (161, 164, 206). The presence of DNCUL5 enhanced the cellular protein level of Vif and abolished the degradation of the A3s (Fig. 3.12B). In contrast, DNCUL2 did not affect the expression of Vif nor the Vif-dependent FcaA3Z3 and FcaA3Z2bZ3 degradation (Fig. 3.12C). However, in the presence of high level of FcaA3Z2b, expression DNCUL2 slightly impaired its degradation by FIV Vif, possible due to DNCUL2-dependent exhaustion of endogenous ElongB/C (Fig. 3.12D). Additionally, I investigated the impact of the proteasome inhibitor MG132 on Vif-mediated A3 degradation. It was found that the degradation of FcaA3Z2bZ3 by FIV Vif was sensitive to MG132 treatment but comparably less sensitive than the HIV-1 Vif-induced degradation of human A3G (Fig. 3.12E). The reasons for these different responses to MG132 are unclear and might indicate different kinetics of degradation.

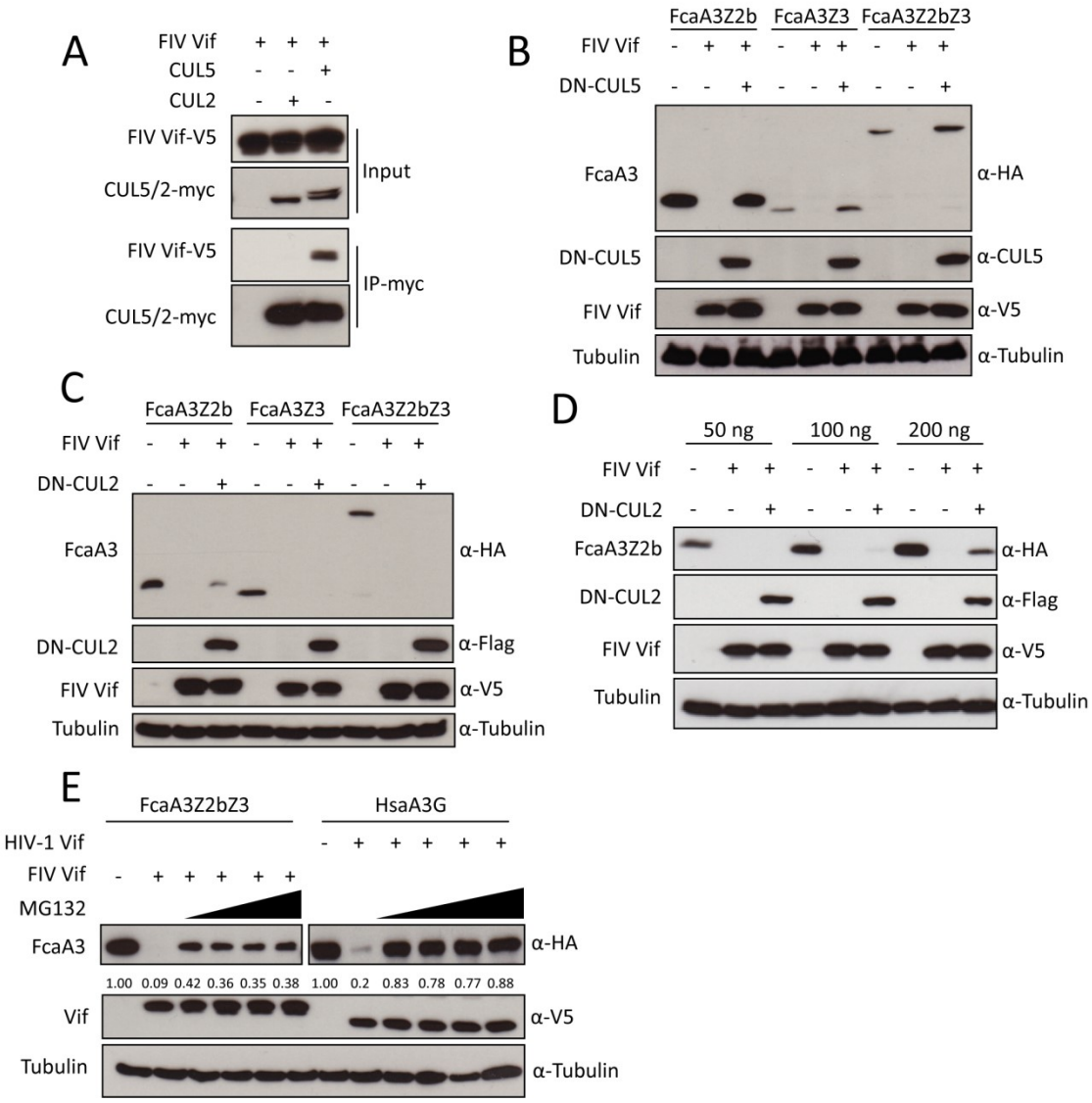

Fig. 3.12 CUL5 is required for FIV Vif induced degradation of feline APOBEC3s. (A) FIV Vif interacts with CUL5, but not CUL2. myc-CUL5 or myc-CUL2 expression plasmids were co-transfected with FIV Vif-V5 expression plasmid. Cell lysates were immunoprecipitated with anti-myc beads and then analyzed by immunoblotting with anti-V5 antibody for FIV Vif and anti-myc antibody for CUL2 and CUL5. (B, C) Dominant-negative (DN)-CUL5, but not DN-CUL2, disrupts the degradation of feline A3s induced by FIV Vif. 293T cells were co-transfected with 300 ng expression plasmids for FcaA3Z2b-HA, FcaA3Z3-HA or FcaA3Z2bZ3-HA; 700 ng of DN-CUL5-FLAG or DN-CUL2-FLAG with 30 ng of FIV Vif-V5. pcDNA3.1 was used as control plasmid to replace the FIV Vif or dominant negative CUL5/2 expression plasmids. Cells were analyzed by immunoblotting using anti-HA, anti-V5, anti-CUL5, anti-Flag and anti-tubulin antibodies, respectively. (D) 293T cells were co-transfected with 50, 100 or 200 ng

expression plasmids for FcaA3Z2b-HA, 700 ng of DN-CUL2-FLAG with 30 ng of FIV Vif-V5. The immunoblotting was performed as (B). (E) FIV Vif induces the degradation of FcaA3s in a proteasome-dependent manner. 293T cells were transfected with HsaA3G-HA or FcaZ2bZ3-HA; HIV-1 Vif-V5 or FIV Vif-V5 expression plasmids, pcDNA3.1 was used as empty plasmid control. The transfected cells were treated with the proteasome inhibitor MG132 (2.5, 5, 7.5 or 10 μM) or DMSO as control 36 h post transfection. Cells were harvested 12 h later (48 h after transfection) and then analyzed by immunoblotting with anti-HA, anti-V5 and anti-tubulin antibodies. The percentage of FcaA3 and human A3G (HsaA3G) were calculated relative to that in the absence of FIV Vif or HIV-1 Vif (set as 1.00).

3.3.2 FIV Vif N-terminal residues are not essential for CUL5 binding.

A previous study suggested that FIV Vif may utilize a novel mechanism for binding CUL5 (168). To investigate which domain of FIV Vif is involved in the CUL5 interaction, I analyzed FIV Vif sequences from different FIV strains. I found several conserved residues at the N-terminal protein region (residues 53 to 132). Thus, I replaced the N-terminal conserved residues (53FI54, 57LR58, 61EGI63, 65WSF67, 68HTR70, 71DYY73, 74IGY76, 77VRE79, 81VAG83, 92MY93, 95YI96, 99PLW101, 105YRP107, 128MED130, and 132IEK134) of FIV Vif by alanines (Fig. 3.13A). All FIV Vif mutants were co-expressed with CUL5-myc in 293T cells (Materials and Methods 2.10). FIV Vif with a TLQ-AAA mutation served as a control because destroying ELOC binding destabilizes the CUL5 interaction (168). Co-immunoprecipitation assays followed by immunoblots were used to evaluate the binding of FIV Vif mutants to CUL5 (Materials and Methods 2.15). The results showed that FIV Vif with mutations in 53FI54, 57LR58, and 77VRE79 bound CUL5, but the binding affinity appeared to be weaker compared to the wild type FIV Vif (Fig. 3.13B). These three FIV Vif mutants had similar binding affinity to FcaA3Z2bZ3 (Fig. 3.13C) and ELOB/C (Fig. 3.13D). Consistent with a reduced CUL5 interaction, these Vif mutants partially lost the function to induce FcaA3Z2bZ3 degradation (Fig. 3.13E). All other Vif mutants showed no change in CUL5 binding (Fig. 3.13B). Overall, it appears that the residues in the N-terminus (53 to 132) of FIV Vif are not important for the CUL5 interaction.

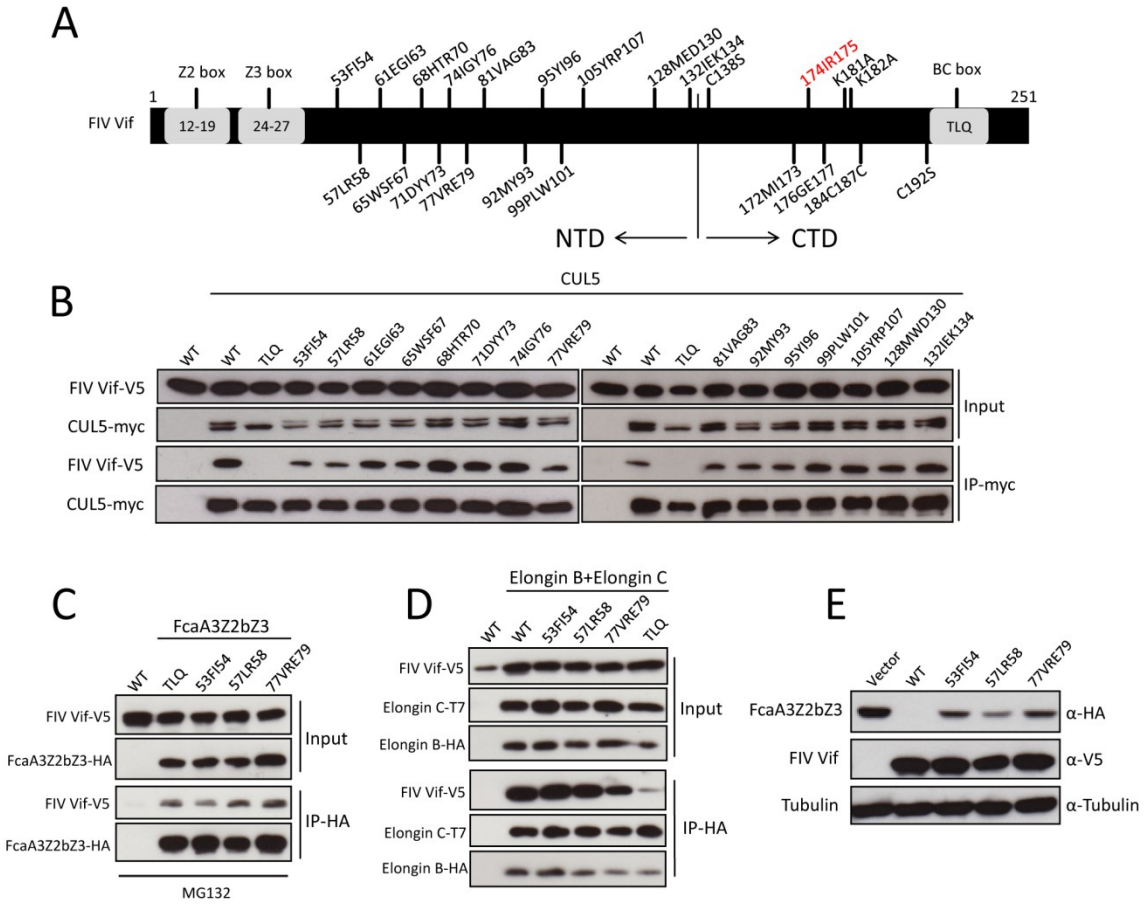

Fig. 3.13 Relevance of FIV Vif N-terminal residues for interaction with CUL5. (A) Schematic structure of FIV Vif. The numbers indicate the positions of amino acids mutated to alanines. The relative positions of the feline A3Z2 and A3Z3 interaction sites (Z2 box, Z3 box) and the Elongin B/C interaction site (BC box) are represented. (B) Co-immunoprecipitation of FIV Vif wild type and mutants with CUL5. myc-CUL5 or pcDNA3.1 empty plasmid were co-transfected with expression plasmids for FIV Vif-V5 wild type or FIV Vif mutants. Immunoprecipitated complexes (IP) were analyzed by immunoblotting with anti-V5 for FIV Vif and anti-myc for CUL5. (C, D) 293T cells were transfected with expression plasmids for FcaZ2bZ3-HA, FIV Vif-V5 wild type, indicated FIV Vif mutants or pcDNA3.1 empty plasmid (C); or FIV Vif-V5 wild type, indicated FIV Vif mutants, T7-ELOC or HA-ELOB and pcDNA3.1 empty plasmid (D). Cells were harvested at 48 h after transfection, protein of cell lysates (input) and immunoprecipitated complexes (IP) were analyzed by immunoblots stained with anti-V5 antibody for FIV Vif, anti-HA antibody for FcaZ2bZ3-HA and HA-ElonginB and anti-T7 antibody for T7-ElonginC. (E) 293T Cells were transfected with FcaA3Z2bZ3-HA and FIV Vif-V5 wild type or indicated FIV Vif mutant expression plasmids or pcDNA3.1 empty plasmid.

Cells were harvested and analyzed by immunoblotting with anti-HA, anti-V5 and anti-tubulin antibodies, respectively.

3.3.3 Identification of determinants in the C-terminus of FIV Vif that regulate binding to CUL5.

It has been shown that in HIV-1 Vif, CUL5 interacts with the C-terminal HCCH box (207-209). Thus, the C-terminal region of Vifs from different FIV strains were analyzed. As in HIV-1, all FIV Vifs contained a TLQ-BC box that is essential for ELOB/C binding (Fig. 3.14A). In addition, a KCCC motif that is similar to the HCCH motif of HIV-1 Vif is found in FIV Vif. In the KCCC motif, I identified a conserved hydrophobic domain (172MIIRGE177; Fig. 3.14A). Despite the low sequence identity of only 13% in this region between FIV Vif and HIV-1 Vif, this hydrophobic domain matched when the C-terminal regions of both Vifs were aligned (Fig. 3.14A). In the complex structure of HIV-1 Vif/CUL5 (158), residues 120IR121 of HIV-1 Vif are involved in the direct interaction with CUL5 (Fig. 3.14B). To investigate whether the equivalent hydrophobic domain 172MIIRGE177 of FIV Vif is also involved in CUL5 binding, 172MI173, 174IR175, or 176GE177 were replaced with alanines (Materials and Methods 2.9; Fig. 3.14C). The binding activities of these FIV Vif mutants with CUL5 were evaluated by co-IP assays (Materials and Methods 2.15). The results showed that FIV Vif 176177GE-AA bound CUL5 similar to the wild type FIV Vif and 172173MI-AA slightly impaired the FIV Vif/CUL5 interaction, while 174175IR-AA impaired binding (Fig. 3.14C). Additionally, single point mutations were introduced at 174IR175 and the I174A and R175A mutations of FIV Vif also decreased the CUL5 interaction (Fig. 3.14C). Taken together, I conclude that the conserved 174IR175 motif of FIV Vif is the main CUL5 binding site.

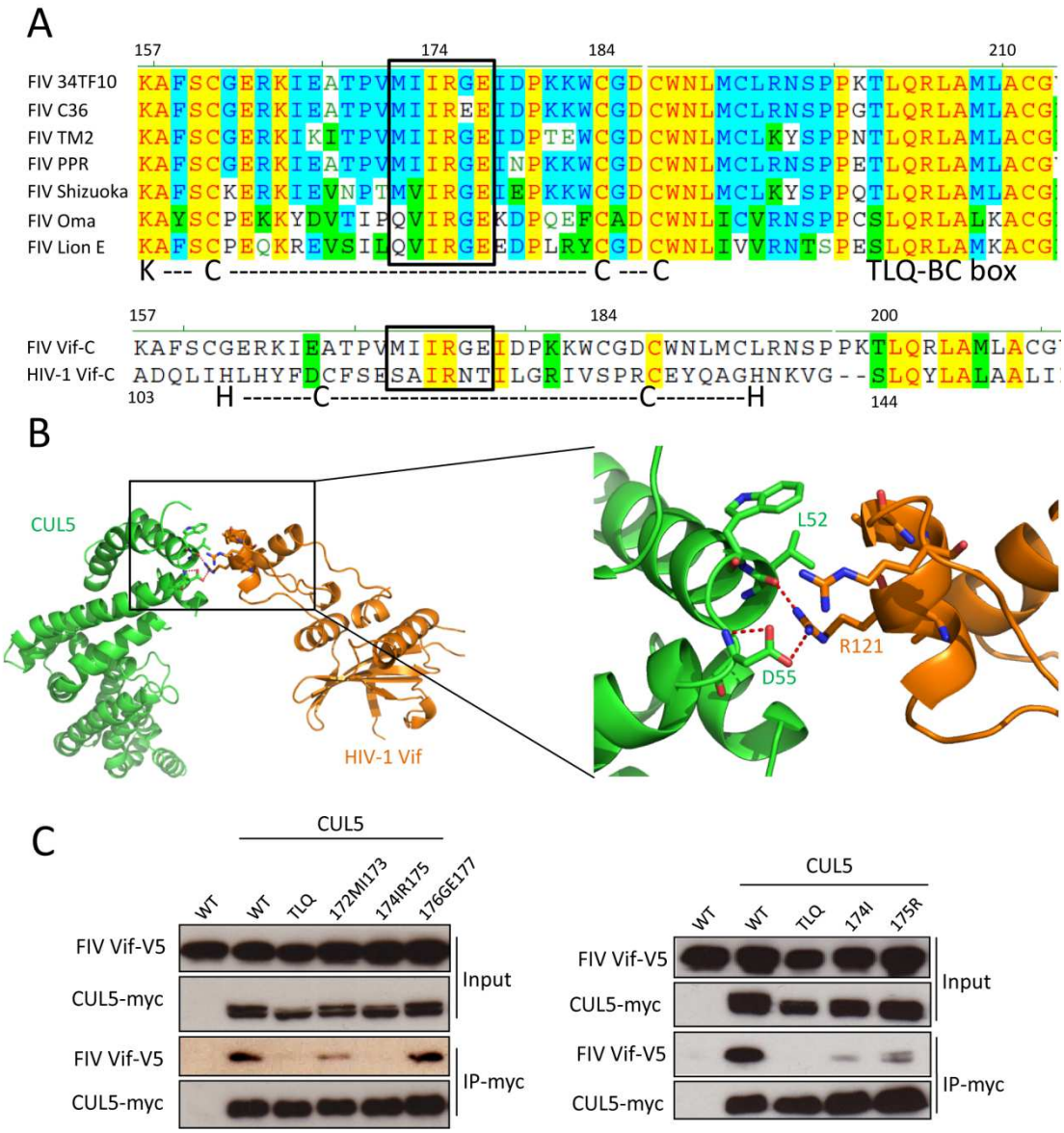

Fig. 3.14 Identification of determinants in the C-terminus of FIV Vif that regulate binding to CUL5. (A) Top: Sequence alignment of FIV Vifs from different FIV strains including 34TF10, C36, TM2, PRR, Shizuoka, Oma (Pallas's cats), and lion subtype E. Bottom: Sequence alignment of C-terminal residues of FIV Vif (clone 34TF10) and HIV-1 Vif (clone NL4-3). KCCC: a motif of FIV Vif similar to the HIV-1 Vif Zinc interaction region HCCH. Boxed region: a conserved hydrophobic motif. Non-similar: black with no background; Conservative: blue with cyan background; Block of similar: black with green background; identical: Ren with yellow background; weakly similar: green with no background. (B) The structure of the HIV-1 Vif-CUL5 complex (Vif, orange; CUL5, green) (PDB entry 4N9F). A close-up view of the HIV-1 Vif-CUL5 interface is shown. The residues that are involved in the HIV-1 Vif-CUL5 interaction

are indicated. Red dashed lines represent hydrogen bonds. (C) myc-CUL5 or pcDNA3.1 empty plasmids were co-transfected with FIV Vif-V5 wild type or indicated FIV Vif mutant expression plasmids. Immunoprecipitated complexes (IP) were analyzed by immunoblotting with anti-V5 for FIV Vif and anti-myc for CUL5.

Next, the degradation activity of FIV Vif 174175IR-AA towards feline A3 was tested (Materials and Methods 2.10 and 2.12). The results showed that FIV Vif 174175IR-AA did not induce degradation of co-expressed FcaA3Z2bZ3 (Fig. 3.15A) and lost the ability to inhibit the anti-FIV activity of FcaA3Z2bZ3 (Fig. 3.15B). These data support the model that CUL5 binding of FIV Vif is essential for its antagonism of feline A3s. Furthermore, I asked whether impairing the CUL5 binding sites of FIV Vif affects its interaction with feline A3 and ELOB/C. To address this question, 293T cells were co-transfected with expression plasmids for wild type FIV Vif or alanine mutations of TLQ or 174IR175 together with expression plasmids for FcaA3Z2bZ3 or ELOB and ELOC. The immunoprecipitation results indicate that alanine mutations of FIV Vif TLQ and 174IR175 variants did not lead to a loss of binding to FcaA3Z2bZ3 (Fig. 3.15C). However, the FIV Vif TLQ-AAA variant lost its interaction with ELOB/C, as shown previously (168). The Vif 174175IR-AA variant bound to ELOB/C similar to the wild type FIV Vif (Fig. 3.15D). Together, these results support that residues 174IR175 of FIV Vif are required for the interaction with CUL5.

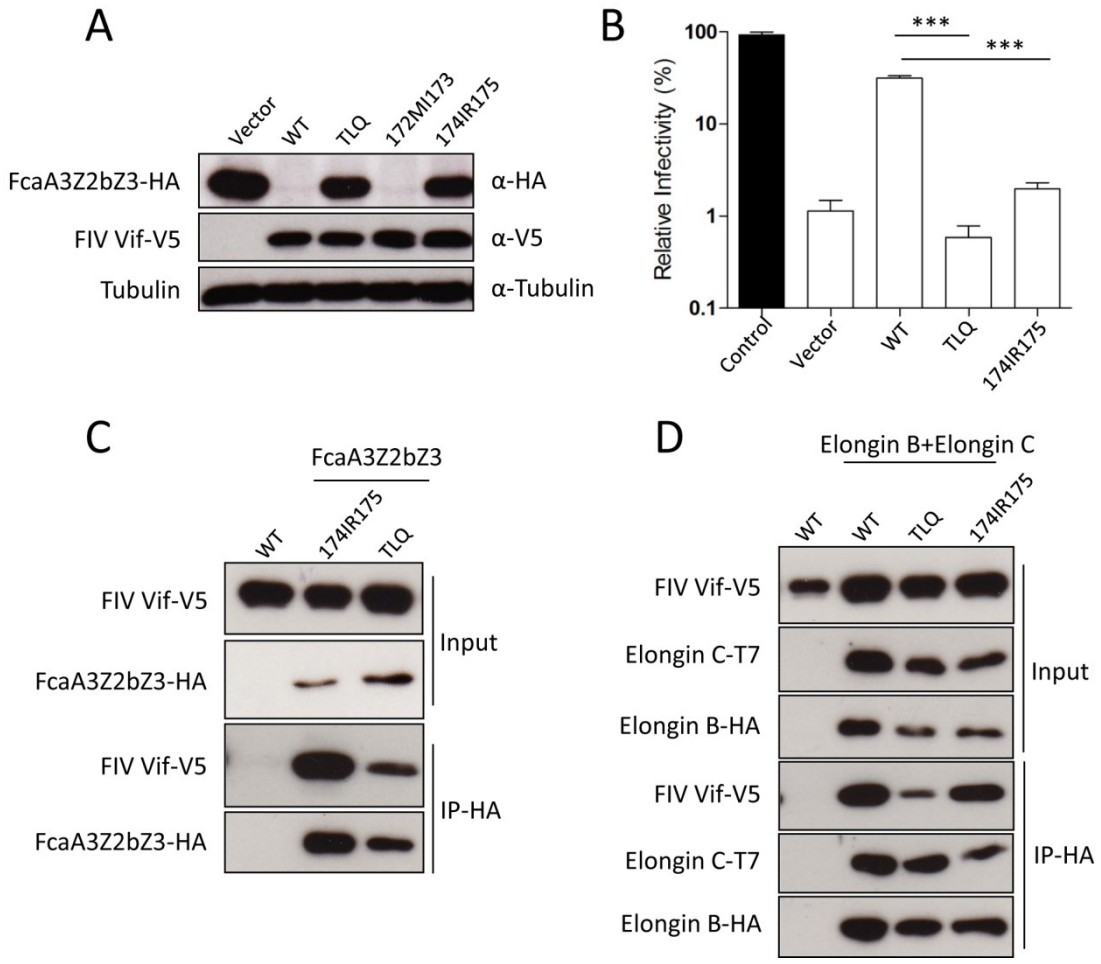

Fig. 3.15 Mutating residues 174IR175 in FIV Vif does not impair interaction with FcaA3s, ELOB and ELOC. (A) Cells were transfected with FcaA3Z2bZ3-HA and FIV Vif-V5 wild type or indicated FIV Vif mutant expression plasmids or pcDNA3.1 empty plasmid. Cells were harvested and analyzed by immunoblotting with anti-HA, anti-V5 and anti-tubulin antibodies, respectively. (B) Single round FIVΔ*vif* luciferase reporter virions were produced in the presence of feline A3 expression plasmids (FcaA3Z2bZ3) with FIV Vif wild type or Vif mutants, pcDNA3.1(+) was added as a control for feline A3 (control) and FIV Vif (vector). Infectivity of reporter vectors was determined by quantification of luciferase activity in 293T cells transduced with normalized amounts of viral vector particles. (C, D) 293T cells were transfected with expression plasmids for FcaZ2bZ3-HA, FIV Vif-V5 wild type, indicated FIV Vif mutants or pcDNA3.1 empty plasmid (C); or FIV Vif-V5 wild type, indicated FIV Vif mutants, T7-ELOC or HA-ELOB and pcDNA3.1 empty plasmid (D). Cells were harvested at 48 h after transfection, protein of cell lysates (input) and immunoprecipitated complexes (IP) were

analyzed by western blots stained with anti-V5 antibody for FIV Vif, anti-HA antibody for FcaZ2bZ3-HA and HA-ElonginB and anti-T7 antibody for T7-ElonginC.

3.3.4 Modeling the FIV Vif/CUL5 complex structure.

To identify further interacting residues in the FIV Vif/CUL5 complex, we, in collaboration with Prof. Holger Gohlke, built a homology model of the complex to guide mutational analyses (Materials and Methods 2.17). As described in the methods section, we incorporated information of the predicted secondary structure of FIV Vif and our results about the importance of residues 174IR175 and the TLQ-BC box for CUL5 binding when generating the sequence alignment of FIV Vif to HIV-1 Vif. We did so due to the sequence identity between FIV and HIV-1 Vif is only 5.2%. In this way, residues corresponding to the FIV 174IR175 and TLQ-BC box motifs were identified in HIV-1. The homology model of the FIV Vif/CUL5 complex showed a contact of the TLQ-BC box with CUL5 and revealed a close proximity of residues 174IR175 of Vif to residues 52LWDD55 of CUL5 (Fig. 3.16A and B). Thus, I mutated 52LW53 and 54DD55 of CUL5 to alanines and tested these CUL5 variants for interaction with FIV Vif (Materials and Methods 2.9 and 2.15). The results showed that CUL5 52LW53-AA no longer bound to FIV Vif; however, the CUL5 54DD55-AA variant still bound Vif similar to the wild type CUL5 (Fig. 3.16C). Additionally, I tested whether the CUL5 52LW53-AA mutant effects FIV Vif induced feline A3s degradation (Materials and Methods 2.10 and 2.12). I expressed the indicated feline A3s together with FIV Vif and the CUL552LW53-AA mutant in 293T cells. Immunoblots of protein extracts from transfected cells were used as readout for the degradation of the respective A3 protein. The results showed that FIV Vif degraded feline A3s with an unchanged efficiency in the presence of this CUL5 mutant (Fig. 3.16D). A model representing the FIV Vif E3 complex is shown in Fig. 3.16E.

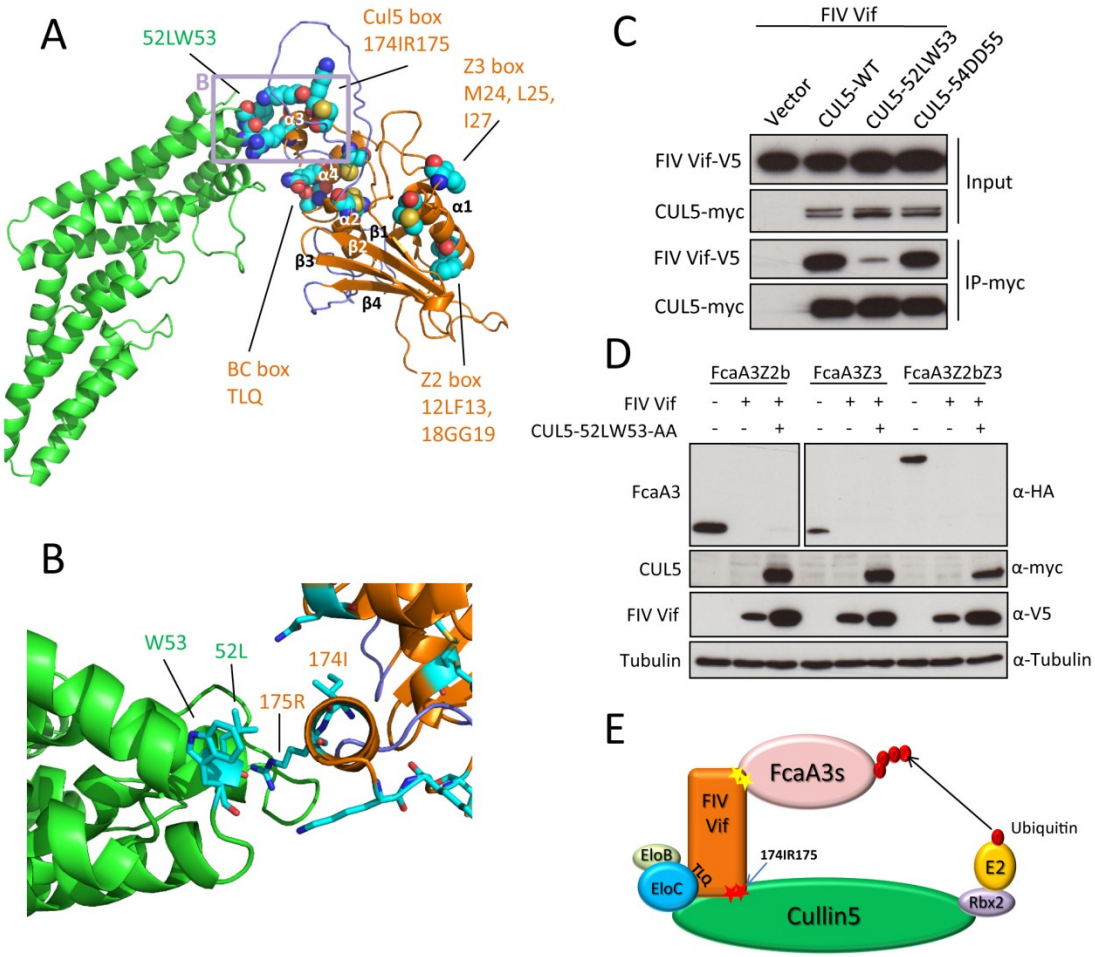

Fig. 3.16 FIV Vif-CUL5 3D structure model. (A) Homology model of the FIV Vif (orange)-CUL5 (green) complex in cartoon representation. Helices α3 and α4 of Vif are interacting with CUL5. The model contains two unstructured loops (navy) before and after helix α2, as no structural template is available for these regions. These loops might be important for binding other parts of the complex. Residues that were subjected to mutational analysis are shown in spheres representation. The region of the close up shown in B is indicated by a light plum rectangle. (B) Close-up view of the homology model of the FIV Vif (orange)-CUL5 (green) complex in cartoon representation, with interacting residues shown in sticks representation. (C) The myc-CUL5 wild type or indicated mutants expression plasmids were co-transfected with FIV Vif-V5 wild type expression plasmid into 293T cells. Cell lysates were immunoprecipitated with anti-myc beads and then analyzed by immunoblotting with anti-V5 antibody for FIV Vif and anti-myc antibody for CUL5. (D) 293T cells were co-transfected with expression plasmids for FcaA3Z2b-HA, FcaA3Z3-HA or FcaA3Z2bZ3-HA; CUL5-52LW53-AA

mutant with FIV Vif-V5. pcDNA3.1 was used as control plasmid to replace the FIV Vif or CUL5 expression plasmids. Cells were analyzed by immunoblotting using anti-HA, anti-V5, anti-CUL5, anti-Flag and anti-tubulin antibodies, respectively. (E) Model of FIV Vif with E3 ligase complex. The CUL5 interaction sites of FIV Vif (174IR175) are shown as red star. Figure A and B are produced by my cooperator Dr. Christoph G. W. Gertzen and Prof. Holger Gohlke, and included into my thesis with permission.

3.3.5 The FIV Vif/CUL5 interaction is zinc-independent.

Several previous studies demonstrated that the zinc binding motif (HCCH) of HIV-1 or SIV Vif regulates Vif/CUL5 interaction (207). Our FIV Vif/CUL5 complex model suggests that helix 3 of FIV Vif-CTD regulates the CUL5 binding (Fig. 3.16 and 3.17A). There are two positively charged lysines (K181 and K182) and several potential zinc-binding cysteines (C138, C161, C184, C187, C192, and C209) at the FIV Vif CTD (Fig. 3.17B). To further address the FIV Vif/CUL5 interaction properties, K181 and K182 were mutated to alanines and several potential zinc-binding residues were mutated to serine (C138S, C161S, C184S, C187S, C192S, and C209S; Materials and Methods 2.9; Fig. 3.17B). The immunoprecipitation results revealed that the C184S and C184C187-SS variants decreased the CUL5 interaction, but Vif mutations K181A, K182A, C187S, C138S, C161S, C192S and C209S did not affect CUL5 binding (Fig. 3.17C). Additionally, I tested the interaction of several FIV C-S mutants (C161S, C184S, C187S and C209S) with endogenous CUL5. The result showed that only C184S mutant lost CUL5 binding activity (Fig. 3.17D). I further investigated the binding property of FIV Vif C184S mutant to feline A3 and ELOB/C. The immunoprecipitation results indicate that FIV Vif C184S mutant has weaker binding affinity to FcaA3Z2bZ3 (Fig. 3.17E), compared with FIV Vif TLQ-AAA mutant and both, FIV Vif TLQ-AAA and C184S, lost interaction with ELOB/C (Fig. 3.17F). I further found that FIV Vif C161S, C184S and C187S mutants completely lost FcaA3Z2bZ3 degradation function, but the other cysteine mutants (C138S, C192S and C209S) efficiently degraded FcaA3Z2bZ3 (Fig. 3.17G). Taken together, these data indicate that C184 of FIV Vif is not specific for CUL5 interaction, and I speculate that C184 may regulate the integral structure of FIV Vif.

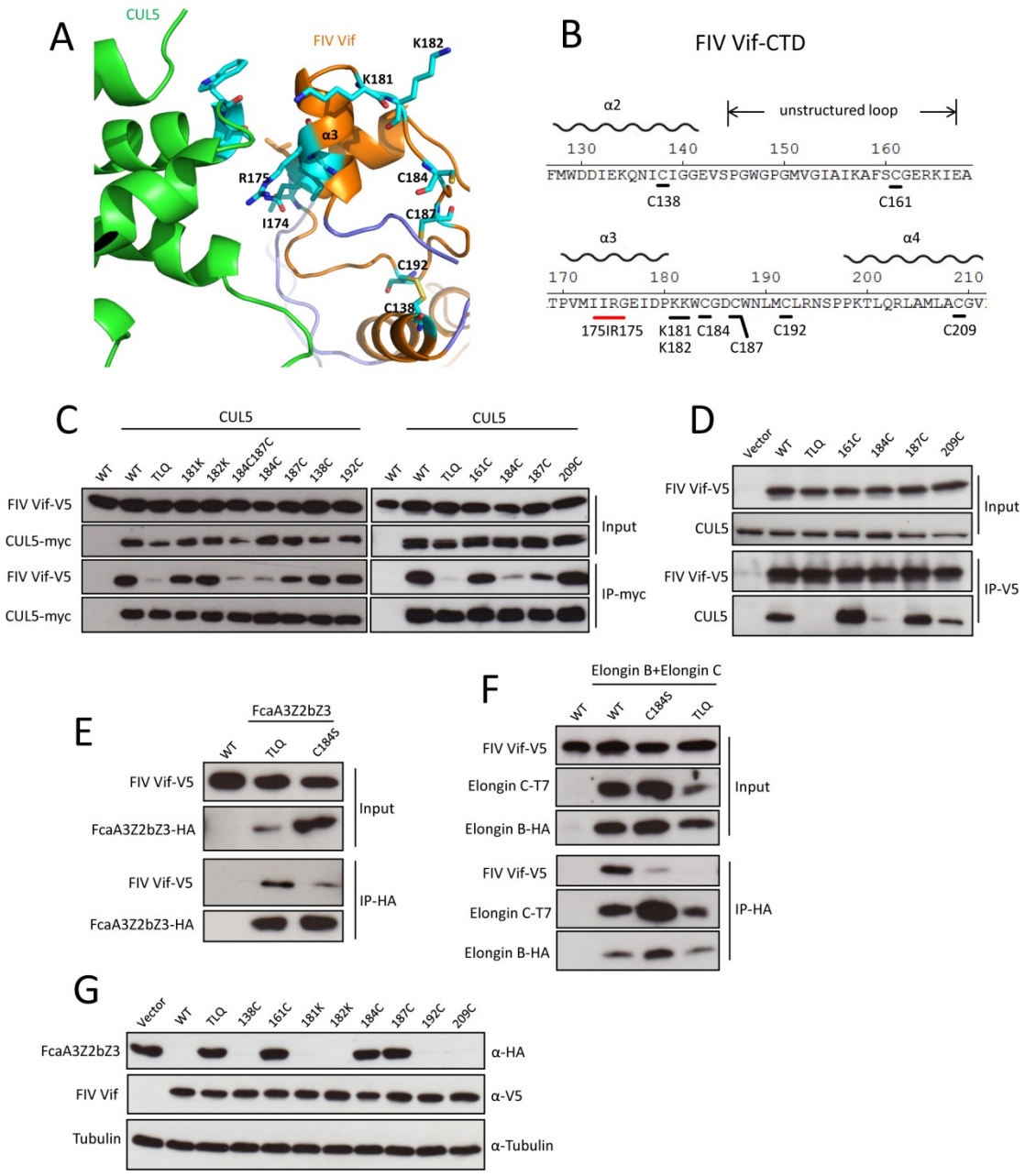

Fig. 3.17 C184 of FIV Vif is essential for Vif-CUL5, Vif-FcaA3 and Vif-ELOB/C interaction (A) Close-up view of the homology model of the FIV Vif (orange)-CUL5 (green) complex in cartoon representation, with residues that underwent mutational analysis shown in sticks representation. These residues are: K181, K182, C184, C187 and C192 in the loop following helix 3 of FIV Vif; C138 that forming a disulfide bond with C192 is also shown. (B) Sequence representation of FIV Vif C terminal domain (CTD). (C) myc-CUL5 or pcDNA3.1 empty plasmid was co-transfected with expression plasmids for FIV Vif-V5 wild type or indicated FIV Vif mutants. Immunoprecipitated complexes (IP) were analyzed by immunoblotting with anti-V5 for FIV Vif and anti-myc for CUL5. (D) 293T cells were transfected with expression plasmids

for FIV Vif-V5 wild type or indicated FIV Vif mutants. Immunoprecipitated complexes (IP) were analyzed by immunoblotting with anti-V5 for FIV Vif and anti-CUL5 for CUL5. (E, F) FIV Vif C184S mutant lost binding capability to FcaA3s, ELOB and ELOC. 293T cells were transfected with expression plasmids for FcaZ2bZ3-HA, FIV Vif-V5 wild type, indicated FIV Vif mutants or pcDNA3.1 empty plasmid (E); or FIV Vif-V5 wild type, indicated FIV Vif mutants, T7-ELOC or HA-ELOB and pcDNA3.1 empty plasmid (F). Cells were harvested at 48 h after transfection, protein of cell lysates (input) and immunoprecipitated complexes (IP) were analyzed by immuno blots stained with anti-V5 antibody for FIV Vif, anti-HA antibody for FcaZ2bZ3-HA and HA-ElonginB and anti-T7 antibody for T7-ElonginC. (G) 293T cells were transfected with FcaA3Z2bZ3-HA and FIV Vif-V5 wild type or indicated FIV Vif mutant expression plasmids or pcDNA3.1 empty plasmid. Cells were harvested and analyzed by immunoblotting with anti-HA, anti-V5 and anti-tubulin antibodies, respectively. Figure A is produced by my cooperator Dr. Christoph G. W. Gertzen and Prof. Holger Gohlke, and included into my thesis with permission.

To test the zinc dependency of the FIV Vif/CUL5 interaction, the cell-permeable zinc chelator TPEN (*N*,*N*,*N*',*N*'-tetrakis (2-pyridylmethyl) ethane-1,2-diamine) was applied in the following experiments. First I tested the effect of TPEN on FIV Vif's ability to induce the degradation of feline A3s.. 293T cells were co-transfected with FIV Vif or HIV-1 Vif and FcaA3Z2bZ3 or HsaA3G and were treated with increasing amounts of TPEN (Materials and Methods 2.10). The immunoblotting results obtained from lysates of these cells indicated that FIV Vif efficiently degraded FcaA3Z2bZ3 in the presence of low concentrations of TPEN (2–4 μM), while higher concentrations of TPEN (5–8 μM) blocked the FIV Vif-induced FcaA3Z2bZ3 degradation (Materials and Methods 2.12; Fig. 3.18A). A similar observation was found in the HIV-1 Vif-HsaA3G degradation assay; however, 4 μM TPEN blocked the HIV-1 Vif-induced HsaA3G degradation, while this concentration of TPEN had no influence on FcaAZ2bZ3 degradation by FIV Vif (Fig. 3.18A and B). Because higher concentrations of TPEN may nonspecifically influence the A3 degradation, I tested the interaction of HIV-1 Vif or FIV Vif with CUL5 by co-IP assays using lysates of cells treated with 5 μM TPEN. The results showed that 5 μM TPEN repressed the HIV-1 Vif/CUL5 interaction, thus supporting the previous

model that HIV-1 Vif/CUL5 interaction is regulated by zinc (Fig. 3.18C) (207-210). In sharp contrast, treatment with 5 μM TPEN did not impair the FIV Vif/CUL5 binding. These data suggest that the FIV Vif/CUL5 interaction is zinc-independent.

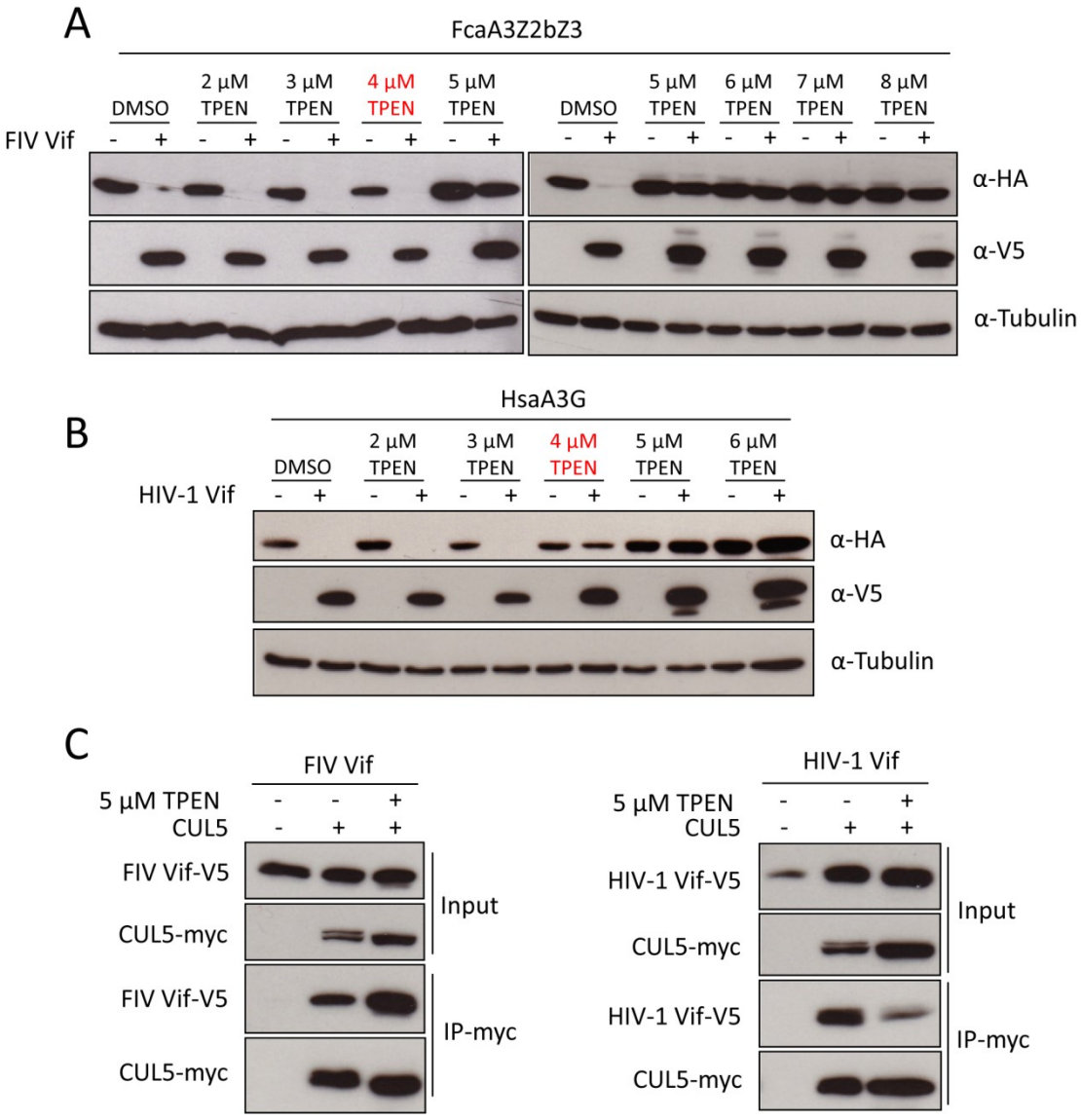

Fig. 3.18 FIV Vif binding to CUL5 is zinc independent. (A, B) 293T cells were transfected with expression plasmids for FcaZ2bZ3-HA (A) or HsaA3G-HA (B); HIV-1 Vif-V5 or FIV Vif-V5, pcDNA3.1 was used as empty plasmid control. The transfected cells were treated with zinc chelator TPEN (2, 3, 4, 5, 6, 7 or 8 μM) or DMSO as control 36 h post transfection. Cells were harvested 12 h later (48 h after transfection) and then analyzed by immunoblotting with anti-HA, anti-V5 and anti-tubulin antibodies. (C) myc-CUL5 expression plasmid was co-transfected with FIV Vif-V5 or HIV-1 Vif-V5 expression plasmids into 293T cells. The

transfected cells were treated with 5 μM TPEN or DMSO 36 h post transfection. Cell lysates were immunoprecipitated with anti-myc beads and then analyzed by immunoblotting with anti-V5 antibody for FIV Vif and HIV-1 Vif, anti-myc antibody for CUL5.

3.4 Cloning domestic cat SERINC3/5 and test their anti-FIV and anti-HIV-1 activities

3.4.1 Cloning and sequencing domestic cat SERINC3/5 gene

Recently, human SERINC3/5 were identified as restriction factors that inhibit the entry of HIV-1, and this restriction is counteracted by HIV-1 Nef (119, 120, 122). However, it is unknown whether domestic cat expresses SERINC3/5 proteins. In the current study, feline SERINC3/5 were cloned from feline CRFK cells. The feline SERINC3/5 cDNAs were verified by sequencing. I then performed the sequence alignment of human and feline SERINC3/5 proteins. The alignment showed that both human and feline SERINC5 contain 461 amino acids, while human and feline SERINC3 include 473 amino acids. Both SERINC3 and SERINC5 are conserved between humans and felines (Fig. 3.19 and 3.20). The different amino acids of SERINC proteins between humans and felines are indicated (black boxes)(Fig. 3.19 and 3.20).

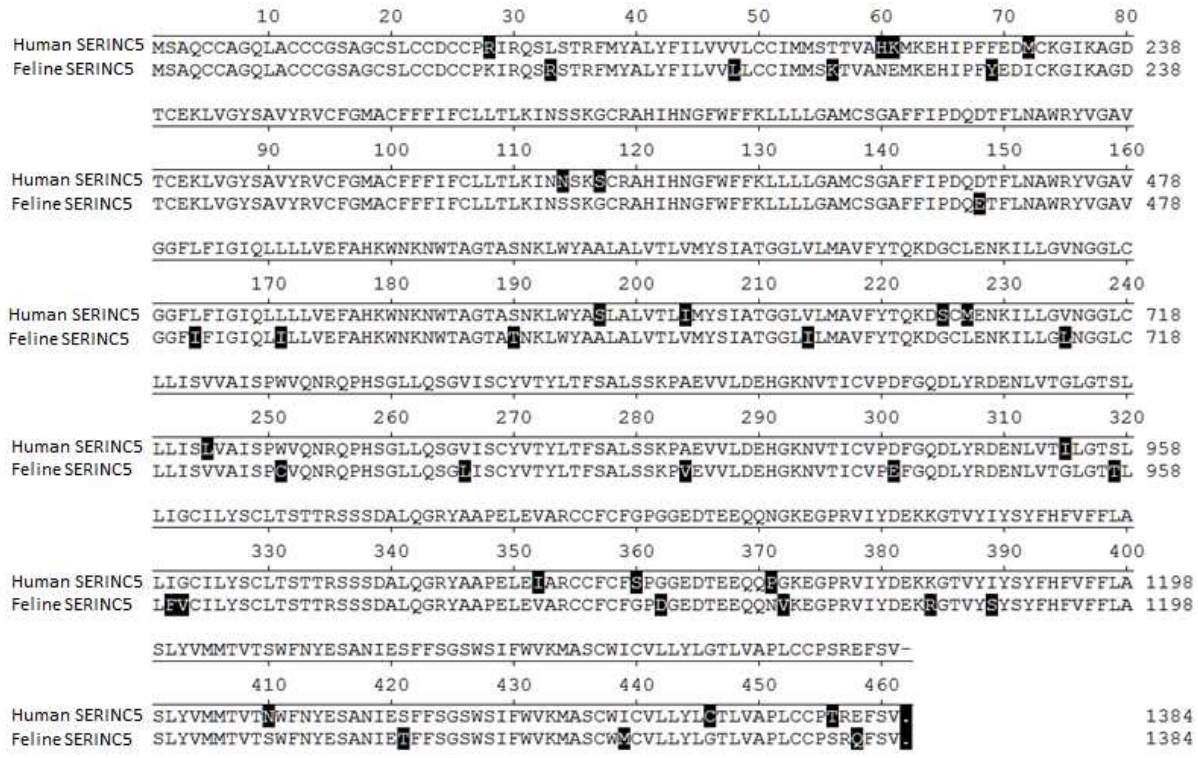

Fig. 3.19 The sequence alignment of human SERINC5 and feline SERINC5. The amino acid sequences of human SERINC5 and feline SERINC5 were aligned by Clustal W method. The black boxes indicate different amino acids.

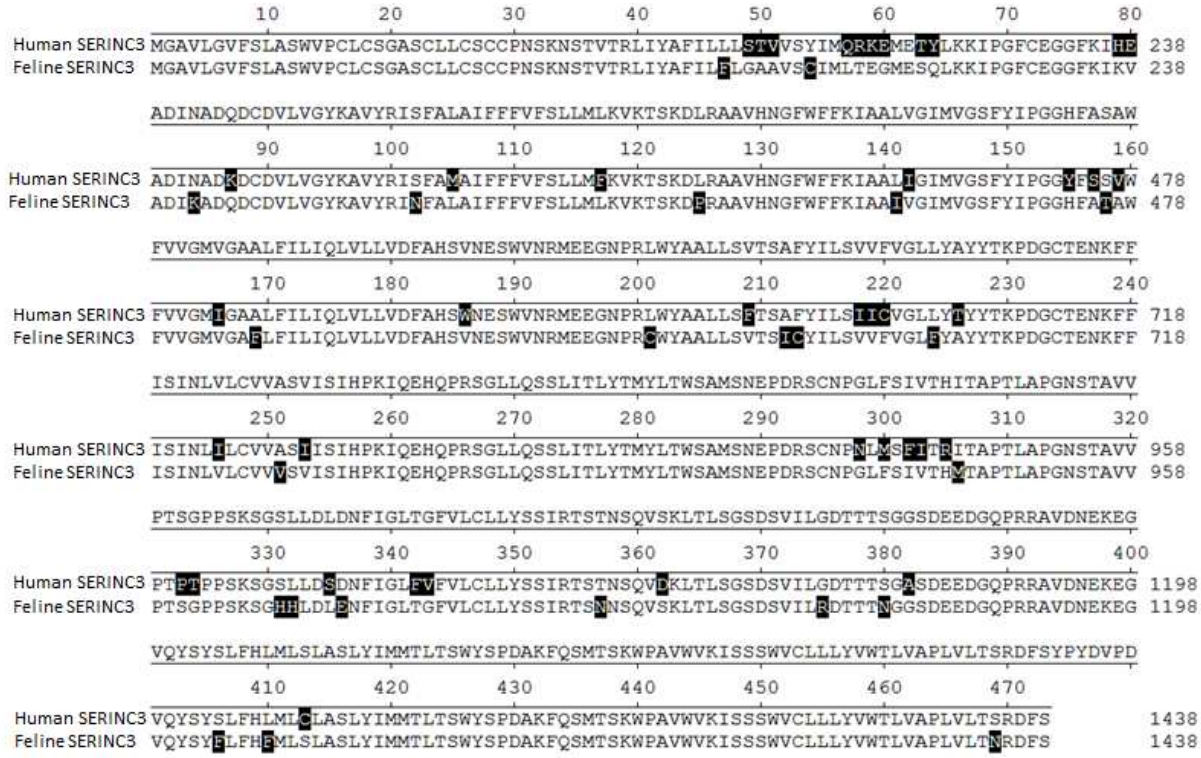

Fig. 3.20 The sequence alignment of human SERINC3 and feline SERINC3. The amino acid sequences of human SERINC3 and feline SERINC3 were aligned by Clustal W method. The black boxes indicate different amino acids.

I also performed a phylogenetic analysis of SERINC3/5 from different species. The results indicated that human, chimpanzee, African green monkey, Rhesus Monkey SERINC5 proteins were found in one clade, and equine and feline SERINC5 proteins clustered into another clade. Rabbit and mouse SERINC5 proteins formed two separate clades, respectively. The phylogenetic analysis of SERINC3 proteins showed the similar classification (Fig. 3.21 and 3.22).

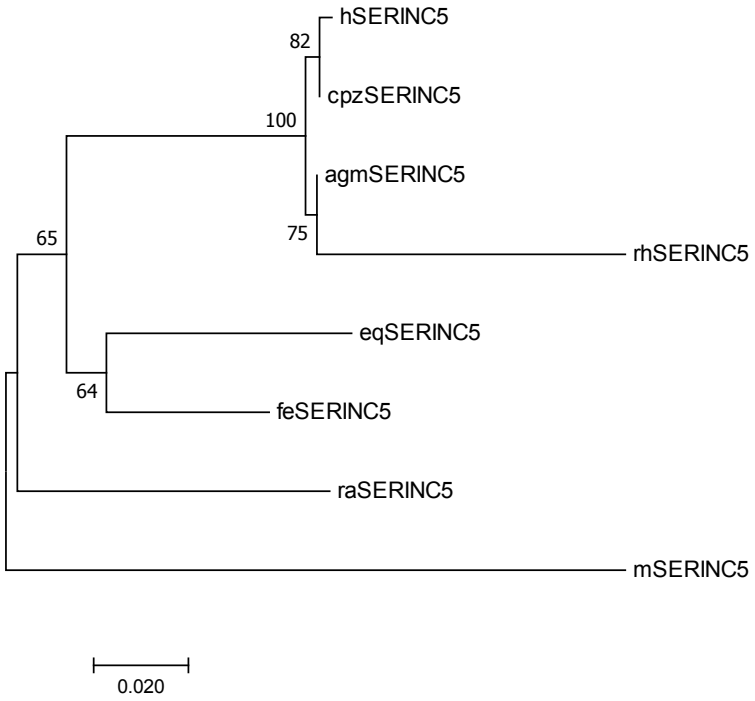

Fig. 3.21 The phylogenetic relationship of SERINC5 from different species. 500 bootstrap replications were performed during calculation and building the tree by using MEGA7 software. The number on each node indicates the bootstrap support. The following SERINC5 sequences were used: Human (h) SERINC5 (NM_178276.6); Chimpanzee (cpz) SERINC5 (XM_016953076.1); African green monkey (agm) SERINC5 (XM_007976640.1); Rhesus Macaque (rh) SERINC5 (XM_015140335.1); Feline (fe) SERINC5 (XM_011284262.3); Equine (eq) SERINC5 (XM_001503874.4); Rabbit (r) SERINC5 (XM_017344548.1); Mouse (m) SERINC5 (NM_172588.2).

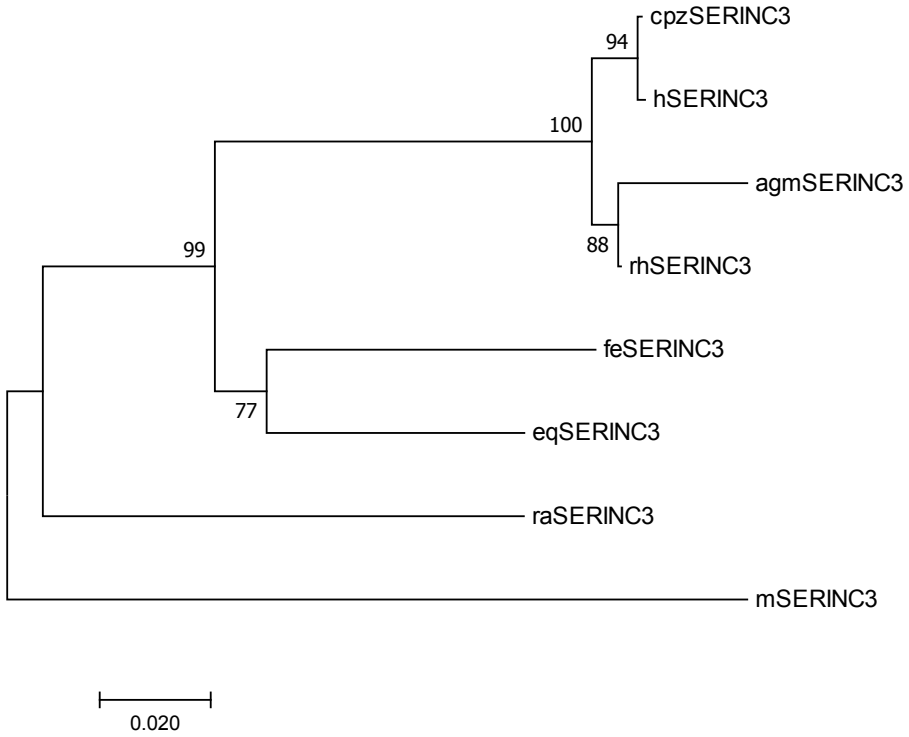

Fig. 3.22 The phylogenetic relationship of SERINC3 from different species. 500 bootstrap replications were performed during calculation and building the tree. The number on each node indicates the bootstrap support. The following SERINC3 were used. Human (h) SERINC3 (NM_006811.3); Chimpanzee (cpz) SERINC3 (NM_001280388.1); African green monkey (agm) SERINC3 (XM_008016564.1); Rhesus Macaque (rh) SERINC3 (NM_001260972.1); Feline (fe) SERINC3 (XM_011280708.3); Equine(eq) SERINC3 (XM_001917430.4); Rabbit (r) SERINC3 (XM_008274475.2); Mouse(m) SERINC3 (NM_012032.4).

Then, the feline SERINC3 and SERINC5 cDNAs were cloned into mammal expression plasmids (pcDNA3.1+ or pBJ6). The expression of these two proteins was detected by immuno blots of cell lysates from transfected 293T cells (Materials and Methods 2.10 and 2.12). Human SERINC5 served as control. The results revealed that feline SERINC3 and SERINC5 proteins have a molecular weight of around 42 KDa. Compared to human SERINC5 and feline SERINC3, feline SERINC5 protein showed a lower expression level (Fig. 3.23).

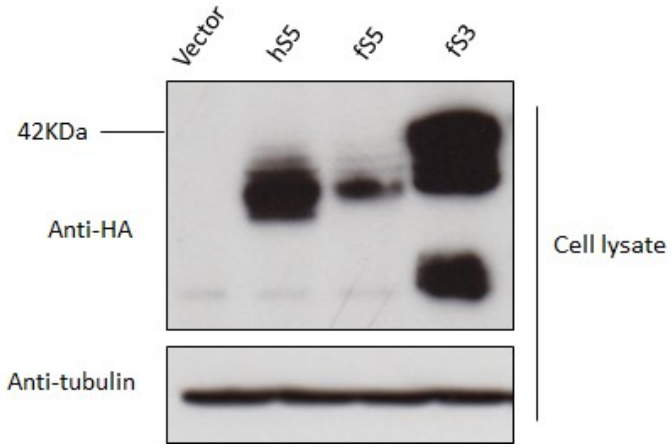

Fig. 3.23 The expression of SERINC in 293T cells. 293T cells were transfected with human SERINC5 (hS5), feline SERINC5 (fS5) and feline SERINC3 (fS3) expression plasmids or pcDNA3.1 empty plasmid. Cells were harvested and analyzed by immunoblotting with anti-HA and anti-tubulin antibodies, respectively.

3.4.2 Domestic cat SERINC3/5 proteins display antiviral activity against HIV-1 and FIV

Human SERINC3/5 display strong inhibition of several retroviruses (HIV-1, EIAV and MLV) in an Env-dependent mechanism (123). The protein similarity of human SERINC and feline SERINC is high. Thus, we tested the anti-HIV activity of feline SERINC3 and SERINC5, in collaboration with Dr. Hanna-Mari Baldauf at the Institute of Virology in Technical University Munich (LMU). Wild type HIV-1 and Nef-deficient HIV-1 were produced in 293T cells in the presence of different SERINC proteins. The viral infectivity was determined by infecting TZM-bl cells. The result indicated that human SERINC5 and feline SERINC3 showed around 50% inhibition against HIV-1Δ*nef.* Feline SERINC5 restricted around 75% infection of HIV-1Δ*nef* (Fig. 3.24). HIV-1 Nef overcame the restriction of human SERINC5 and recovered viral infectivity to the similar level of vector control (Fig. 3.24). Interestingly, HIV-1 Nef also had capability of antagonizing the restrictions of feline SERINC5 and SERINC3, which indicates a conserved Nef counteraction mechanism (Fig. 3.24).

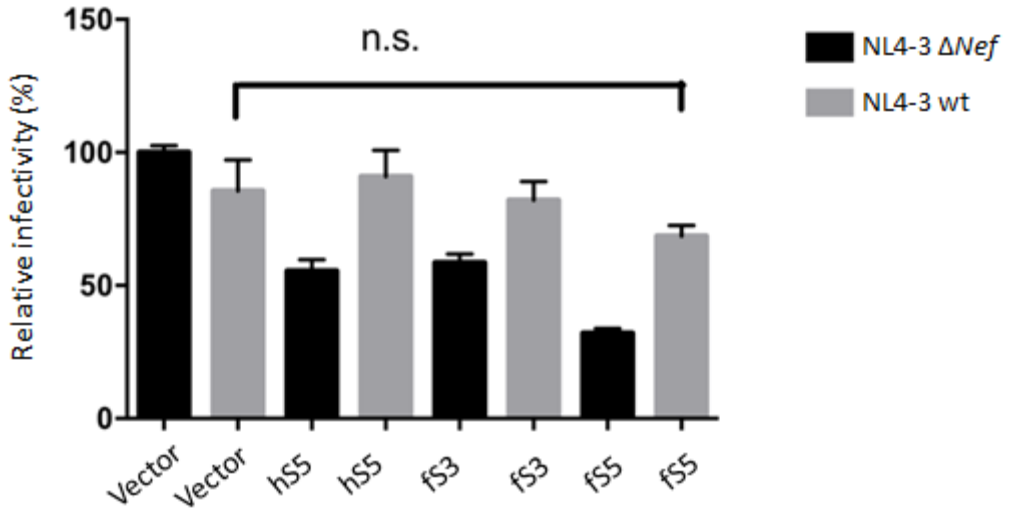

Fig. 3.24 The anti-HIV activity of feline SERINC. HIV-1Δ*nef* or HIV-1 wild type virions were produced in the presence of human SERINC5 (hS5) or feline SERINC expression plasmids (fS5 or fS3), pBJ6 empty vector was added as a control (vector). Viral Infectivity was determined by quantification of luciferase activity in TZM-bl cells transduced with particles. This figure is produced by my cooperator Patrícia Pereira, and included into my thesis with permission.

In addition, I tested feline SERINC restriction against FIV by using FIV based single round infection assays. Env- or VSV-G-pseudotyped FIVs were produced in the presence of SERINC in transfected 293T cells. The viral infectivity was determined by infecting feline CRFK-CD134 cells. The results revealed that human SERINC5 and feline SERINC5 displayed strong restriction against Env-pseudotyped FIV (Fig. 3.25A). In contrast, no inhibition was observed by feline SERINC3 (Fig. 3.25A). Interestingly, I did not observe any antiviral activity of human SERINC5, feline SERINC5 and feline SERINC3 when FIV was pseudotyped with VSV-G (Fig. 3.25B). These data indicate that feline SERINC5 suppresses FIV infection by an Env-dependent mechanism.

Next, I produced complete (full length) FIV virions in the presence of feline SERINC and the FIV reporter transfer vector pLinSin from 293T cells (Materials and Methods 2.10). The viral infectivity data indicated that human SERINC5 and feline SERINC5 showed strong restriction against PPR-based FIV (Petaluma strain), while feline SERINC3 had less inhibition (Materials and Methods 2.11; Fig 3.26A). FIV-C36 belongs to FIV subtype C, and this clone was obtained

by lambda cloning from cats that developed severe immunodeficiency disease when infected with CABCpady00C (Abbotsford, British Columbia, Canada) (Sohela de Rozie`res et al. 2004 JVI). Human SERINC5 and feline SERINC5 also strongly inhibited FIV-C36 infection (Fig. 3.26B). These data suggest that FIV has no capability of counteraction the antiviral function of feline SERINC.

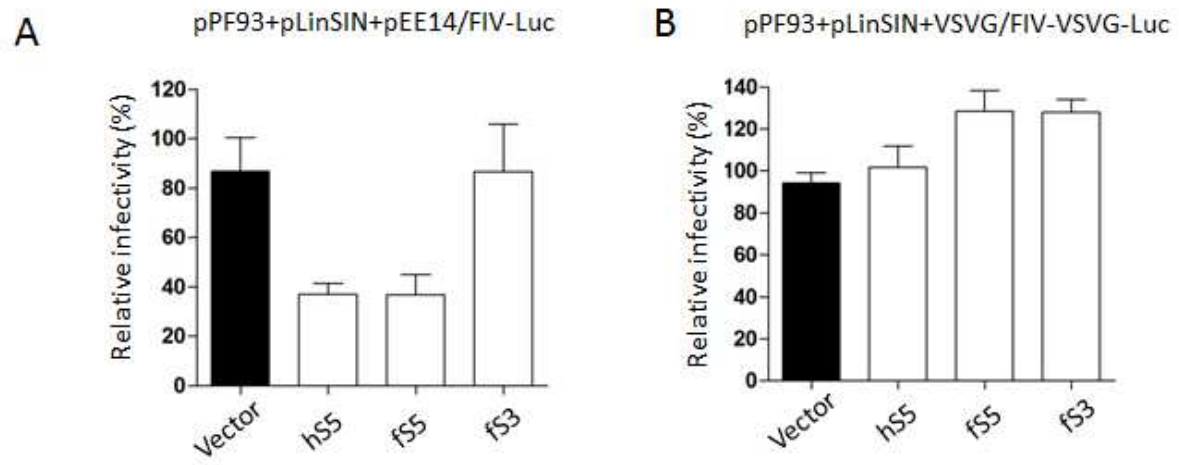

Fig. 3.25 The anti-FIV activity of feline SERINC. Single-round Env or VSV-G pseudotyped FIV luciferase reporter virions ("3-plasmid system" including pPF93, pLinSin, and pEE14 or pMD.G) were produced in the presence of human SERINC5 (hS5) or feline SERINC expression plasmids (fS5 or fS3), pBJ6 empty vector was added as a control (vector). Infectivity of reporter vectors (normalized by reverse transcriptase activity) was determined by quantification of luciferase activity in CRFK-CD134 cells transduced with vector particles.

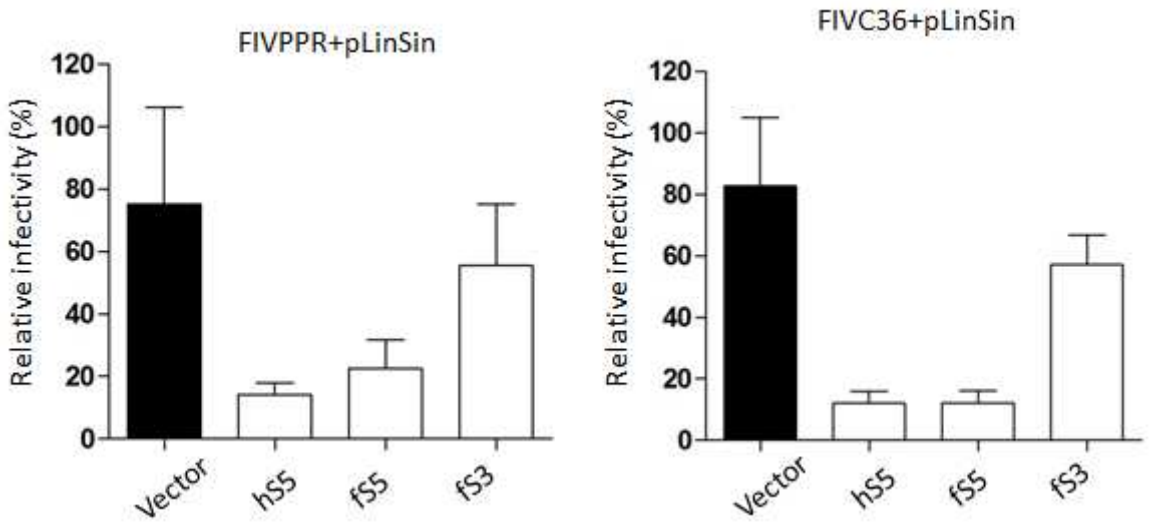

Fig. 3.26 FIV does not counteract feline SERINC restriction. Full length FIV molecular clones (PPR or C36) and FIV luciferase transfer vector (pLinSin) were transfected together with human SERINC5 (hS5) or feline SERINC expression plasmids (fS5 or fS3), pBJ6 empty vector was added as a control (vector). Viral infectivity was determined after normalization for reverse transcriptase activity by quantification of luciferase activity in CRFK-CD134 cells infected with FIV particles.

Furthermore, the incorporation of feline SERINC into viral particles was investigated. Full length FIV (PPR) virions were produced in the presence of SERINC in 293T cells (Materials and Methods 2.10). Viral particles were concentrated by centrifugation, and the presence of SERINC proteins were detected by immuno blots (Materials and Methods 2.12). The results revealed that human SERINC5, feline SERINC5 and feline SERINC3 were packaged into FIV viral particles (Fig. 3.27). Interestingly, I observed that human SERINC5 and feline SERINC5 increased the FIV particle release compared to vector control (Fig. 3.27). However, feline SERINC3 had no effect on p24 capsid level of FIV in viral supernatants (Fig. 3.27).

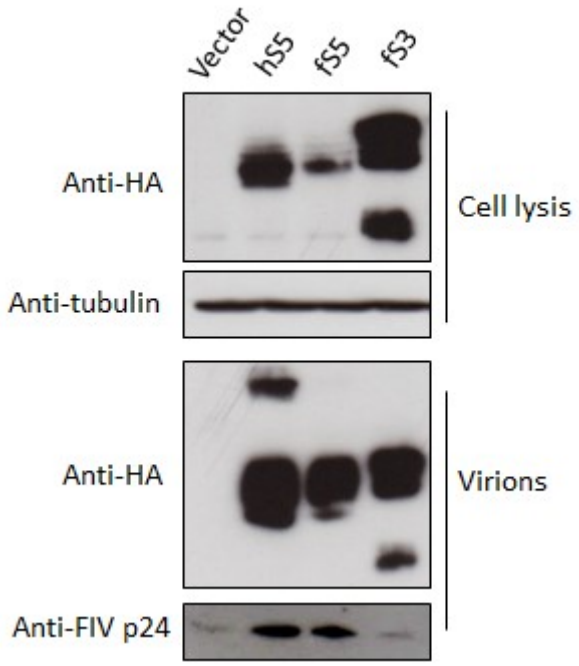

Fig. 3.27 Feline SERINC5 and SERINC3 are packaged into FIV particles. A full length FIV molecular clone (PPR) was transfected together with pcDNA3.1(+) based human SERINC5 (hS5) or feline SERINC expression plasmids (fS5 or fS3), pcDNA3.1(+) empty vector was added as a control (vector). FIV particles were concentrated by centrifugation. The expression of SERINC in 293T cells was detected by anti-HA antibody. Cell lysates were also analyzed for equal amounts of total proteins using anti-tubulin antibody. Feline SERINC5 and SERINC3 packaged into FIV particles were detected by anti-HA antibodies. FIV virions were detected by anti-FIV p24 antibodies.

4. Discussion

In this study, I characterized the interaction of FIV Vif with feline A3 proteins and Cullin5. The Vif protein has the capacity to form a multi-protein complex that includes the different A3 restrictions factors and cellular E3 ligase proteins. First, I identified potential specific interaction sites in FIV Vif for the degradation of feline A3Z2 and A3Z3. Several motifs of FIV Vif were also identified that were important for the degradation of all feline A3s. Then, I described essential domains in the feline A3Z2 and A3Z3 proteins for FIV Vif induced their degradation. Together, these results provide important insights for future experiments describing the FIV Vif interaction with A3s and other cellular proteins.

As mentioned, Vif binds to several diverse proteins at the same time. The molecular interaction of FIV Vif with Elongin C was already identified (168). In addition, Cullin 5 forms the E3-ligase complex. Thus, the goal was to characterize the FIV Vif binding to CUL5. The less expected results show that the presumed FIV Vif-CUL5 interaction surface, structurally mirrors the one in HIV-1 Vif, even if the zinc dependency of both Vifs is different.. Positive selection is not seen in mammalian CUL5 and, thus, the data that Vif protein interaction with CUL5 show evolutionarily preserved interfaces. In contrast, after cross-species transmissions, the lentiviruses adapt to rather variable A3 proteins, which are under positive selection. Furthermore, the current study shows for the first time that feline SERINC5 is an antiviral restriction factor against both FIV and HIV-1Δ*nef*, while feline SERINC3 only inhibits the infection of HIV-1Δ*nef* with less restriction for FIV. In addition, FIV seems to be unable to antagonize the restriction of feline SERINC5, while HIV-1 utilizes its Nef protein to overcome that restriction.

4.1 The interaction between FIV Vif and feline A3s

4.1.1 Comparison of HIV-1 Vif and FIV Vif sites that important for degradation A3s

Previous studies have identified several determinants in HIV-1 Vif, which confer selective interactions with A3F or A3G (e.g. 39YRHHY44 for interaction with A3G, 13DRMR17 for interaction with A3F) (185, 188, 211, 212). Additionally, some motifs of HIV-1 Vif regulate its binding to both A3G and A3F (e.g. 55VxIPx$_4$L64, 69YxxL72 and 96TQx$_5$ADx$_2$I107, x can be any amino acid) (211, 213, 214). In this study, I identified two motifs (12LF13 and 18GG19) in the

FIV Vif N-terminal region that specifically determine its interaction with feline A3Z2 (Fig. 3.2). I also found that the residues M24, L25 and I27 of FIV Vif mediate the selective interaction with feline A3Z3 (Fig. 3.4). Only by impairing the feline A3Z2 and A3Z3 interaction sites together, was it possible to generate a FIV Vif that lost its counteractivity against the feline double domain A3Z2Z3 (Fig. 3.4C and D). In addition, nine discontinuous, conserved Vif motifs (Y26, 53FI54, 57LR58, 61EGI63, 65WSF67, 81VAG83, 95YI96, 119VN120 and 126GFM128) were identified that were shown to be necessary for inducing degradation of all three feline A3s (Fig. 3.3B and C). Why mutations in these residues blocked the degradation of feline A3s was not investigated here. I can speculate that amino acid changes in some of these motifs affect the integrity of the Vif protein. However, some conserved residues of Vif likely form part of the Vif-A3 interface. In addition, some of these residues may interact with cellular proteins important for A3 degradation. Recently, the HIV-1 Vif structure was reported, and it shows that the region forming the β1, β6 strands and α2 helix of HIV-1 Vif are involved in CBF-β binding (158). Impairing the α2 helix (T(Q/D/E)x_5ADx_2(I/L)) of HIV-1 Vif disrupted the neutralizing activity of HIV-1 Vif towards both A3G and A3F (213). Whether the nine discontinuous motifs of FIV Vif are involved in the interaction with the E3 ligase or an unknown co-factor needs more investigation.

A previous study demonstrated that A3F.E289 and HIV-1 Vif.R15 display a strong interaction by applying molecular docking (179). Additionally, it was reported that several electrostatic interfaces of HIV-1 Vif are involved in binding to A3F and A3C (179, 212). In this study, the specific feline A3Z3 interaction sites (M24, L25 and I27) of FIV Vif belong to hydrophobic residues, and FIV Vif counteraction against feline A3Z3 was also determined by the size of the side chain of FIV Vif residue 25 (Fig. 3.3C and D). These results may indicate that the interactions of FIV Vif with feline A3Z3 and HIV-1 Vif with human A3s are quite different. Yoshikawa *et al.* demonstrated that the exposed surface area of feline A3Z3 residue 65 determines its interaction with FIV Vif (190). Whether M24, L25 or I27 of FIV Vif directly interact with I65 of feline A3Z3 by the specific spatial distance needs further investigation.

4.1.2 FIV Vif cellular localization

In this study, I found that FIV Vif protein localized to both cytoplasm and nucleus, but was mainly found be cytoplasmic (Fig. 3.5), which is consistent with a previous observation (202).

I also observed that the FIV Vif protein formed several puncta in the cytoplasm that may be caused by Vif oligomerization (Fig. 3.5). Previous reports showed that HIV-1 Vif also localized to both the cytoplasm and nucleus compartments (215, 216). Mutations of feline A3Z2 and A3Z3 interaction sites of FIV Vif did not alter the cellular localization of Vif (Fig. 3.5). However, the relationship between Vif localization and A3s degradation is still unclear.

4.1.3 FIV Vif-feline A3 interaction and degradation

Unexpectedly, the specific FIV Vif mutations I found that are relevant for feline A3 degradation did not disrupt the binding of FIV Vif to feline A3Z2 and A3Z3 in pull-down assays (Fig. 3.6). When I tested different N-terminal Vif fragments, the region from amino acid 50 to 110 of FIV Vif was found to be important for binding to feline A3s and may explain why mutations in conserved residues of FIV Vif 50 to 110 regions disrupted the degradation activity of FIV Vif against all three feline A3s (Fig. 3.3B). Several previous observations describe that Vif binding to A3s is important but insufficient to induce degradation (162, 217, 218). Based on a recent wobble model (179), I speculate that the region of FIV Vif 50 to 110 contains the main Vif-A3 interaction interface, whereas the specific feline A3Z2 and A3Z3 interaction sites at the N-terminal 1-50 region provide additional stabilizing contacts.

4.1.4 Conservation of FIV Vif functional sites

The A3G and A3F interaction sites of Vif from different HIV-1 strains are relatively conserved. The feline A3Z2 and A3Z3 interaction sites identified in this study are conserved in Vif from different FIV subtype stains of domestic cat, one FIV of Pallas cats, and two FIV subtype strains of lion (Fig. 3.7). Vifs of puma and bobcat FIVs (FIVpco) are quite different from the other FIV Vifs (Fig. 3.7B). It was reported that puma FIV has a high divergence, and multiple puma FIV strains circulate in pumas (45, 47, 219). One recent study demonstrated that puma FIV Vif is inactive against A3Z3s derived from puma and the domestic cat (191). However, it is important to point out that the described Vif was derived from puma FIV subtype B, which has two deletions at the N-terminal region (Fig. 3.7B). Puma FIV can cause infections in domestic cats, but these infections often are abortive (220-222), which indicates an immune defense from the domestic cat. Specifically, increased A3-related G to A mutations were

detected in viral genomes of puma FIV subtype B during infections in domestic cats (223). These observations indicate that the two N-terminal Vif deletions in puma FIV subtype B might impair viral cross-species transmission. However, it is also important to clarify how this virus evades the restriction from its host A3s.

4.1.5 FIV Vif targets different domain of feline A3Z2 and Z3 for degradation

Our knowledge about the interaction regions of A3s and of human and non-human lentivirus Vifs is limited. It was discussed that Vif is not simply a linker between the substrate A3 and the E3 ubiquitin ligase (218, 224). In this study I investigated the interaction of three groups of Vif proteins (FIV, HIV-2/SIV, HIV-1) with feline A3s. I found that HIV-2 and SIVmac Vifs are able to induce feline A3Z2Z3 degradation by targeting the linker domain, in agreement with two previous studies (164, 173).

A previous study described that the residue A65 in feline A3Z3 modulates the sensitivity to FIV Vif (205). I identified here two additional residues (L41, I42) in feline A3Z3 whose combined mutation resulted in an A3 protein that was resistant even to degradation by very high amounts of co-expressed FIV Vif. My colleague demonstrated that the mutated feline A3Z3 protein clearly showed reduced binding to FIV Vif, supporting the model that Vif binding to A3 is needed for A3 degradation.

In feline A3Z2 residues D165 and H166 were also found to regulate the FIV Vif induced degradation (Fig. 3.10), but it was demonstrated by my colleagues that these mutations did not block feline A3Z2 binding to FIV Vif in co-immunoprecipitation assays. This observation demonstrates that Vif binding to A3s is not sufficient for A3 degradation. Supporting evidence that Vif interaction is necessary but not sufficient is coming from reports describing that HIV-1 NL4-3 Vif binds A3C mutants, A3B and A3H without inducing APOBEC3 degradation (217, 218, 225). The binding of mutated feline A3Z2.DH-YN to FIV Vif appeared to be robust, indicating a more complex mechanism. Studies on HIV-1 Vif binding to human A3B and A3H similarly concluded that the interaction strength is not the only determinant for complete Vif-mediated degradation, and the individual interfaces of the A3-Vif pair additionally regulate degradation (217).

Recently, Richards *et al.* (179) presented a wobble model of the evolution of the Vif-A3 interaction. This model implicates that Vif forms several interactions, of which some are essential and some provide additional stabilizing contacts. Based on this idea, only if Vif forms a sufficient network of interactions with its A3 binding partner, a functional interaction is made. Suboptimal, destabilized interactions could be restored by the evolution of compensatory changes in Vif–A3 interface. It is thus possible that in feline A3Z3 residue A65 and L41, I42 are major independent interactions in the Vif-A3 interface, whereas in feline A3Z2 D165 and H166 represent one of the relevant interacting points for FIV Vif complex formation, while additional contact points still exist. Such a suboptimal Vif-A3 interaction might, for example, not be sufficient to facilitate E3 ligase conjugation of K48-linked polyubiquitin chains that are generally recognized by the proteasome.

4.2 The interaction between FIV Vif and CUL5

4.2.1 The involvement of FIV Vif N terminus in interaction with CUL5

FIV Vif interacts with CUL5, ELOB, and ELOC to form an E3 complex to induce degradation of feline A3s (168). The interaction properties of FIV Vif with feline A3s and ELOB/C were previously identified (162, 168, 206). However, the interface between FIV Vif and CUL5 was not characterized.

Feline CUL5 and human CUL5 only differ in one amino acid, and this mutation does not affect its interaction with FIV Vif (168). It was also shown that FIV Vif can induce the degradation of feline A3s in both feline CRFK and human 293T cells, thus supporting that FIV Vif can interact with human and feline CUL5 (168, 206). In this study, I first identified that three FIV Vif N-terminal mutants (53FI54, 57LR58, and 77VRE79) partially lost CUL5 binding, compared to wildtype FIV Vif (Fig. 3.13B). These Vif mutants only partially degraded feline A3s, clearly less efficient than wildtype Vif. The N-terminus of FIV Vif does not directly bind CUL5, according to our FIV Vif/CUL5 structural model (Fig. 3.16A). Thus, I speculate that these residues rather interact with an unknown factor that regulates the FIV Vif/CUL5 binding. Indeed, a previous study suggested that FIV Vif requires an unknown factor to stabilize the FIV Vif/CUL5/ELOB/C complex (170).

4.2.2 Comparison of FIV Vif-CUL5 and other adaptors-CUL5 interface

CUL5-type ubiquitin ligases have a variety of adaptors that induce degradation of different cellular substrates (see recent review (150)). The adaptors of CUL5 share one common domain, *i.e.*, the SOCS box, which consists of a BC box and a CUL5 box (150). The CUL5 box has a common sequence, -LPθP-θ-YL, in which θ represents a hydrophobic residue, and CUL5 box is localized downstream of the BC box (150). Such a CUL5-like box is also found in HIV-1 Vif (PPLP motif), but this region does not interact with CUL5 (226, 227). In fact, HIV-1 Vif uses a hydrophobic region of helix 3 to interact with CUL5 (158, 208, 209). In FIV Vif, a typical CUL5 box is also missing (168). However, I found that FIV Vif, similar to HIV Vif, uses a hydrophobic region of helix 3 upstream of the BC box, position 174 and 175, to interact with CUL5 (Fig. 3.14 and 3.16). Vif proteins are not unique in applying unusual CUL5 boxes. For example, the adenovirus serotype 5 (Ad5) protein E4orf6 does not have a typical CUL5 box either, but it still interacts with CUL5 and forms an E3 ligase complex to degrade p53 (228).

4.2.3 FIV Vif function is zinc independent

Three HIV/SIV accessory proteins (Vpr, Vpx, and Vif) bind zinc, which is essential for the assembly of their E3 ligase complexes (229-231). Zinc is also required for BIV Vif/CUL2 binding, while MVV Vif/CUL5 interaction does not need zinc (232). In this study, I used the cell-permeable zinc chelator TPEN to investigate whether this chelator impairs the function of FIV Vif or HIV-1 Vif in A3 degradation. I found that TPEN inhibited both FcaA3 and HsaA3 degradation induced by FIV Vif and HIV-1 Vif, respectively (Fig. 3.18A and B). It is important to point out that high concentrations of TPEN will repress cellular pathways, such as those of the cellular lysosome and autophagy (233). Thus, it is possible that high concentrations of TPEN may impact upon many cellular degradation pathways. However, I found that 4 µM TPEN inhibited the HIV-1 Vif-induced HsaA3G degradation, while this concentration of TPEN had no influence on FcaAZ2bZ3 degradation by FIV Vif (Fig. 3.18A and B). In addition, the presence of 5 µM TPEN did not allow the isolation of HIV-1 Vif/CUL5 complexes, whereas FIV Vif/CUL5 complexes could still be detected (Fig. 3.18). Thus, the data support that zinc is not important for the FIV Vif/CUL5 interaction, as discussed previously (168). Other studies have demonstrated that TPEN treatment blocks the function of HIV-1 Vif, Vpr, and SIVmac Vpx

(229). These findings indicate that, in the group of lentiviruses, there are zinc-dependent (*e.g.,* HIV-1, BIV) and zinc-independent (*e.g.,* FIV, MVV) Vif proteins. The inter-Vif diversity is high, and HIV-1 Vif shares only around 16% and 5.2% identical residues with BIV or FIV Vif, respectively. Thus, the requirement and structural consequences of zinc binding in Vifs are currently unclear. However, whether other metals (Mg^{2+} or Ca^{2+}) bind FIV or MVV Vif needs more investigation. The SOCS3/CUL5 and E4orf6/CUL5 interactions are also zinc-independent (228, 234), which, together, indicates that zinc is not necessary for binding of CUL5.

4.2.4 FIV Vif structural homology model

As the sequence of FIV Vif is 59 amino acids longer than that of HIV-1 Vif and no other structural template is available, an unstructured loop is found in our model between helices 2 and 3 (Fig. 3.16A). This loop could be involved in the binding of CUL5 or other cofactors; however, without a structural template, its function remains unknown. Whether this loop is specific for FIV Vif requires further investigation. Despite the low sequence identity between FIV and HIV-1 Vif and their difference in sequence length, our homology model of the FIV Vif/CUL5 complex is apparently accurate enough to predict interacting residues between these proteins. Our data from the CUL5 alanine variant of 52LW53 (Fig. 3.16C) and our homology model suggest that the interaction between Vif and CUL5 is also mediated by a hydrophobic contact. This is similar to the importance of the hydrophobic motif in the CUL5 BC box. In our homology model, helix 3 of Vif, which interacts with CUL5, is followed by C184. This cysteine was shown to be important for CUL5 interaction, and for feline A3 or ELOB/C interaction, which differs from a previous study (168). As C184 is neither located in the Vif/CUL5 interface according to our homology model nor involved in zinc binding, I speculate that it might contribute to stabilizing the integral structure of FIV Vif. Overall, while our model certainly cannot be expected to be a perfect structural representation of the FIV Vif/CUL5 complex given the low sequence identity between FIV and HIV-1 Vif, we were able to successfully predict interacting residues between the two proteins in those regions with a higher sequence similarity.

4.2.5 Further methods for investigation of protein-protein interactions

Currently, many methods are available to investigate protein-protein interactions (PPI), such as tandem affinity purification (TAP), pull-down assay, co-immunoprecipitation (CoIP), protein chip, bimolecular fluorescence complementation (BiFC), Far-Western blotting, affinity electrophoresis, label transfer, and photoreactive amino acid analogs. In my investigations, CoIP and protein homology modeling were the main methods used. CoIP is a common method to study protein-protein interactions, especially for endogenous proteins. In this study, I tested the interaction of both over-expressed proteins (with a tag) and endogenous proteins (not tagged) by the CoIP method. The target protein is isolated by a specific antibody or an antibody conjugated to agarose beads. The partner proteins that bind the target protein are simultaneously isolated and detected by Western blotting. However, only according to the CoIP results, it is not sufficient to conclude that the identified residues involve in direct protein-protein binding. The protein-protein interaction was also suggested by homology modeling, to illustrate the direct protein binding surface. In turn, I used CoIP to confirm the protein-protein interface. By combining CoIP and protein homology methods, I exactly discovered the FIV Vif-Cul5 binding interface. In fact, nuclear magnetic resonance (NMR) and gel filtration are also commonly used by biochemist to investigate the direct protein-protein binding. However, these two methods require purified proteins, and in some cases they are not applicable due to the insolubility and instability of protein.

4.3 The antiviral activity of feline SERINC

Feline A3s, especially feline A3Z3 and A3Z2Z3, are strong restriction factors that inhibit the infection of FIVΔ*vif*. A new human restriction factor, named as SERINC, was recently identified displaying strong inhibition for lentiviruses, while little is known about feline SERINC. Thus, I cloned feline SERINC3 and SERINC5 cDNAs. After expression and infections assays, I found that feline SERINC5 suppressed the infectivity of both HIV-1 and FIV (Fig.3.24 and 3.25), consistent with the antiviral activity of human SERINC5 (119, 120, 122). These results indicate a common antiviral mechanism of feline and human SERINC5 proteins. Interestingly, feline SERINC3 inhibited HIV-1 infection, while it displayed quite less restriction against FIV (Fig. 3.24 and 3.25). This observation suggests that FIV may escape the restriction

from feline SERINC3. However, it is still unclear how FIV counteracts the inhibition of feline SERINC5. Further investigation is required to evaluate the expression level of feline SERINC proteins in FIV targeted cells (CRFK, T cells or macrophages). Feline SERINC knockout experiments are also required to investigate the effect of SERINC on FIV replication and pathogenesis.

FIV infection in cat is an animal model for HIV-1. In addition, previous studies indicated that feline A3s are main barriers for HIV-1 replication in cat cell lines and that HIV-1 with vif of FIV can replicate in feline cells (161, 164). Here, I demonstrated that HIV-1 Nef is able to overcome the restriction of feline SERINC5 and SERINC3 (Fig. 3.24). This result suggests that feline SERINC proteins are not considerable issues during construction animal model of HIV-1 infected cat.

4.4 Limitation of our study

All the current studies use cellular molecular biology methods to test the molecular interaction between FIV Vif and its interactome. Even we use homology method to model the structure of FIV Vif, our model certainly cannot be expected to be a perfect structural due to the low sequence identity between FIV and HIV-1 Vif. We need biochemistry method to deeply resolve the exact 3D structure of FIV Vif. But generation a high resolution structure of Vif is difficult, because FIV Vif is highly insoluble when I expressed it in *E.coli* (data not shown).

5. Summary

The apolipoprotein B mRNA-editing enzyme, catalytic polypeptide-like (APOBEC3, A3) family of DNA cytidine deaminases are intrinsic restriction factors against retroviruses. In felids such as the domestic cat (*Felis catus, Fca*), the APOBEC3 (A3) genes code for the A3Z2s, A3Z3, and A3Z2Z3 antiviral cytidine deaminases. Only A3Z3 and A3Z2Z3 inhibit viral infectivity factor (Vif)-deficient feline immunodeficiency virus (FIV). FIV Vif protein interacts with Cullin (CUL), Elongin B (ELOB), and Elongin C (ELOC) to form an E3 ubiquitination complex to induce the degradation of feline A3s. The functional domains in FIV Vif for interaction with FcaA3s are poorly understood. Here, I have identified several motifs in FIV Vif that are important for selective degradation of different FcaA3s. I initially proposed that FIV Vif would selectively interact with the Z2 and the Z3 A3s. Indeed, I identified two N-terminal Vif motifs (12LF13 and 18GG19) that specifically interacted with the FcaA3Z2 protein but not with A3Z3. In contrast, the exclusive degradation of FcaA3Z3 was regulated by a region of three residues (M24, L25 and I27). Only a FIV Vif carrying a combination of mutations from both interaction sites lost the capacity to degrade and counteract FcaA3Z2Z3. However, alterations in the specific A3s interaction sites did not affect the cellular localization of the FIV Vif protein and binding to feline A3s. Pull-down experiments suggested that the A3 binding region localized to FIV Vif residues 50 to 80, outside the specific A3 interaction domain. Finally, we found that the Vif sites specific to individual A3s are conserved in several FIV lineages of domestic cat and non-domestic cats, while being absent in the FIV Vif of pumas. Our data support a complex model of multiple Vif-A3 interactions in which the specific region for selective A3 counteraction is discrete from a general A3 binding domain.

Additionally, the functional domains in FIV Vif for interaction with Cullin are poorly understood. In this study, I found that the expression of dominant-negative CUL5 prevented the degradation of feline A3s by FIV Vif, while dominant-negative CUL2 had no influence on the degradation of A3. In co-immunoprecipitation assays, FIV Vif bound to CUL5 but not CUL2. To identify the CUL5 interaction site in FIV Vif, the conserved amino acids from position 47 to 160 of FIV Vif were mutated, but these mutations did not impair the binding of Vif to CUL5. By focusing on a potential zinc-binding motif (K175– C161—C184–C187) of FIV Vif, I found a conserved hydrophobic region (174IR175) that is important for CUL5

interaction. Mutating this region also impaired the FIV Vif-induced degradation of feline A3s. Based on a structural model of the FIV Vif/CUL5 interaction, residues 52LW53 in CUL5 were identified as mediating the binding to FIV Vif. By comparing our results to the human immunodeficiency virus type 1 (HIV-1) Vif/CUL5 interaction surface (120IR121, a hydrophobic region that is localized in the zinc-binding motif), we suggest that the CUL5 interaction surface in the diverse HIV-1 and FIV Vif is evolutionarily conserved indicating a strong structural constraint. However, the FIV Vif/CUL5 interaction is zinc-independent, which differs from the zinc-dependency of HIV-1 Vif.

6. Zusammenfassung

APOBEC3-Prtoteine (A3, apolipoprotein B mRNA-editing enzyme catalytic polypeptide-like) gehören zur Familie der DNA-Cytidin-Desaminasen und sind intrinsische Restriktionsfaktoren gegen Retroviren. In Felidae wie der Hauskatze (*Felis catus, Fca*) kodieren die APOBEC3-Gene für die antiviralen Cytidin-Deaminasen A3Z2, A3Z3 und A3Z2Z3. Nur A3Z3 und A3Z2Z3 inhibieren das Vif (viral infectivity factor)-defiziente feline Immundefizienz-Virus (FIV). Das Vif-Protein von FIV interagiert mit Cullin (CUL), Elongin B (ELOB) und Elongin C (ELOC), um einen E3-Ubiquitinierungskomplex zu formieren und die Degradierung feliner A3s zu induzieren. Bisher war über die funktionalen Domänen des FIV-Vif, die mit FcaA3 interagieren, wenig bekannt. In dieser Arbeit habe ich diverse Motive des FIV-Vif entdeckt, die für die selektive Degradierung verschiedener FcaA3 von Bedeutung sind. Meine ursprüngliche Hypothese war, dass FIV-Vif selektiv mit A3Z2 und A3Z3 interagiert. Tatsächlich identifizierte ich zwei N-terminale Vif-Motive (12LF13 und 18GG19), die spezifisch mit dem FcaA3Z2- nicht aber mit dem A3Z3-Protein interagieren. Im Gegensatz dazu wird die exklusive Degradierung des FcaA3Z3 durch eine Region aus drei Aminosäureresten reguliert (M24, L25 und I27) bestimmt. Nur das FIV-Vif mit einer Kombination aus Mutationen an beiden Interaktionsstellen verliert die Fähigkeit FcaA3Z2Z3 zu degradieren und zu neutralisieren. Dagegen hatten Veränderungen an den spezifischen A3-Interaktionsstellen keinen Einfluss auf die Bindung an feline A3s und verändern auch nicht die zelluläre Lokalisation des FIV-Vif-Proteins. Pull-down-Experimente deuten darauf hin, dass die A3-Bindungsregion in den Aminosäureresten 50 bis 80 des FIV-Vifs, außerhalb der spezifischen A3-Interaktionsdomäne, lokalisiert ist. Außerdem stellte ich fest, dass die Vif-Stellen, die spezifisch für individuelle A3s sind, in diversen FIV-Linien der Hauskatze und anderer Felidae konserviert sind, aber nicht im FIV-Vif des Pumas vorkommen. Unsere Daten unterstützen ein komplexes Modell mit multiplen Vif-A3-Interaktionen, bei denen sich die spezifische Region für selektive A3-Gegenwirkung von einer generellen A3-Bindungsdomäne unterscheidet.

Außerdem ist über die Interaktion der funktionellen Domänen des FIV-Vif mit Cullin wenig bekannt. In dieser Arbeit habe ich herausgefunden, dass die Expression von dominant-negativem CUL5 vor einer Degradierung feliner A3 durch FIV-Vif schützt, während die Expression von dominant-negativem CUL2 keinen Einfluss auf diese Degradierung hatte. In

Koimmunopräzipitations-Assays band FIV-Vif an CUL5, nicht aber an CUL2. Um die CUL5-Interaktionsstelle des FIV-Vif zu identifizieren wurden die konservierten Aminosäuren der Positionen 47 bis 160 des FIV-Vif mutiert, was aber zu keiner verminderten Bindung des Vif an CUL5 führte. Während der Fokussierung auf ein potentielles Zink-bindendes Motiv (K175–C161—C184–C187) des FIV-Vif fand ich eine konservierte hydrophobe Region (174IR175), die eine wichtig Rolle bei der CUL5-Interaktion spielt. Mutationen in dieser Region verringern die FIV-Vif-induzierte Degradierung der felinen A3. Basierend auf einem Strukturmodell der FIV-Vif/CUL5-Interaktion wurden die Aminosäurereste 52LW53 des CUL5 als wichtig für die Bindung an FIV-Vif identifiziert. Vergleicht man unsere Ergebnisse mit der Vif/CUL5-Interaktionsfläche des humanen Immundefizienz-Virus Typ 1 (HIV-1) (120IR121, eine hydrophobe Region, die im Zink-bindenden Motiv lokalisiert ist) schlagen wir ein Modell vor, bei dem die CUL5-Interaktionsfläche in diversen HIV-1- und FIV-Vif evolutionär konserviert ist, was auf einen optimale strukturelle Bindung mit wenig Freiheitsgraden schließen lässt. Im Gegensatz zum Zink-abhängigen HIV-1-Vif, ist die FIV-Vif/CUL5-Interaktion unabhängig von Zink.

7. References

1. **Rous P.** 1911. A Sarcoma of the Fowl Transmissible by an Agent Separable from the Tumor Cells. J Exp Med **13:**397-411.
2. **Latarjet R, Duplan JF.** 1962. Experiment and discussion on leukaemogenesis by cell-free extracts of radiation-induced leukaemia in mice. Int J Radiat Biol Relat Stud Phys Chem Med **5:**339-344.
3. **Gross L, Dreyfuss Y.** 1978. Relative loss of oncogenic potency of mouse leukemia virus (Gross) after prolonged propagation in tissue culture. Proc Natl Acad Sci U S A **75:**3989-3992.
4. **Sharp PM, Hahn BH.** 2011. Origins of HIV and the AIDS pandemic. Cold Spring Harb Perspect Med **1:**a006841.
5. **Pandrea I, Apetrei C.** 2010. Where the wild things are: pathogenesis of SIV infection in African nonhuman primate hosts. Curr HIV/AIDS Rep **7:**28-36.
6. **Ayouba A, Akoua-Koffi C, Calvignac-Spencer S, Esteban A, Locatelli S, Li H, Li Y, Hahn BH, Delaporte E, Leendertz FH, Peeters M.** 2013. Evidence for continuing cross-species transmission of SIVsmm to humans: characterization of a new HIV-2 lineage in rural Cote d'Ivoire. AIDS **27:**2488-2491.
7. **Olmsted RA, Barnes AK, Yamamoto JK, Hirsch VM, Purcell RH, Johnson PR.** 1989. Molecular cloning of feline immunodeficiency virus. Proc Natl Acad Sci U S A **86:**2448-2452.
8. **Pedersen NC, Yamamoto JK, Ishida T, Hansen H.** 1989. Feline immunodeficiency virus infection. Vet Immunol Immunopathol **21:**111-129.
9. **Willett BJ, Flynn JN, Hosie MJ.** 1997. FIV infection of the domestic cat: an animal model for AIDS. Immunol Today **18:**182-189.
10. **Weiss RA.** 1996. Retrovirus classification and cell interactions. J Antimicrob Chemother **37 Suppl B:**1-11.
11. **Griffiths DJ.** 2001. Endogenous retroviruses in the human genome sequence. Genome Biol **2:**REVIEWS1017.
12. **Platt EJ, Wehrly K, Kuhmann SE, Chesebro B, Kabat D.** 1998. Effects of CCR5 and CD4 cell surface concentrations on infections by macrophagetropic isolates of human immunodeficiency virus type 1. J Virol **72:**2855-2864.
13. **Shimojima M, Miyazawa T, Ikeda Y, McMonagle EL, Haining H, Akashi H, Takeuchi Y, Hosie MJ, Willett BJ.** 2004. Use of CD134 as a primary receptor by the feline immunodeficiency virus. Science **303:**1192-1195.
14. **de Parseval A, Chatterji U, Sun P, Elder JH.** 2004. Feline immunodeficiency virus targets activated CD4+ T cells by using CD134 as a binding receptor. Proc Natl Acad Sci U S A **101:**13044-13049.
15. **Willett BJ, McMonagle EL, Ridha S, Hosie MJ.** 2006. Differential utilization of CD134 as a functional receptor by diverse strains of feline immunodeficiency virus. J Virol **80:**3386-3394.
16. **Zhang Z, Ma J, Zhang X, Su C, Yao QC, Wang X.** 2015. Equine Infectious Anemia Virus Gag Assembly and Export Are Directed by Matrix Protein through trans-Golgi Networks and Cellular Vesicles. J Virol **90:**1824-1838.
17. **Fevrier M, Dorgham K, Rebollo A.** 2011. CD4+ T cell depletion in human immunodeficiency virus (HIV) infection: role of apoptosis. Viruses **3:**586-612.
18. **Campo J, Perea MA, del Romero J, Cano J, Hernando V, Bascones A.** 2006. Oral transmission of HIV, reality or fiction? An update. Oral Dis **12:**219-228.
19. **Cohen MS, Smith MK, Muessig KE, Hallett TB, Powers KA, Kashuba AD.** 2013. Antiretroviral treatment of HIV-1 prevents transmission of HIV-1: where do we go from here? Lancet **382:**1515-1524.
20. **Wensing AM, Calvez V, Gunthard HF, Johnson VA, Paredes R, Pillay D, Shafer RW, Richman DD.** 2017. 2017 Update of the Drug Resistance Mutations in HIV-1. Top Antivir Med **24:**132-133.

21. **D'Arc M, Ayouba A, Esteban A, Learn GH, Boue V, Liegeois F, Etienne L, Tagg N, Leendertz FH, Boesch C, Madinda NF, Robbins MM, Gray M, Cournil A, Ooms M, Letko M, Simon VA, Sharp PM, Hahn BH, Delaporte E, Mpoudi Ngole E, Peeters M.** 2015. Origin of the HIV-1 group O epidemic in western lowland gorillas. Proc Natl Acad Sci U S A **112:**E1343-1352.
22. **Hemelaar J.** 2012. The origin and diversity of the HIV-1 pandemic. Trends Mol Med **18:**182-192.
23. **Gottlieb GS, Sow PS, Hawes SE, Ndoye I, Coll-Seck AM, Curlin ME, Critchlow CW, Kiviat NB, Mullins JI.** 2003. Molecular epidemiology of dual HIV-1/HIV-2 seropositive adults from Senegal, West Africa. AIDS Res Hum Retroviruses **19:**575-584.
24. **Visseaux B, Damond F, Matheron S, Descamps D, Charpentier C.** 2016. Hiv-2 molecular epidemiology. Infect Genet Evol **46:**233-240.
25. **Frankel AD, Young JA.** 1998. HIV-1: fifteen proteins and an RNA. Annu Rev Biochem **67:**1-25.
26. **Hartmann K.** 2015. Efficacy of antiviral chemotherapy for retrovirus-infected cats: What does the current literature tell us? J Feline Med Surg **17:**925-939.
27. **Uhl EW, Martin M, Coleman JK, Yamamoto JK.** 2008. Advances in FIV vaccine technology. Vet Immunol Immunopathol **123:**65-80.
28. **Hartmann K.** 2011. Clinical aspects of feline immunodeficiency and feline leukemia virus infection. Vet.Immunol.Immunopathol.
29. **de Rozieres S, Mathiason CK, Rolston MR, Chatterji U, Hoover EA, Elder JH.** 2004. Characterization of a highly pathogenic molecular clone of feline immunodeficiency virus clade C. J Virol **78:**8971-8982.
30. **Diehl LJ, Mathiason-Dubard CK, O'Neil LL, Obert LA, Hoover EA.** 1995. Induction of accelerated feline immunodeficiency virus disease by acute-phase virus passage. J Virol **69:**6149-6157.
31. **Obert LA, Hoover EA.** 2000. Feline immunodeficiency virus clade C mucosal transmission and disease courses. AIDS Res Hum Retroviruses **16:**677-688.
32. **Lehman TL, O'Halloran KP, Hoover EA, Avery PR.** 2010. Utilizing the FIV model to understand dendritic cell dysfunction and the potential role of dendritic cell immunization in HIV infection. Vet Immunol Immunopathol **134:**75-81.
33. **Yamamoto JK, Sanou MP, Abbott JR, Coleman JK.** 2010. Feline immunodeficiency virus model for designing HIV/AIDS vaccines. Curr HIV Res **8:**14-25.
34. **Elder JH, Lin YC, Fink E, Grant CK.** 2010. Feline immunodeficiency virus (FIV) as a model for study of lentivirus infections: parallels with HIV. Curr HIV Res **8:**73-80.
35. **O'Brien SJ, Troyer JL, Brown MA, Johnson WE, Antunes A, Roelke ME, Pecon-Slattery J.** 2012. Emerging viruses in the Felidae: shifting paradigms. Viruses **4:**236-257.
36. **Hayward JJ, Rodrigo AG.** 2010. Molecular epidemiology of feline immunodeficiency virus in the domestic cat (Felis catus). Vet Immunol Immunopathol **134:**68-74.
37. **Hutson CA, Rideout BA, Pedersen NC.** 1991. Neoplasia associated with feline immunodeficiency virus infection in cats of southern California. J Am Vet Med Assoc **199:**1357-1362.
38. **Troyer JL, Roelke ME, Jespersen JM, Baggett N, Buckley-Beason V, MacNulty D, Craft M, Packer C, Pecon-Slattery J, O'Brien SJ.** 2011. FIV diversity: FIV Ple subtype composition may influence disease outcome in African lions. Vet Immunol Immunopathol **143:**338-346.
39. **Troyer JL, Vandewoude S, Pecon-Slattery J, McIntosh C, Franklin S, Antunes A, Johnson W, O'Brien SJ.** 2008. FIV cross-species transmission: an evolutionary prospective. Vet Immunol Immunopathol **123:**159-166.
40. **Pecon-Slattery J, McCracken CL, Troyer JL, VandeWoude S, Roelke M, Sondgeroth K, Winterbach C, Winterbach H, O'Brien SJ.** 2008. Genomic organization, sequence divergence, and recombination of feline immunodeficiency virus from lions in the wild. BMC Genomics **9:**66.

41. **Lee JS, Bevins SN, Serieys LE, Vickers W, Logan KA, Aldredge M, Boydston EE, Lyren LM, McBride R, Roelke-Parker M, Pecon-Slattery J, Troyer JL, Riley SP, Boyce WM, Crooks KR, VandeWoude S.** 2014. Evolution of puma lentivirus in bobcats (Lynx rufus) and mountain lions (Puma concolor) in North America. J Virol **88:**7727-7737.
42. **VandeWoude S, Troyer J, Poss M.** 2010. Restrictions to cross-species transmission of lentiviral infection gleaned from studies of FIV. Vet Immunol Immunopathol **134:**25-32.
43. **Pecon-Slattery J, Troyer JL, Johnson WE, O'Brien SJ.** 2008. Evolution of feline immunodeficiency virus in Felidae: implications for human health and wildlife ecology. Vet Immunol Immunopathol **123:**32-44.
44. **Lee J, Malmberg JL, Wood BA, Hladky S, Troyer R, Roelke M, Cunningham M, McBride R, Vickers W, Boyce W, Boydston E, Serieys L, Riley S, Crooks K, VandeWoude S.** 2017. Feline Immunodeficiency Virus Cross-Species Transmission: Implications for Emergence of New Lentiviral Infections. J Virol **91**.
45. **Carpenter MA, Brown EW, Culver M, Johnson WE, Pecon-Slattery J, Brousset D, O'Brien SJ.** 1996. Genetic and phylogenetic divergence of feline immunodeficiency virus in the puma (Puma concolor). J Virol **70:**6682-6693.
46. **Nishimura Y, Goto Y, Yoneda K, Endo Y, Mizuno T, Hamachi M, Maruyama H, Kinoshita H, Koga S, Komori M, Fushuku S, Ushinohama K, Akuzawa M, Watari T, Hasegawa A, Tsujimoto H.** 1999. Interspecies transmission of feline immunodeficiency virus from the domestic cat to the Tsushima cat (Felis bengalensis euptilura) in the wild. J Virol **73:**7916-7921.
47. **Troyer JL, Pecon-Slattery J, Roelke ME, Johnson W, VandeWoude S, Vazquez-Salat N, Brown M, Frank L, Woodroffe R, Winterbach C, Winterbach H, Hemson G, Bush M, Alexander KA, Revilla E, O'Brien SJ.** 2005. Seroprevalence and genomic divergence of circulating strains of feline immunodeficiency virus among Felidae and Hyaenidae species. J Virol **79:**8282-8294.
48. **Franklin SP, Troyer JL, Terwee JA, Lyren LM, Boyce WM, Riley SP, Roelke ME, Crooks KR, Vandewoude S.** 2007. Frequent transmission of immunodeficiency viruses among bobcats and pumas. J Virol **81:**10961-10969.
49. **Zielonka J, Münk C.** 2011. Cellular restriction factors of feline immunodeficiency virus. Viruses **3:**1986-2005.
50. **Münk C, Beck T, Zielonka J, Hotz-Wagenblatt A, Chareza S, Battenberg M, Thielebein J, Cichutek K, Bravo IG, O'Brien SJ, Löchelt M, Yuhki N.** 2008. Functions, structure, and read-through alternative splicing of feline APOBEC3 genes. Genome Biol **9:**R48.
51. **Hong Y, Fink E, Hu QY, Kiosses WB, Elder JH.** 2010. OrfA downregulates feline immunodeficiency virus primary receptor CD134 on the host cell surface and is important in viral infection. J Virol **84:**7225-7232.
52. **Troyer RM, Thompson J, Elder JH, VandeWoude S.** 2013. Accessory genes confer a high replication rate to virulent feline immunodeficiency virus. J Virol **87:**7940-7951.
53. **Sundstrom M, Chatterji U, Schaffer L, de Rozieres S, Elder JH.** 2008. Feline immunodeficiency virus OrfA alters gene expression of splicing factors and proteasome-ubiquitination proteins. Virology **371:**394-404.
54. **Goff SP, Berg P.** 1976. Construction of hybrid viruses containing SV40 and lambda phage DNA segments and their propagation in cultured monkey cells. Cell **9:**695-705.
55. **Cavazzana-Calvo M, Hacein-Bey S, de Saint Basile G, Gross F, Yvon E, Nusbaum P, Selz F, Hue C, Certain S, Casanova JL, Bousso P, Deist FL, Fischer A.** 2000. Gene therapy of human severe combined immunodeficiency (SCID)-X1 disease. Science **288:**669-672.
56. **Pao W, Klimstra DS, Fisher GH, Varmus HE.** 2003. Use of avian retroviral vectors to introduce transcriptional regulators into mammalian cells for analyses of tumor maintenance. Proc Natl Acad Sci U S A **100:**8764-8769.

57. **Sharon D, Kamen A.** 2018. Advancements in the design and scalable production of viral gene transfer vectors. Biotechnol Bioeng **115:**25-40.
58. **Zhang W, Ehrhardt A.** 2017. Getting genetic access to natural adenovirus genomes to explore vector diversity. Virus Genes **53:**675-683.
59. **McCarty DM, Monahan PE, Samulski RJ.** 2001. Self-complementary recombinant adeno-associated virus (scAAV) vectors promote efficient transduction independently of DNA synthesis. Gene Ther **8:**1248-1254.
60. **Parolin C, Sodroski J.** 1995. A defective HIV-1 vector for gene transfer to human lymphocytes. J Mol Med (Berl) **73:**279-288.
61. **Poeschla EM, Wong-Staal F, Looney DJ.** 1998. Efficient transduction of nondividing human cells by feline immunodeficiency virus lentiviral vectors. Nat Med **4:**354-357.
62. **Haskell EC, Bressloff PC.** 2003. On the formation of persistent states in neuronal network models of feature selectivity. J Integr Neurosci **2:**103-123.
63. **Saenz DT, Barraza R, Loewen N, Teo W, Poeschla EM.** 2012. Feline immunodeficiency virus-based lentiviral vectors. Cold Spring Harb Protoc **2012:**71-76.
64. **Doyle T, Goujon C, Malim MH.** 2015. HIV-1 and interferons: who's interfering with whom? Nat Rev Microbiol **13:**403-413.
65. **Sauter D.** 2014. Counteraction of the multifunctional restriction factor tetherin. Front Microbiol **5:**163.
66. **Hotter D, Sauter D, Kirchhoff F.** 2013. Emerging role of the host restriction factor tetherin in viral immune sensing. J Mol Biol **425:**4956-4964.
67. **Yin X, Hu Z, Gu Q, Wu X, Zheng YH, Wei P, Wang X.** 2014. Equine tetherin blocks retrovirus release and its activity is antagonized by equine infectious anemia virus envelope protein. J Virol **88:**1259-1270.
68. **Neil SJ.** 2013. The antiviral activities of tetherin. Curr Top Microbiol Immunol **371:**67-104.
69. **Morrison JH, Guevara RB, Marcano AC, Saenz DT, Fadel HJ, Rogstad DK, Poeschla EM.** 2014. Feline immunodeficiency virus envelope glycoproteins antagonize tetherin through a distinctive mechanism that requires virion incorporation. J Virol **88:**3255-3272.
70. **Dietrich I, McMonagle EL, Petit SJ, Vijayakrishnan S, Logan N, Chan CN, Towers GJ, Hosie MJ, Willett BJ.** 2011. Feline tetherin efficiently restricts release of feline immunodeficiency virus but not spreading of infection. J Virol **85:**5840-5852.
71. **Celestino M, Calistri A, Del Vecchio C, Salata C, Chiuppesi F, Pistello M, Borsetti A, Palu G, Parolin C.** 2012. Feline tetherin is characterized by a short N-terminal region and is counteracted by the feline immunodeficiency virus envelope glycoprotein. J Virol **86:**6688-6700.
72. **Forshey BM, von Schwedler U, Sundquist WI, Aiken C.** 2002. Formation of a human immunodeficiency virus type 1 core of optimal stability is crucial for viral replication. J Virol **76:**5667-5677.
73. **Dismuke DJ, Aiken C.** 2006. Evidence for a functional link between uncoating of the human immunodeficiency virus type 1 core and nuclear import of the viral preintegration complex. J Virol **80:**3712-3720.
74. **Takeda E, Kono K, Hulme AE, Hope TJ, Nakayama EE, Shioda T.** 2015. Fluorescent image analysis of HIV-1 and HIV-2 uncoating kinetics in the presence of old world monkey TRIM5alpha. PLoS One **10:**e0121199.
75. **Reymond A, Meroni G, Fantozzi A, Merla G, Cairo S, Luzi L, Riganelli D, Zanaria E, Messali S, Cainarca S, Guffanti A, Minucci S, Pelicci PG, Ballabio A.** 2001. The tripartite motif family identifies cell compartments. EMBO J **20:**2140-2151.
76. **Nisole S, Stoye JP, Saib A.** 2005. TRIM family proteins: retroviral restriction and antiviral defence. Nat Rev Microbiol **3:**799-808.
77. **Yap MW, Nisole S, Stoye JP.** 2005. A single amino acid change in the SPRY domain of human Trim5alpha leads to HIV-1 restriction. Curr Biol **15:**73-78.

78. **Nakayama EE, Miyoshi H, Nagai Y, Shioda T.** 2005. A specific region of 37 amino acid residues in the SPRY (B30.2) domain of African green monkey TRIM5alpha determines species-specific restriction of simian immunodeficiency virus SIVmac infection. J Virol **79:**8870-8877.
79. **Rakoff-Nahoum S, Kuebler PJ, Heymann JJ, M ES, Ortiz GM, G SO, Barbour JD, Lenz J, Steinfeld AD, Nixon DF.** 2006. Detection of T lymphocytes specific for human endogenous retrovirus K (HERV-K) in patients with seminoma. AIDS Res Hum Retroviruses **22:**52-56.
80. **Li X, Li Y, Stremlau M, Yuan W, Song B, Perron M, Sodroski J.** 2006. Functional replacement of the RING, B-box 2, and coiled-coil domains of tripartite motif 5alpha (TRIM5alpha) by heterologous TRIM domains. J Virol **80:**6198-6206.
81. **Saenz DT, Teo W, Olsen JC, Poeschla EM.** 2005. Restriction of feline immunodeficiency virus by Ref1, Lv1, and primate TRIM5alpha proteins. J Virol **79:**15175-15188.
82. **Roganowicz MD, Komurlu S, Mukherjee S, Plewka J, Alam SL, Skorupka KA, Wan Y, Dawidowski D, Cafiso DS, Ganser-Pornillos BK, Campbell EM, Pornillos O.** 2017. TRIM5alpha SPRY/coiled-coil interactions optimize avid retroviral capsid recognition. PLoS Pathog **13:**e1006686.
83. **Stremlau M, Song B, Javanbakht H, Perron M, Sodroski J.** 2006. Cyclophilin A: an auxiliary but not necessary cofactor for TRIM5alpha restriction of HIV-1. Virology **351:**112-120.
84. **McEwan WA, Schaller T, Ylinen LM, Hosie MJ, Towers GJ, Willett BJ.** 2009. Truncation of TRIM5 in the Feliformia explains the absence of retroviral restriction in cells of the domestic cat. J Virol **83:**8270-8275.
85. **Dietrich I, Macintyre A, McMonagle E, Price AJ, James LC, McEwan WA, Hosie MJ, Willett BJ.** 2010. Potent lentiviral restriction by a synthetic feline TRIM5 cyclophilin A fusion. J Virol **84:**8980-8985.
86. **Li M, Zhang D, Zhu M, Shen Y, Wei W, Ying S, Korner H, Li J.** 2017. Roles of SAMHD1 in antiviral defense, autoimmunity and cancer. Rev Med Virol **27**.
87. **Mlcochova P, Sutherland KA, Watters SA, Bertoli C, de Bruin RA, Rehwinkel J, Neil SJ, Lenzi GM, Kim B, Khwaja A, Gage MC, Georgiou C, Chittka A, Yona S, Noursadeghi M, Towers GJ, Gupta RK.** 2017. A G1-like state allows HIV-1 to bypass SAMHD1 restriction in macrophages. EMBO J **36:**604-616.
88. **Yang S, Zhan Y, Zhou Y, Jiang Y, Zheng X, Yu L, Tong W, Gao F, Li L, Huang Q, Ma Z, Tong G.** 2016. Interferon regulatory factor 3 is a key regulation factor for inducing the expression of SAMHD1 in antiviral innate immunity. Sci Rep **6:**29665.
89. **Wittmann S, Behrendt R, Eissmann K, Volkmann B, Thomas D, Ebert T, Cribier A, Benkirane M, Hornung V, Bouzas NF, Gramberg T.** 2015. Phosphorylation of murine SAMHD1 regulates its antiretroviral activity. Retrovirology **12:**103.
90. **Arnold LH, Groom HC, Kunzelmann S, Schwefel D, Caswell SJ, Ordonez P, Mann MC, Rueschenbaum S, Goldstone DC, Pennell S, Howell SA, Stoye JP, Webb M, Taylor IA, Bishop KN.** 2015. Phospho-dependent Regulation of SAMHD1 Oligomerisation Couples Catalysis and Restriction. PLoS Pathog **11:**e1005194.
91. **Laguette N, Sobhian B, Casartelli N, Ringeard M, Chable-Bessia C, Segeral E, Yatim A, Emiliani S, Schwartz O, Benkirane M.** 2011. SAMHD1 is the dendritic- and myeloid-cell-specific HIV-1 restriction factor counteracted by Vpx. Nature **474:**654-657.
92. **Hrecka K, Hao C, Gierszewska M, Swanson SK, Kesik-Brodacka M, Srivastava S, Florens L, Washburn MP, Skowronski J.** 2011. Vpx relieves inhibition of HIV-1 infection of macrophages mediated by the SAMHD1 protein. Nature **474:**658-661.
93. **Jang S, Zhou X, Ahn J.** 2016. Substrate Specificity of SAMHD1 Triphosphohydrolase Activity Is Controlled by Deoxyribonucleoside Triphosphates and Phosphorylation at Thr592. Biochemistry **55:**5635-5646.

94. **Chen Z, Zhu M, Pan X, Zhu Y, Yan H, Jiang T, Shen Y, Dong X, Zheng N, Lu J, Ying S, Shen Y.** 2014. Inhibition of Hepatitis B virus replication by SAMHD1. Biochem Biophys Res Commun **450:**1462-1468.
95. **Jeong GU, Park IH, Ahn K, Ahn BY.** 2016. Inhibition of hepatitis B virus replication by a dNTPase-dependent function of the host restriction factor SAMHD1. Virology **495:**71-78.
96. **Gramberg T, Kahle T, Bloch N, Wittmann S, Mullers E, Daddacha W, Hofmann H, Kim B, Lindemann D, Landau NR.** 2013. Restriction of diverse retroviruses by SAMHD1. Retrovirology **10:**26.
97. **White TE, Brandariz-Nunez A, Valle-Casuso JC, Amie S, Nguyen L, Kim B, Brojatsch J, Diaz-Griffero F.** 2013. Contribution of SAM and HD domains to retroviral restriction mediated by human SAMHD1. Virology **436:**81-90.
98. **Asadian P, Finnie G, Bienzle D.** 2018. The expression profile of sterile alpha motif and histidine-aspartate domain-containing protein 1 (SAMHD1) in feline tissues. Vet Immunol Immunopathol **195:**7-18.
99. **Haller O.** 2013. Dynamins are forever: MxB inhibits HIV-1. Cell Host Microbe **14:**371-373.
100. **Manz B, Dornfeld D, Gotz V, Zell R, Zimmermann P, Haller O, Kochs G, Schwemmle M.** 2013. Pandemic influenza A viruses escape from restriction by human MxA through adaptive mutations in the nucleoprotein. PLoS Pathog **9:**e1003279.
101. **Gao S, von der Malsburg A, Dick A, Faelber K, Schroder GF, Haller O, Kochs G, Daumke O.** 2011. Structure of myxovirus resistance protein a reveals intra- and intermolecular domain interactions required for the antiviral function. Immunity **35:**514-525.
102. **Zimmermann P, Manz B, Haller O, Schwemmle M, Kochs G.** 2011. The viral nucleoprotein determines Mx sensitivity of influenza A viruses. J Virol **85:**8133-8140.
103. **Goujon C, Moncorge O, Bauby H, Doyle T, Ward CC, Schaller T, Hue S, Barclay WS, Schulz R, Malim MH.** 2013. Human MX2 is an interferon-induced post-entry inhibitor of HIV-1 infection. Nature **502:**559-562.
104. **Kane M, Yadav SS, Bitzegeio J, Kutluay SB, Zang T, Wilson SJ, Schoggins JW, Rice CM, Yamashita M, Hatziioannou T, Bieniasz PD.** 2013. MX2 is an interferon-induced inhibitor of HIV-1 infection. Nature **502:**563-566.
105. **Goujon C, Greenbury RA, Papaioannou S, Doyle T, Malim MH.** 2015. A triple-arginine motif in the amino-terminal domain and oligomerization are required for HIV-1 inhibition by human MX2. J Virol **89:**4676-4680.
106. **Dicks MD, Goujon C, Pollpeter D, Betancor G, Apolonia L, Bergeron JR, Malim MH.** 2015. Oligomerization Requirements for MX2-Mediated Suppression of HIV-1 Infection. J Virol **90:**22-32.
107. **Alvarez FJD, He S, Perilla JR, Jang S, Schulten K, Engelman AN, Scheres SHW, Zhang P.** 2017. CryoEM structure of MxB reveals a novel oligomerization interface critical for HIV restriction. Sci Adv **3:**e1701264.
108. **Buffone C, Schulte B, Opp S, Diaz-Griffero F.** 2015. Contribution of MxB oligomerization to HIV-1 capsid binding and restriction. J Virol **89:**3285-3294.
109. **Fribourgh JL, Nguyen HC, Wolfe LS, Dewitt DC, Zhang W, Yu XF, Rhoades E, Xiong Y.** 2014. Core binding factor beta plays a critical role by facilitating the assembly of the Vif-cullin 5 E3 ubiquitin ligase. J Virol **88:**3309-3319.
110. **Fribourgh JL, Nguyen HC, Matreyek KA, Alvarez FJD, Summers BJ, Dewdney TG, Aiken C, Zhang P, Engelman A, Xiong Y.** 2014. Structural insight into HIV-1 restriction by MxB. Cell Host Microbe **16:**627-638.
111. **Bähr A, Singer A, Hain A, Vasudevan AA, Schilling M, Reh J, Riess M, Panitz S, Serrano V, Schweizer M, Konig R, Chanda S, Häussinger D, Kochs G, Lindemann D, Münk C.** 2016. Interferon but not MxB inhibits foamy retroviruses. Virology **488:**51-60.

112. **Fricke T, White TE, Schulte B, de Souza Aranha Vieira DA, Dharan A, Campbell EM, Brandariz-Nunez A, Diaz-Griffero F.** 2014. MxB binds to the HIV-1 core and prevents the uncoating process of HIV-1. Retrovirology **11:**68.
113. **Opp S, Vieira DA, Schulte B, Chanda SK, Diaz-Griffero F.** 2015. MxB Is Not Responsible for the Blocking of HIV-1 Infection Observed in Alpha Interferon-Treated Cells. J Virol **90:**3056-3064.
114. **Opp S, Fricke T, Shepard C, Kovalskyy D, Bhattacharya A, Herkules F, Ivanov DN, Kim B, Valle-Casuso J, Diaz-Griffero F.** 2017. The small-molecule 3G11 inhibits HIV-1 reverse transcription. Chem Biol Drug Des **89:**608-618.
115. **Busnadiego I, Kane M, Rihn SJ, Preugschas HF, Hughes J, Blanco-Melo D, Strouvelle VP, Zang TM, Willett BJ, Boutell C, Bieniasz PD, Wilson SJ.** 2014. Host and viral determinants of Mx2 antiretroviral activity. J Virol **88:**7738-7752.
116. **Mitchell PS, Young JM, Emerman M, Malik HS.** 2015. Evolutionary Analyses Suggest a Function of MxB Immunity Proteins Beyond Lentivirus Restriction. PLoS Pathog **11:**e1005304.
117. **Inuzuka M, Hayakawa M, Ingi T.** 2005. Serinc, an activity-regulated protein family, incorporates serine into membrane lipid synthesis. J Biol Chem **280:**35776-35783.
118. **Beitari S, Ding S, Pan Q, Finzi A, Liang C.** 2017. Effect of HIV-1 Env on SERINC5 Antagonism. J Virol **91**.
119. **Rosa A, Chande A, Ziglio S, De Sanctis V, Bertorelli R, Goh SL, McCauley SM, Nowosielska A, Antonarakis SE, Luban J, Santoni FA, Pizzato M.** 2015. HIV-1 Nef promotes infection by excluding SERINC5 from virion incorporation. Nature **526:**212-217.
120. **Usami Y, Wu Y, Gottlinger HG.** 2015. SERINC3 and SERINC5 restrict HIV-1 infectivity and are counteracted by Nef. Nature **526:**218-223.
121. **Sood C, Marin M, Chande A, Pizzato M, Melikyan GB.** 2017. SERINC5 protein inhibits HIV-1 fusion pore formation by promoting functional inactivation of envelope glycoproteins. J Biol Chem **292:**6014-6026.
122. **Heigele A, Kmiec D, Regensburger K, Langer S, Peiffer L, Sturzel CM, Sauter D, Peeters M, Pizzato M, Learn GH, Hahn BH, Kirchhoff F.** 2016. The Potency of Nef-Mediated SERINC5 Antagonism Correlates with the Prevalence of Primate Lentiviruses in the Wild. Cell Host Microbe **20:**381-391.
123. **Chande A, Cuccurullo EC, Rosa A, Ziglio S, Carpenter S, Pizzato M.** 2016. S2 from equine infectious anemia virus is an infectivity factor which counteracts the retroviral inhibitors SERINC5 and SERINC3. Proc Natl Acad Sci U S A **113:**13197-13202.
124. **Harris RS, Dudley JP.** 2015. APOBECs and virus restriction. Virology **479-480:**131-145.
125. **Simon V, Bloch N, Landau NR.** 2015. Intrinsic host restrictions to HIV-1 and mechanisms of viral escape. Nat Immunol **16:**546-553.
126. **Huthoff H, Malim MH.** 2007. Identification of amino acid residues in APOBEC3G required for regulation by human immunodeficiency virus type 1 Vif and Virion encapsidation. J Virol **81:**3807-3815.
127. **Mangeat B, Turelli P, Caron G, Friedli M, Perrin L, Trono D.** 2003. Broad antiretroviral defence by human APOBEC3G through lethal editing of nascent reverse transcripts. Nature **424:**99-103.
128. **Refsland EW, Hultquist JF, Harris RS.** 2012. Endogenous origins of HIV-1 G-to-A hypermutation and restriction in the nonpermissive T cell line CEM2n. PLoS Pathog **8:**e1002800.
129. **Zhang H, Yang B, Pomerantz RJ, Zhang C, Arunachalam SC, Gao L.** 2003. The cytidine deaminase CEM15 induces hypermutation in newly synthesized HIV-1 DNA. Nature **424:**94-98.
130. **Bishop KN, Holmes RK, Sheehy AM, Malim MH.** 2004. APOBEC-mediated editing of viral RNA. Science **305:**645.

131. **Mariani R, Chen D, Schröfelbauer B, Navarro F, König R, Bollman B, Münk C, Nymark-McMahon H, Landau NR.** 2003. Species-specific exclusion of APOBEC3G from HIV-1 virions by Vif. Cell **114:**21-31.
132. **Yang B, Chen K, Zhang C, Huang S, Zhang H.** 2007. Virion-associated uracil DNA glycosylase-2 and apurinic/apyrimidinic endonuclease are involved in the degradation of APOBEC3G-edited nascent HIV-1 DNA. J Biol Chem **282:**11667-11675.
133. **Gillick K, Pollpeter D, Phalora P, Kim EY, Wolinsky SM, Malim MH.** 2013. Suppression of HIV-1 infection by APOBEC3 proteins in primary human CD4(+) T cells is associated with inhibition of processive reverse transcription as well as excessive cytidine deamination. J Virol **87:**1508-1517.
134. **Iwatani Y, Chan DS, Wang F, Maynard KS, Sugiura W, Gronenborn AM, Rouzina I, Williams MC, Musier-Forsyth K, Levin JG.** 2007. Deaminase-independent inhibition of HIV-1 reverse transcription by APOBEC3G. Nucleic Acids Res **35:**7096-7108.
135. **Holmes RK, Koning FA, Bishop KN, Malim MH.** 2007. APOBEC3F can inhibit the accumulation of HIV-1 reverse transcription products in the absence of hypermutation. Comparisons with APOBEC3G. J Biol Chem **282:**2587-2595.
136. **Mbisa JL, Barr R, Thomas JA, Vandegraaff N, Dorweiler IJ, Svarovskaia ES, Brown WL, Mansky LM, Gorelick RJ, Harris RS, Engelman A, Pathak VK.** 2007. Human immunodeficiency virus type 1 cDNAs produced in the presence of APOBEC3G exhibit defects in plus-strand DNA transfer and integration. J Virol **81:**7099-7110.
137. **Mbisa JL, Bu W, Pathak VK.** 2010. APOBEC3F and APOBEC3G inhibit HIV-1 DNA integration by different mechanisms. J Virol **84:**5250-5259.
138. **Wang X, Ao Z, Chen L, Kobinger G, Peng J, Yao X.** 2012. The cellular antiviral protein APOBEC3G interacts with HIV-1 reverse transcriptase and inhibits its function during viral replication. J Virol **86:**3777-3786.
139. **Pollpeter D, Parsons M, Sobala AE, Coxhead S, Lang RD, Bruns AM, Papaioannou S, McDonnell JM, Apolonia L, Chowdhury JA, Horvath CM, Malim MH.** 2017. Deep sequencing of HIV-1 reverse transcripts reveals the multifaceted antiviral functions of APOBEC3G. Nat Microbiol.
140. **Finley D, Ciechanover A, Varshavsky A.** 2004. Ubiquitin as a central cellular regulator. Cell **116:**S29-32, 22 p following S32.
141. **Kimura Y, Tanaka K.** 2010. Regulatory mechanisms involved in the control of ubiquitin homeostasis. J Biochem **147:**793-798.
142. **Glickman MH, Ciechanover A.** 2002. The ubiquitin-proteasome proteolytic pathway: destruction for the sake of construction. Physiol Rev **82:**373-428.
143. **Glickman MH, Maytal V.** 2002. Regulating the 26S proteasome. Curr Top Microbiol Immunol **268:**43-72.
144. **Mukhopadhyay D, Dasso M.** 2007. Modification in reverse: the SUMO proteases. Trends Biochem Sci **32:**286-295.
145. **Schnell JD, Hicke L.** 2003. Non-traditional functions of ubiquitin and ubiquitin-binding proteins. J Biol Chem **278:**35857-35860.
146. **Lamsoul I, Uttenweiler-Joseph S, Moog-Lutz C, Lutz PG.** 2016. Cullin 5-RING E3 ubiquitin ligases, new therapeutic targets? Biochimie **122:**339-347.
147. **Bloom J, Amador V, Bartolini F, DeMartino G, Pagano M.** 2003. Proteasome-mediated degradation of p21 via N-terminal ubiquitinylation. Cell **115:**71-82.
148. **Metzger MB, Hristova VA, Weissman AM.** 2012. HECT and RING finger families of E3 ubiquitin ligases at a glance. J Cell Sci **125:**531-537.
149. **Nakayama KI, Nakayama K.** 2006. [Ubiquitin system regulating G1 and S phases of cell cycle]. Tanpakushitsu Kakusan Koso **51:**1362-1369.
150. **Okumura F, Joo-Okumura A, Nakatsukasa K, Kamura T.** 2016. The role of cullin 5-containing ubiquitin ligases. Cell Div **11:**1.

151. **Burnatowska-Hledin MA, Barney CC.** 2014. New insights into the mechanism for VACM-1/cul5 expression in vascular tissue in vivo. Int Rev Cell Mol Biol **313:**79-101.
152. **Byrd PJ, Stankovic T, McConville CM, Smith AD, Cooper PR, Taylor AM.** 1997. Identification and analysis of expression of human VACM-1, a cullin gene family member located on chromosome 11q22-23. Genome Res **7:**71-75.
153. **Hurbin A, Orcel H, Ferraz C, Moos FC, Rabie A.** 2000. Expression of the genes encoding the vasopressin-activated calcium-mobilizing receptor and the dual angiotensin II/vasopressin receptor in the rat central nervous system. J Neuroendocrinol **12:**677-684.
154. **Burnatowska-Hledin M, Lazdins IB, Listenberger L, Zhao P, Sharangpani A, Folta V, Card B.** 1999. VACM-1 receptor is specifically expressed in rabbit vascular endothelium and renal collecting tubule. Am J Physiol **276:**F199-209.
155. **Jager S, Kim DY, Hultquist JF, Shindo K, LaRue RS, Kwon E, Li M, Anderson BD, Yen L, Stanley D, Mahon C, Kane J, Franks-Skiba K, Cimermancic P, Burlingame A, Sali A, Craik CS, Harris RS, Gross JD, Krogan NJ.** 2012. Vif hijacks CBF-beta to degrade APOBEC3G and promote HIV-1 infection. Nature **481:**371-375.
156. **Sheehy AM, Gaddis NC, Choi JD, Malim MH.** 2002. Isolation of a human gene that inhibits HIV-1 infection and is suppressed by the viral Vif protein. Nature **418:**646-650.
157. **Yu X, Yu Y, Liu B, Luo K, Kong W, Mao P, Yu XF.** 2003. Induction of APOBEC3G ubiquitination and degradation by an HIV-1 Vif-Cul5-SCF complex. Science **302:**1056-1060.
158. **Guo Y, Dong L, Qiu X, Wang Y, Zhang B, Liu H, Yu Y, Zang Y, Yang M, Huang Z.** 2014. Structural basis for hijacking CBF-beta and CUL5 E3 ligase complex by HIV-1 Vif. Nature **505:**229-233.
159. **LaRue RS, Andresdottir V, Blanchard Y, Conticello SG, Derse D, Emerman M, Greene WC, Jonsson SR, Landau NR, Löchelt M, Malik HS, Malim MH, Münk C, O'Brien SJ, Pathak VK, Strebel K, Wain-Hobson S, Yu XF, Yuhki N, Harris RS.** 2009. Guidelines for naming nonprimate APOBEC3 genes and proteins. J Virol **83:**494-497.
160. **Münk C, Willemsen A, Bravo IG.** 2012. An ancient history of gene duplications, fusions and losses in the evolution of APOBEC3 mutators in mammals. BMC Evol Biol **12:**71.
161. **Zielonka J, Marino D, Hofmann H, Yuhki N, Löchelt M, Münk C.** 2010. Vif of feline immunodeficiency virus from domestic cats protects against APOBEC3 restriction factors from many felids. J Virol **84:**7312-7324.
162. **Zhang Z, Gu Q, Jaguva Vasudevan AA, Hain A, Kloke BP, Hasheminasab S, Mulnaes D, Sato K, Cichutek K, Häussinger D, Bravo IG, Smits SH, Gohlke H, Münk C.** 2016. Determinants of FIV and HIV Vif sensitivity of feline APOBEC3 restriction factors. Retrovirology **13:**46.
163. **Larue RS, Lengyel J, Jonsson SR, Andresdottir V, Harris RS.** 2010. Lentiviral Vif degrades the APOBEC3Z3/APOBEC3H protein of its mammalian host and is capable of cross-species activity. J Virol **84:**8193-8201.
164. **Stern MA, Hu C, Saenz DT, Fadel HJ, Sims O, Peretz M, Poeschla EM.** 2010. Productive replication of Vif-chimeric HIV-1 in feline cells. J Virol **84:**7378-7395.
165. **de Castro FL, Junqueira DM, de Medeiros RM, da Silva TR, Costenaro JG, Knak MB, de Matos Almeida SE, Campos FS, Roehe PM, Franco AC.** 2014. Analysis of single-nucleotide polymorphisms in the APOBEC3H gene of domestic cats (Felis catus) and their association with the susceptibility to feline immunodeficiency virus and feline leukemia virus infections. Infect Genet Evol **27:**389-394.
166. **Löchelt M, Romen F, Bastone P, Muckenfuss H, Kirchner N, Kim YB, Truyen U, Rosler U, Battenberg M, Saib A, Flory E, Cichutek K, Münk C.** 2005. The antiretroviral activity of APOBEC3 is inhibited by the foamy virus accessory Bet protein. Proc Natl Acad Sci U S A **102:**7982-7987.
167. **Münk C, Zielonka J, Constabel H, Kloke BP, Rengstl B, Battenberg M, Bonci F, Pistello M, Löchelt M, Cichutek K.** 2007. Multiple restrictions of human immunodeficiency virus type 1 in feline cells. J Virol **81:**7048-7060.

168. **Wang J, Zhang W, Lv M, Zuo T, Kong W, Yu X.** 2011. Identification of a Cullin5-ElonginB-ElonginC E3 complex in degradation of feline immunodeficiency virus Vif-mediated feline APOBEC3 proteins. J Virol **85:**12482-12491.
169. **Zhang W, Du J, Evans SL, Yu Y, Yu XF.** 2012. T-cell differentiation factor CBF-beta regulates HIV-1 Vif-mediated evasion of host restriction. Nature **481:**376-379.
170. **Kane JR, Stanley DJ, Hultquist JF, Johnson JR, Mietrach N, Binning JM, Jonsson SR, Barelier S, Newton BW, Johnson TL, Franks-Skiba KE, Li M, Brown WL, Gunnarsson HI, Adalbjornsdottir A, Fraser JS, Harris RS, Andresdottir V, Gross JD, Krogan NJ.** 2015. Lineage-Specific Viral Hijacking of Non-canonical E3 Ubiquitin Ligase Cofactors in the Evolution of Vif Anti-APOBEC3 Activity. Cell Rep **11:**1236-1250.
171. **Ai Y, Zhu D, Wang C, Su C, Ma J, Ma J, Wang X.** 2014. Core-binding factor subunit beta is not required for non-primate lentiviral Vif-mediated APOBEC3 degradation. J Virol **88:**12112-12122.
172. **Han X, Liang W, Hua D, Zhou X, Du J, Evans SL, Gao Q, Wang H, Viqueira R, Wei W, Zhang W, Yu XF.** 2014. Evolutionarily conserved requirement for core binding factor beta in the assembly of the human immunodeficiency virus/simian immunodeficiency virus Vif-cullin 5-RING E3 ubiquitin ligase. J Virol **88:**3320-3328.
173. **Yoshikawa R, Takeuchi JS, Yamada E, Nakano Y, Ren F, Tanaka H, Münk C, Harris RS, Miyazawa T, Koyanagi Y, Sato K.** 2015. Vif determines the requirement for CBF-beta in APOBEC3 degradation. J Gen Virol **96:**887-892.
174. **Letko M, Booiman T, Kootstra N, Simon V, Ooms M.** 2015. Identification of the HIV-1 Vif and Human APOBEC3G Protein Interface. Cell Rep **13:**1789-1799.
175. **Zhen A, Wang T, Zhao K, Xiong Y, Yu XF.** 2010. A single amino acid difference in human APOBEC3H variants determines HIV-1 Vif sensitivity. J Virol **84:**1902-1911.
176. **Ooms M, Letko M, Binka M, Simon V.** 2013. The resistance of human APOBEC3H to HIV-1 NL4-3 molecular clone is determined by a single amino acid in Vif. PLoS One **8:**e57744.
177. **Kitamura S, Ode H, Nakashima M, Imahashi M, Naganawa Y, Kurosawa T, Yokomaku Y, Yamane T, Watanabe N, Suzuki A, Sugiura W, Iwatani Y.** 2012. The APOBEC3C crystal structure and the interface for HIV-1 Vif binding. Nat Struct Mol Biol **19:**1005-1010.
178. **Zhang Z, Gu Q, Jaguva Vasudevan AA, Jeyaraj M, Schmidt S, Zielonka J, Perkovic M, Heckel JO, Cichutek K, Häussinger D, Smits SH, Münk C.** 2016. Vif Proteins from Diverse Human Immunodeficiency Virus/Simian Immunodeficiency Virus Lineages Have Distinct Binding Sites in A3C. J Virol **90:**10193-10208.
179. **Richards C, Albin JS, Demir O, Shaban NM, Luengas EM, Land AM, Anderson BD, Holten JR, Anderson JS, Harki DA, Amaro RE, Harris RS.** 2015. The Binding Interface between Human APOBEC3F and HIV-1 Vif Elucidated by Genetic and Computational Approaches. Cell Rep **13:**1781-1788.
180. **Smith JL, Pathak VK.** 2010. Identification of specific determinants of human APOBEC3F, APOBEC3C, and APOBEC3DE and African green monkey APOBEC3F that interact with HIV-1 Vif. J Virol **84:**12599-12608.
181. **Nakashima M, Ode H, Kawamura T, Kitamura S, Naganawa Y, Awazu H, Tsuzuki S, Matsuoka K, Nemoto M, Hachiya A, Sugiura W, Yokomaku Y, Watanabe N, Iwatani Y.** 2015. Structural Insights into HIV-1 Vif-APOBEC3F Interaction. J Virol **90:**1034-1047.
182. **Albin JS, LaRue RS, Weaver JA, Brown WL, Shindo K, Harjes E, Matsuo H, Harris RS.** 2010. A single amino acid in human APOBEC3F alters susceptibility to HIV-1 Vif. J Biol Chem **285:**40785-40792.
183. **Land AM, Shaban NM, Evans L, Hultquist JF, Albin JS, Harris RS.** 2014. APOBEC3F determinants of HIV-1 Vif sensitivity. J Virol **88:**12923-12927.
184. **Zennou V, Bieniasz PD.** 2006. Comparative analysis of the antiretroviral activity of APOBEC3G and APOBEC3F from primates. Virology **349:**31-40.

185. **Russell RA, Pathak VK.** 2007. Identification of two distinct human immunodeficiency virus type 1 Vif determinants critical for interactions with human APOBEC3G and APOBEC3F. J Virol **81:**8201-8210.
186. **Binka M, Ooms M, Steward M, Simon V.** 2012. The activity spectrum of Vif from multiple HIV-1 subtypes against APOBEC3G, APOBEC3F, and APOBEC3H. J Virol **86:**49-59.
187. **Salter JD, Morales GA, Smith HC.** 2014. Structural insights for HIV-1 therapeutic strategies targeting Vif. Trends Biochem Sci **39:**373-380.
188. **Dang Y, Davis RW, York IA, Zheng YH.** 2010. Identification of 81LGxGxxIxW89 and 171EDRW174 domains from human immunodeficiency virus type 1 Vif that regulate APOBEC3G and APOBEC3F neutralizing activity. J Virol **84:**5741-5750.
189. **Smith JL, Izumi T, Borbet TC, Hagedorn AN, Pathak VK.** 2014. HIV-1 and HIV-2 Vif interact with human APOBEC3 proteins using completely different determinants. J Virol **88:**9893-9908.
190. **Yoshikawa R, Izumi T, Yamada E, Nakano Y, Misawa N, Ren F, Carpenter MA, Ikeda T, Münk C, Harris RS, Miyazawa T, Koyanagi Y, Sato K.** 2016. A Naturally Occurring Domestic Cat APOBEC3 Variant Confers Resistance to Feline Immunodeficiency Virus Infection. J Virol **90:**474-485.
191. **Yoshikawa R, Nakano Y, Yamada E, Izumi T, Misawa N, Koyanagi Y, Sato K.** 2016. Species-specific differences in the ability of feline lentiviral Vif to degrade feline APOBEC3 proteins. Microbiol Immunol **60:**272-279.
192. **Zielonka J, Marino D, Hofmann H, Yuhki N, Löchelt M, Münk C.** 2010. Vif of Feline Immunodeficiency Virus from Domestic Cats Protects against APOBEC3 Restriction Factors from Many Felids. J.Virol. **84:**7312-7324.
193. **Russell RA, Wiegand HL, Moore MD, Schafer A, McClure MO, Cullen BR.** 2005. Foamy virus Bet proteins function as novel inhibitors of the APOBEC3 family of innate antiretroviral defense factors. J Virol **79:**8724-8731.
194. **Jin J, Ang XL, Shirogane T, Wade Harper J.** 2005. Identification of substrates for F-box proteins. Methods Enzymol **399:**287-309.
195. **Ohta T, Michel JJ, Schottelius AJ, Xiong Y.** 1999. ROC1, a homolog of APC11, represents a family of cullin partners with an associated ubiquitin ligase activity. Mol Cell **3:**535-541.
196. **Lonergan KM, Iliopoulos O, Ohh M, Kamura T, Conaway RC, Conaway JW, Kaelin WG, Jr.** 1998. Regulation of hypoxia-inducible mRNAs by the von Hippel-Lindau tumor suppressor protein requires binding to complexes containing elongins B/C and Cul2. Mol Cell Biol **18:**732-741.
197. **Ohh M, Park CW, Ivan M, Hoffman MA, Kim TY, Huang LE, Pavletich N, Chau V, Kaelin WG.** 2000. Ubiquitination of hypoxia-inducible factor requires direct binding to the beta-domain of the von Hippel-Lindau protein. Nat Cell Biol **2:**423-427.
198. **Loewen N, Barraza R, Whitwam T, Saenz DT, Kemler I, Poeschla EM.** 2003. FIV Vectors. Methods Mol Biol **229:**251-271.
199. **Eswar N, Webb B, Marti-Renom MA, Madhusudhan MS, Eramian D, Shen MY, Pieper U, Sali A.** 2006. Comparative protein structure modeling using Modeller. Curr Protoc Bioinformatics **Chapter 5:**Unit-5 6.
200. **Jones DT.** 1999. Protein secondary structure prediction based on position-specific scoring matrices. J Mol Biol **292:**195-202.
201. **De Filippis V, Sander C, Vriend G.** 1994. Predicting local structural changes that result from point mutations. Protein Eng **7:**1203-1208.
202. **Chatterji U, Grant CK, Elder JH.** 2000. Feline immunodeficiency virus Vif localizes to the nucleus. J Virol **74:**2533-2540.
203. **Stern MA, Hu C, Saenz DT, Fadel HJ, Sims O, Peretz M, Poeschla EM.** 2010. Productive replication of Vif-chimeric HIV-1 in feline cells. J.Virol. **84:**7378-7395.

204. **Münk C, Beck T, Zielonka J, Hotz-Wagenblatt A, Chareza S, Battenberg M, Thielebein J, Cichutek K, Bravo IG, O'Brien SJ, Löchelt M, Yuhki N.** 2008. Functions, structure, and read-through alternative splicing of feline APOBEC3 genes. Genome Biol. **9:**R48.
205. **Yoshikawa R, Izumi T, Yamada E, Nakano Y, Misawa N, Ren F, Carpenter MA, Ikeda T, Munk C, Harris RS, Miyazawa T, Koyanagi Y, Sato K.** 2015. A naturally occurring domestic cat APOBEC3 variant confers resistance to FIV infection. Journal of virology.
206. **Gu Q, Zhang Z, Cano Ortiz L, Franco AC, Häussinger D, Münk C.** 2016. Feline Immunodeficiency Virus Vif N-Terminal Residues Selectively Counteract Feline APOBEC3s. J Virol **90:**10545-10557.
207. **Luo K, Xiao Z, Ehrlich E, Yu Y, Liu B, Zheng S, Yu XF.** 2005. Primate lentiviral virion infectivity factors are substrate receptors that assemble with cullin 5-E3 ligase through a HCCH motif to suppress APOBEC3G. Proc Natl Acad Sci U S A **102:**11444-11449.
208. **Xiao Z, Ehrlich E, Yu Y, Luo K, Wang T, Tian C, Yu XF.** 2006. Assembly of HIV-1 Vif-Cul5 E3 ubiquitin ligase through a novel zinc-binding domain-stabilized hydrophobic interface in Vif. Virology **349:**290-299.
209. **Xiao Z, Xiong Y, Zhang W, Tan L, Ehrlich E, Guo D, Yu XF.** 2007. Characterization of a novel Cullin5 binding domain in HIV-1 Vif. J Mol Biol **373:**541-550.
210. **Mehle A, Thomas ER, Rajendran KS, Gabuzda D.** 2006. A zinc-binding region in Vif binds Cul5 and determines cullin selection. J Biol Chem **281:**17259-17265.
211. **He Z, Zhang W, Chen G, Xu R, Yu XF.** 2008. Characterization of conserved motifs in HIV-1 Vif required for APOBEC3G and APOBEC3F interaction. J Mol Biol **381:**1000-1011.
212. **Nakashima M, Ode H, Kawamura T, Kitamura S, Naganawa Y, Awazu H, Tsuzuki S, Matsuoka K, Nemoto M, Hachiya A, Sugiura W, Yokomaku Y, Watanabe N, Iwatani Y.** 2016. Structural Insights into HIV-1 Vif-APOBEC3F Interaction. J Virol **90:**1034-1047.
213. **Dang Y, Wang X, York IA, Zheng YH.** 2010. Identification of a critical T(Q/D/E)x5ADx2(I/L) motif from primate lentivirus Vif proteins that regulate APOBEC3G and APOBEC3F neutralizing activity. J Virol **84:**8561-8570.
214. **Pery E, Rajendran KS, Brazier AJ, Gabuzda D.** 2009. Regulation of APOBEC3 proteins by a novel YXXL motif in human immunodeficiency virus type 1 Vif and simian immunodeficiency virus SIVagm Vif. J Virol **83:**2374-2381.
215. **Farrow MA, Somasundaran M, Zhang C, Gabuzda D, Sullivan JL, Greenough TC.** 2005. Nuclear localization of HIV type 1 Vif isolated from a long-term asymptomatic individual and potential role in virus attenuation. AIDS Res Hum Retroviruses **21:**565-574.
216. **Wichroski MJ, Ichiyama K, Rana TM.** 2005. Analysis of HIV-1 viral infectivity factor-mediated proteasome-dependent depletion of APOBEC3G: correlating function and subcellular localization. J Biol Chem **280:**8387-8396.
217. **Baig TT, Feng Y, Chelico L.** 2014. Determinants of efficient degradation of APOBEC3 restriction factors by HIV-1 Vif. J Virol **88:**14380-14395.
218. **Zhang W, Huang M, Wang T, Tan L, Tian C, Yu X, Kong W, Yu XF.** 2008. Conserved and non-conserved features of HIV-1 and SIVagm Vif mediated suppression of APOBEC3 cytidine deaminases. Cell Microbiol **10:**1662-1675.
219. **Carpenter MA, O'Brien SJ.** 1995. Coadaptation and immunodeficiency virus: lessons from the Felidae. Curr Opin Genet Dev **5:**739-745.
220. **VandeWoude S, O'Brien SJ, Langelier K, Hardy WD, Slattery JP, Zuckerman EE, Hoover EA.** 1997. Growth of lion and puma lentiviruses in domestic cat cells and comparisons with FIV. Virology **233:**185-192.
221. **VandeWoude S, O'Brien SJ, Hoover EA.** 1997. Infectivity of lion and puma lentiviruses for domestic cats. J Gen Virol **78 (Pt 4):**795-800.
222. **VandeWoude S, Hageman CL, Hoover EA.** 2003. Domestic cats infected with lion or puma lentivirus develop anti-feline immunodeficiency virus immune responses. J Acquir Immune Defic Syndr **34:**20-31.

223. **Poss M, Ross HA, Painter SL, Holley DC, Terwee JA, Vandewoude S, Rodrigo A.** 2006. Feline lentivirus evolution in cross-species infection reveals extensive G-to-A mutation and selection on key residues in the viral polymerase. J Virol **80:**2728-2737.
224. **He Z, Zhang W, Chen G, Xu R, Yu XF.** 2008. Characterization of conserved motifs in HIV-1 Vif required for APOBEC3G and APOBEC3F interaction. J.Mol.Biol. **381:**1000-1011.
225. **Marin M, Golem S, Rose KM, Kozak SL, Kabat D.** 2008. Human immunodeficiency virus type 1 Vif functionally interacts with diverse APOBEC3 cytidine deaminases and moves with them between cytoplasmic sites of mRNA metabolism. J Virol **82:**987-998.
226. **Bergeron JR, Huthoff H, Veselkov DA, Beavil RL, Simpson PJ, Matthews SJ, Malim MH, Sanderson MR.** 2010. The SOCS-box of HIV-1 Vif interacts with ElonginBC by induced-folding to recruit its Cul5-containing ubiquitin ligase complex. PLoS Pathog **6:**e1000925.
227. **Wolfe LS, Stanley BJ, Liu C, Eliason WK, Xiong Y.** 2010. Dissection of the HIV Vif interaction with human E3 ubiquitin ligase. J Virol **84:**7135-7139.
228. **Luo K, Ehrlich E, Xiao Z, Zhang W, Ketner G, Yu XF.** 2007. Adenovirus E4orf6 assembles with Cullin5-ElonginB-ElonginC E3 ubiquitin ligase through an HIV/SIV Vif-like BC-box to regulate p53. FASEB J **21:**1742-1750.
229. **Wang H, Guo H, Su J, Rui Y, Zheng W, Gao W, Zhang W, Li Z, Liu G, Markham RB, Wei W, Yu XF.** 2017. Inhibition of Vpx-Mediated SAMHD1 and Vpr-Mediated Host Helicase Transcription Factor Degradation by Selective Disruption of Viral CRL4 (DCAF1) E3 Ubiquitin Ligase Assembly. J Virol **91**.
230. **Schwefel D, Groom HC, Boucherit VC, Christodoulou E, Walker PA, Stoye JP, Bishop KN, Taylor IA.** 2014. Structural basis of lentiviral subversion of a cellular protein degradation pathway. Nature **505:**234-238.
231. **Wu Y, Zhou X, Barnes CO, DeLucia M, Cohen AE, Gronenborn AM, Ahn J, Calero G.** 2016. The DDB1-DCAF1-Vpr-UNG2 crystal structure reveals how HIV-1 Vpr steers human UNG2 toward destruction. Nat Struct Mol Biol **23:**933-940.
232. **Zhang J, Wu J, Wang W, Wu H, Yu B, Wang J, Lv M, Wang X, Zhang H, Kong W, Yu X.** 2014. Role of cullin-elonginB-elonginC E3 complex in bovine immunodeficiency virus and maedi-visna virus Vif-mediated degradation of host A3Z2-Z3 proteins. Retrovirology **11:**77.
233. **Lee SJ, Koh JY.** 2010. Roles of zinc and metallothionein-3 in oxidative stress-induced lysosomal dysfunction, cell death, and autophagy in neurons and astrocytes. Mol Brain **3:**30.
234. **Kim YK, Kwak MJ, Ku B, Suh HY, Joo K, Lee J, Jung JU, Oh BH.** 2013. Structural basis of intersubunit recognition in elongin BC-cullin 5-SOCS box ubiquitin-protein ligase complexes. Acta Crystallogr D Biol Crystallogr **69:**1587-1597.